Decadal to centennial variability of daily wind over Northern Europe and its application to migrating dunes in the Baltic Sea region.

Dissertation zur Erlangung des Doktorgrades
an der Fakultät für Mathematik, Informatik und Naturwissenschaften
Fachbereich Geowissenschaften
der Universität Hamburg

vorgelegt von
Svenja E. Bierstedt

Hamburg, Oktober 2015

Tag der Disputation:	04.12.2015
Gutachter:	Prof. Dr. Dr. h.c. Hans von Storch
	Dr. Birgit Hünicke

"We know accurately only when we know little, with knowledge doubt increases."

Johann Wolfgang von Goethe

Abstract

The present work is focused on the analysis of the variability of extreme daily winds in Northern Europe, their relationship to mean winds and to large-scale climate patterns. In particular, this work has the aim of investigating the following four research questions: 1. Are mean wind statistics a useful tool to draw conclusions on extreme wind statistics over the Baltic Sea? 2. What pressure patterns drive extreme westerly winds over the Baltic Sea? 3. What large-scale atmospheric parameters drive changes in the wind speed distribution over Northern Europe? 4. Can internal dune structures at the southern Baltic be applied to reconstruct the seasonal wind climate?

The study uses different data sets ranging from the last decades, using observation-based reconstructions, to the last millennium, using model simulations:

To answer the first research question the study compares the statistics of seasonal mean and daily extreme wind events over the Baltic Sea in three aspects: direction distribution, regional differences and seasonal variability. The results exhibited differences between mean and extreme wind events in all three facets. Therefore, the overall conclusion is that the hypothesis that the statistics of mean wind can serve as a proxy for statistics of extreme wind does not hold for the Baltic Sea region.

The second part investigates daily wind extremes from west and south-west in the Baltic Sea region during winter and their relationship to circulation types. After identifying eight circulation types, four patterns showed relations to the frequencies of extreme west/south-west winds. The temporal evolution of three of these patterns showed clear similarities to extreme west/south-west wind frequencies.

The third part analyses the influence of potential large-scale atmospheric drivers to modulate the probability distribution of daily wind speed in winter over Northern Europe. The considered drivers are the mean temperature, the meridional temperature gradient and the North Atlantic Oscillation. The main result of this study is that in the analysed climate simulations there is no clear systematic relationship detectable between the analysed atmospheric parameters and the wind speed distribution. Further analysis is needed regarding the linkage of large-scale and small-scale dynamics.

The last part of this study validates a dune record compiled in cooperation with geologists (Ludwig et al., 2015). The dune layers can be seen as an analog to tree ring width records with annual resolution, and hence for the validation a dendrochronological method was applied. This proxy is believed to record the frequency of daily wind from particular directions. The measures of statistical skill are found to be acceptable, compared to tree ring reconstructions. Hence, this study statistically verifies a rare instance of a proxy that can be used to reconstruct past wind conditions with high temporal resolution.

Zusammenfassung

Die vorliegende Arbeit analysiert die Variabilität von extremen Winden über Nordeuropa und deren Beziehung zu mittleren Winden und zu großskaligen Klimaparametern. Dazu werden unterschiedliche Datensätze untersucht, die die letzten Dekaden - durch die Nutzung von beobachtungs-basierten Rekonstruktionen - bis zum letzten Millennium - durch die Nutzung von Modellsimulationen - abdecken. Die Analyse hat zum Ziel, die folgenden Fragen zu beantworten: 1. Können Statistiken von mittleren Winden genutzt werden, um Aussagen über Statistiken von extremen Winden zu treffen? 2. Welche Luftdruckmuster beeinflussen extreme Winde aus Westen? 3. Welche großskaligen atmosphärischen Parameter beeinflussen die Verteilung der Windgeschwindigkeit? 4. Können Internstrukturen von Küstendünen der südlichen Ostsee als Proxy genutzt werden, um eine Rekonstruktion des saisonalen Windklimas zu erstellen?

Um die erste Frage zu beantworten, werden mittlere und extreme Windereignisse über der Ostseeregion in drei Aspekten verglichen: Verteilung der Windrichtungen, regionale Unterschiede und saisonale Variabilität. Die Ergebnisse zeigen Unterschiede in allen drei Punkten. Aus diesem Grund wird die Hypothese abgelehnt, dass die Statistik von mittleren Winden als Vertreter für die Statistik von extremen Winden über der Ostseeregion verwendet werden kann.

Der zweite Teil untersucht extreme West und Süd-West Winde im Winter über der Ostsee und deren Beziehung zu Zirkulationsklassen, die mit Hilfe des Drucks auf Meeresniveau bestimmt wurden. Nach der Identifikation von acht Zirkulationsklassen zeigen vier Muster eine Verbindung zu den Häufigkeiten von West und Süd-West Winden, die das 95te Perzentil überschreiten. Die zeitliche Entwicklung dreier Muster zeigt deutliche Übereinstimmungen mit den Häufigkeiten von extremen West und Süd-West Winden.

Im dritten Teil wird der Einfluss potenzieller, großskaliger atmosphärischer Antriebe auf die Verteilung der Windgeschwindigkeit über Nordeuropa untersucht. Eine Hauptaussage ist, dass mit den untersuchten Klimasimulationen keine klare systematische Verbindung zwischen den analysierten atmosphärischen Parametern und der Verteilung der Windgeschwindigkeit gefunden werden kann. Es werden weitere Untersuchungen bezüglich der Kopplung von großskaligen und kleinskaligen Dynamiken benötigt.

Der letzte Teil der Arbeit validiert einen Dünendatensatz, der in Kooperation mit Geologen (Ludwig el al., 2015) erarbeitet wurde. Dieser weist starke Ähnlichkeiten zu Baumringdatensätzen auf und wurde aus diesem Grund mit einer dendrochronologischen Methode validiert, dies führte zu akzeptablen Validationsmaßen, vergleichbar zu Werten, die für Baumringrekonstruktionen erreicht werden. Folglich beweist die vorliegende Untersuchung die statistische Legitimität von wandernden Küstendünen als Wind-Proxy.

Contents

1 Introduction

1.1 Motivation

Nowadays the scientific community has high confidence about the anthropogenic induced climate change (IPCC, 2013) due to greenhouse gas emissions and land-use changes. Greenhouse gas concentrations in the atmosphere have significantly increased since the 1850^{th} and the last century is characterised by globally increasing temperatures over most regions of the globe. On a regional perspective, annual temperature over the northern Baltic Sea region increased up to 1.5 K from 1871 to 2011 (von Storch et al., 2015). Depending on future emitted greenhouse gases this increase could proceed by a further 1 to 8 K over the next 100 years (Christensen et al., 2015). This warming may also have an affect on other atmospheric parameters including atmospheric circulation and related changes in mean and extreme wind.

Changes in wind climate may have a direct impact on different aspects: A reduction of wind speed can reduce the productivity of wind farms, whereas an increase of wind speed might increase this productivity. In contrast to increasing wind speeds an increase in the frequency of severe winds e.g. storms may harm the available capacity of power supply (Nolan et al., 2012). For central Europe and the Baltic Sea region, extreme winds are the natural hazards that are most relevant for economic losses, leading to damages of buildings and infrastructure, and they may cause loss of life or lead to storm surges which can extent these damages (Rutgersson et al., 2015). Storm surges are frequently occurring events because of the Baltic Sea shape, promoting extreme wind effects, and the existence of shallow beach areas exposed to the direction of strong winds. Furthermore, extreme sea levels in the Baltic Sea are mainly induced by wind (Hünicke et al., 2015).

Due to the importance of wind events in Europe it is of high public and economic interest to analyse and understand long-term changes in wind speeds and wind directions. Furthermore, the assessment of past wind climate changes helps to broaden the knowledge of this important climate parameter and helps to distinguish between changes and trends due to anthropogenic influences and natural climate variability (Krueger, 2014).

1.2 North Atlantic, European and Baltic Sea wind

The focus of this study lies on the Baltic Sea region. Besides processes occurring at the regional scale, this area is strongly influenced by the North-Atlantic and Northern-Europe area, including sea level air-pressure, temperature, precipitation, and especially wind.

The wind field over the Baltic Sea area depends on large-scale pressure patterns over the North-Atlantic-European area. The most important pattern is the North-Atlantic-Oscillation (NAO). This pattern is characterised by the difference of a pressure low over Iceland and high pressure near the Azores (Rutgersson et al., 2015). The temporal evolution of this atmospheric sea-saw can be described by the NAO index which describes a large part of the pressure variability during winter time and strongly influences other climate variables (e.g. temperature, wind speed and wind direction) over Europe and hence the Baltic Sea. A positive (negative) NAO index is connected to higher (lower) pressure differences between Iceland-Low and Azores-High and is related to stronger (weaker) westerlies (Hurrell et al., 2003).
Moreover, the Baltic Sea is strongly influenced by westerly winds, which are in theory dependent on the large-scale meridional temperature gradient. This temperature difference between the North and South North-Atlantic-European region is strongest during winter, because of the stronger surface radiation difference between these regions during this season (Leppäranta and Myrberg, 2009). Thus, on average, the highest wind speeds over the Baltic Sea occur during the winter-half season from October to February (Weidemann, 2014).
The following subsections give an overview about the state-of-the-art knowledge of the scientific community regarding past changes of wind speed and wind direction for the above mentioned regions.

1.2.1 Wind speed

Wind speed, storm intensities and frequency have been analysed on different temporal and spatial resolutions covering various time periods from a few decades to centuries. In general, it can be concluded that the resulting trends and low-frequency variations strongly depend on the time periods and data sets taken under consideration (Feser et al., 2015). Donat et al. (2011) analysed the 20CR reanalysis (Compo et al., 2011) covering the period since 1871 and reported a positive long-term trend in storminess during winter over Northern Europe. This is in contradiction with proxy-based studies covering the last 130 years (e.g. Matulla et al., 2007) which concluded that values of extreme geostrophic winds since the mid 1990s returned later back to the values more typical of the periods before the 1960s. Krueger et al. (2013) analysed 20CR storminess in greater detail by comparing the results with storminess time series derived from a storm-proxy based on geostrophic winds. Their results showed that 20CR data differ in large parts from the proxy-based observations and that this was most likely due to the increasing number of observations assimilated into 20CR over time.
Since time series of direct wind measurements are found to be too inhomogeneous in time for comprehensive long-term wind analyses (Trenberth et al., 2007) numerous studies of

the European wind climate are based on the storm-proxy derived from air-pressure observation (e.g. Alexandersson et al., 2000; Bärring and von Storch, 2004; WASA, 1998). The corresponding analyses showed an increase in storms since 1960 until the mid 1990's followed by a decrease afterwards. This development was also reported for the Baltic Sea region (Hurrell et al., 2003).
In shorter periods, Lehmann et al. (2011) analysed SMHI meteorological data and found the mean winter geostrophic wind speed increasing by about 1.5 m/s in the period 1989 to 2007 compared to 1970 to 1998 over the Baltic Sea region. This increase occurred simultaneously with an increased number of storms over the southern North Sea identified by Weisse et al. (2005). Station data analysis for Estonia reported a decrease in mean wind speeds and an increase in extreme wind speeds over the past 50 years (Jaagus, 2009; Jaagus and Kull, 2011).
Studies concerning long-term time series since 1800 (Bärring and von Storch, 2004) suggest that these trends are part of decadal variations and that there is no long-term centennial trend in storm activity over Europe (Bärring and Fortuniak, 2009).
The results of these studies have been summarised for the Baltic Sea region by Rutgersson et al. (2015) concluding that there are no long-term trends in annual wind statistics since the nineteenth century, but pronounced variability at decadal time scales.

1.2.2 Wind direction

Similar to wind speed, changes in wind directions are also related to large-scale atmospheric circulation. Changes in Northern hemispheric sea-level-pressure (SLP) are discussed in detail by Serreze et al. (2000) for the last half of the 20^{th} century. They observed a significant decrease in SLP over the Arctic with an increase over South-Europe. This intensification of the pressure gradient caused stronger westerlies. Furthermore Jaagus and Kull (2011) reported comparable results regarding trends of the large-scale NAO pressure pattern, closely related to wind statistics over the Baltic Sea.
A study regarding atmospheric circulation patterns over Europe showed changes for the last years of the period from 1881 to 1989 (Bárdossy and Caspary, 1990). These authors reported a positive trend for the frequency of the zonal circulation since 1973 for winter and a negative trend for spring. Additionally, a negative trend in the frequency of easterly winds occurred for winters since 1980.
The study by Lehmann et al. (2011) analysed the period from 1958 to 2009 regarding climate variability in the Baltic Sea and found changes in the distribution of wind directions. The results indicated a negative trend for wind from the south-west sector and a positive trend for easterly winds during autumn. The winter season showed trends with the opposite sign, with increasing westerly winds and decreasing easterly winds.
Other studies focusing exclusively on changes in the frequency of wind direction are available for Estonia (Jaagus, 2009; Jaagus and Kull, 2011; Keevallik, 2008; Kull, 2005), where

higher frequencies for south-west winds are documented. At the 500 hPa level, zonal wind velocity significantly increased during 1953 to 1998 for winter, whereas the meridional component increased in March (Keevallik and Rajasalub, 2001).

1.3 Data bases

A number of studies uses near-surface wind speed measurements averaged over different time spans as data basis. Direct measurements are, for example, used by Chaverot et al. (2008) for analysis at the northern coast of France or by Jaagus (2009); Jaagus and Kull (2011) for investigations of wind in Estonia. However, these kind of data sets are commonly known to be affected by inhomogeneities due to station relocation or changes in measurement techniques (Krueger, 2014).
Therefore, other studies rely on proxy data that can be derived e.g. from direct air-pressure measurements (e.g. Alexandersson et al., 2000; Bärring and Fortuniak, 2009; Bärring and von Storch, 2004; Hanna et al., 2008; Krueger et al., 2013). These data sets are particularly advantageous for analysis of long-term evolution because pressure readings are partly documented already since 1750 (e.g. Matulla et al., 2011). This proxy allows for the analysis of wind statistics by the derivation of the geostrophical wind. The WASA-project (Carretero et al., 1998) investigated the storm and wave climate for the North-Atlantic based on observations of air-pressure, air-pressure tendencies and variabilities of sea-level. Sea-level is another example of the usage of proxies in regard to wind analysis. Dahm et al. (2005); Ekman (2007) used sea-level data to draw conclusions on storm frequencies for the North-Atlantic and the Baltic Sea, respectively. Furthermore, there are studies using documented damages as wind proxies. For example De Kraker (1999) used dike breaches in the northern part of Flanders to analyse storm surge frequencies. Additionally there are studies revealing wind proxies in sedimentary archives, such as coastal dunes in Denmark (Clemmensen et al., 2014) or the Swina barrier in Poland (Reimann et al., 2011).
This study uses different data bases, including reanalysis, model and proxy data:

1.3.1 Reanalysis data

Some wind analysis rely on reanalysis data (e.g. Della-Marta et al., 2009; Paciorek et al., 2002). The reanalysis method assimilates different observations (e.g. from stations and satellites) into a weather prediction model which is used to produce a homogeneous, gridded data set about past climate parameters. One advantage of these data sets relates to their temporal and spatial homogeneity in comparison with direct station time series, since the model used to produce the meteorological reanalysis is frozen-in and not improved over time as it happens in the usual weather forecast. Inhomogeneities may, however, arise, if

the volume or nature of observational data set that is assimilated is changing over time (Krueger et al., 2013).

1.3.2 Model data

Free-running climate model simulations, without data assimilation, also allow to derive information on time periods without observations. Moreover, they allow for estimations about possible climate changes due to increasing greenhouse gas emissions into the atmosphere (Zorita, 2012). However, one needs to keep in mind that one model simulation is always only one possible trajectory of the state of the Earth under a given external climate forcing and other trajectories, also physically consistent, may have been possible. Nevertheless, simulations still allow to derive conclusions about climate statistics on time periods when no observations are available. Many studies rely on climate model data with different temporal and spatial resolutions (e.g. Fischer-Bruns et al., 2005; Gómez-Navarro et al., 2013; Knippertz et al., 2000).

Wind in the Baltic region may depend on changes in the external forcing factors but also are closely related to large-scale climate variability modes like the NAO. To make predictions about future wind changes its response to external forcings and its connection to internal climate variability need to be understood. The response of wind to external forcing can be assessed by analysing climate simulations over the past centuries, which have been subject to a variety of external forcings like volcanic eruptions or solar irradiance. This response may be caused by the direct thermal effect to radiative forcing or mediated by the response of large-scale climate modes (e.g. NAO) to the external forcing. For instance, it has been shown that the NAO may respond to volcanic forcing (Scaife et al., 2013; Zanchettin et al., 2012) and thus it is plausible to assume that volcanic forcing may also influence the wind in the Baltic region.

The relative influence of external forcing and internal variability on the total variability may be different for different variables. For temperature, the influence of external forcing is relatively clear. The evolution of the temperature of the past millennium has been reconstructed from proxies and showed a generally warm period in the early centuries (the Medieval Warm Period; 1000–1300 AD) and generally colder centuries around 1700 (the Little Ice Age), with the subsequent warming leading to the current recent warm period. This alternation of warm and cold periods is believed to have been caused by external climate forcing, for other variables like precipitation or wind the internal variability might have been more dominant (Gómez-Navarro et al., 2012). Thus, the last millennium provides a suitable period to test whether the variability of winds may follow an alternation in time similar to temperature or if wind changes are more strongly dominated by internal climate variations.

When analysing climate model data, one model limitation is the uncertainty in the realism of the model. In the case of wind, this realism is strongly determined by the limited

spatial resolution of current climate models, which precludes a direct simulation of smaller scale eddies and turbulence. These processes need to be represented indirectly by the so called parametrisation. Parametrisations are ad-hoc representations of small-scale fluxes, e.g. of momentum, as a function of the large-scale flow. Although parametrisations are intended to represent as realistically as possible small scale dynamics, they are only an approximation and depend on the climate model used, as different modelling groups apply different strategies. Therefore, parametrisations may be an inadequate representation of physical processes and the model resolution may be unfavourable (Gómez-Navarro et al., 2013).

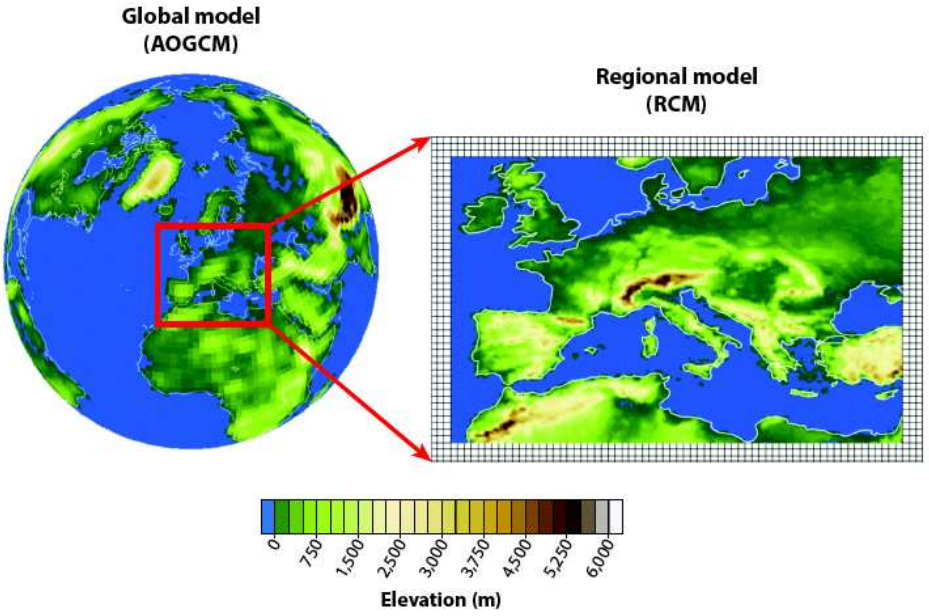

FIGURE 1.1: The figure shows the refinement in topography and coastlines that can be obtained from the use of an RCM. (AOGCM – atmosphere-ocean general circulation model; RCM – regional climate model) Figure is taken from Giorgi and Gutowski Jr. (2015).

The spatial resolution is especially important for extremes. Global climate models are not totally adequate to represent realistically extreme events, even more so in regions with complex coastlines (Hall, 2014). Recent global climate models have a spatial resolution between one to three geographical degrees. For the Baltic Sea region this means a representation by about 20 grid cells, with a width of 200–400 km each (Zorita, 2012). Regional climate models, driven at their boundaries by the fields simulated by global climate models, can provide a better representation (10-50 km) of small scale processes and of the land-sea contrasts, and thus are more suitable for the simulation of extreme events. The difference between global circulation model and regional model resolution can be seen in Figure 1.1.

These limitations imply that single simulations demonstrate only one realisation of numerous possible past climate evolutions. Hence, perfect agreements between different model simulations and/or reconstructions are unlikely.

1.3.3 Proxy data

Proxy-based reconstructions enable investigations of climatic conditions for regions and time periods without reliable observational data sets. They potentially allow for the validation of model simulations. One commonly known example are tree rings, because tree growth rates are often sensitive to the mean temperature during the growing season, and hence they can provide estimations of annually resolved temperature, once the relationship between tree-ring width and temperature is established. This process is known as proxy calibration and usually is conducted with a statistical model that represents the physical link between the proxy and the environmental conditions. The statistical calibration is performed with observations and it is extrapolated to the longer proxy time series to reconstruct past climate conditions. The processes of calibration may be cumbersome, because a number of different options may be possible. First, the choice of driving environmental variable, (e.g. temperature or precipitation) and its seasonality must be investigated. Then, the form of the statistical model, for instance linear or non-linear, has to be explored. Finally, the statistical uncertainty of the reconstruction has also to be estimated based on the good-of-fit of the statistical model to the observations.
Whereas, there is a growing body of temperature and precipitation proxies that cover the past centuries, there is a dearth of proxies that may represent past wind conditions. Therefore, the analysis of any wind proxy is interesting. There are already some wind proxies which have been mentioned above, however, because one part of this study deals with a sedimentary archive as a possible wind proxy the basic concept using dunes as a proxy archive for climate, i.e. wind climate reconstructions will be outlined in the following:
Wind has a close relationship with sedimentary processes forming and shaping dunes. Therefore dunes are a potential archive of past wind variations. A number of studies already used aeolian dunes as wind archives to draw conclusions on e.g. changes in storminess (Clemmensen et al., 2014; Costas, 2013; Reimann et al., 2011). There are studies dealing with changes in dominant wind directions (Costas et al., 2012b; Lancaster et al., 2002) and studies analysing changes of wind speed intensities or storm numbers (Costas et al., 2012a; Lancaster et al., 2002; Yao et al., 2007). A shortcoming of the according studies relates to the low temporal resolution on millennial changes, although some studies address decadal changes. However, higher temporal resolution e.g. annually would be a noticeable contribution for the scientific community.

1.4 Thesis objective

The objective of this thesis originates from a collaboration of geoscientists and climate researchers within the Helmholtz Climate Initiative REKLIM (Regional Climate Change), a joint research project of the Helmholtz Association of German Research Centres (HGF). The REKLIM project covers a variety of topics of natural and social sciences. This thesis belongs to the REKLIM topic 8: "Abrupt climate change derived from proxy data", which aims at the investigation of spatial and temporal patterns of climate variability in different regions. The focus lies on time scales from years to millennia and on the analysis of the rapid climate change during previous thermal changes (e.g. Little Ice Age, Medieval Warm Period) (www.reklim.de). In the framework of Topic 8 this thesis is part of the research project "Climate Signals in Coastal Deposits" (CLISCODE) which has the general aim of identifying a new wind proxy in migrating coastal dunes at the polish Baltic Sea coast. Therefore, the variability of the wind on time scales from decades to the last millennium over the Baltic Sea region and Northern Europe will be investigated here. In particular, temporal changes of predominant wind directions will be analysed. The relationship between large-scale climatic patterns and the wind climate shall be evaluated. This may help identifying large-scale processes that are related to the changing storminess at Baltic coastal areas. Therefore, reanalysis and model data are investigated. Finally, these results are used to validate a new wind-proxy derived from coastal deposits.

The thesis consists of two main parts. The first part deals with the variability of mean and extreme wind speeds and directions on different time scales from the last decades to the last millennium. Furthermore, wind variability is investigated regarding its relation to large-scale atmospheric drivers such as the regional mean temperature, the meridional temperature gradient and air pressure patterns. The focus of this thesis lies on the Baltic Sea, but as this region is also strongly influenced by climate conditions on a larger scale, the analysis, in parts, also covers Northern Europe. In the second part of the thesis, the wind variability is used to verify a new wind proxy, identified in cooperation with geologists of the University of Hamburg, which is recorded in migrating coastal dunes at the polish coastline. I try to answer the following research question within these two parts:

Part 1: Analyses of the variability of wind on different time scales regarding mean and extreme wind events.

- Are mean wind statistics a useful tool to draw conclusions on extreme wind statistics over the Baltic Sea?
- What pressure patterns drive extreme westerly winds over the Baltic Sea?

- What large-scale atmospheric parameters drive changes in the wind speed distribution over Northern Europe?

Part 2: A statistical analysis validating a new wind proxy in migrating coastal dunes.

- Can internal dune structures at the southern Baltic be applied to reconstruct the seasonal wind climate?

1.5 Thesis outline

The thesis is framed with this introductory chapter and a chapter including a summary, conclusions and an outlook. The main part of this thesis is divided in four Chapters. Chapter 2, 3 and 4 aim at answering the research questions of part 1 and Chapter 5 is directed at the research question of part 2, as presented in the previous section. Each Chapter has already been prepared for peer review journals and can therefore be read largely independently from the others, because each Chapter contains its own introduction, description of data sets and methods, discussion and conclusions. Therefore, some repetitions of the contents will unavoidable occur for the sake of clarity. In the following a brief overview about the context of these main Chapters is given:

Chapter 2
One open question in the scientific community is whether and how mean and extreme winds are connected. This Chapter addresses this question with the aim of identifying the relationship between the variations of seasonal mean winds and seasonal extreme winds for the Baltic Sea area. Thereby two observation-based reconstructions are analysed, namely coastDat2 and HiResAFF, which span the periods 1948-2009 and 1850-2009, respectively. The variability of mean and extreme wind events are compared in three different aspects: the wind speed distributions, the regional differences and the seasonal patterns and their persistence. Additionally to these three main investigations, the seasonal co-variability of mean and extreme wind events are compared and the connection to the NAO is analysed. The results of this study showed that the variations of mean and extreme wind variations are rather uncoupled and that changes in the mean winds are not directly related to changes in extreme winds in the Baltic Sea region.

Chapter 3
This Chapter analyses changes of wind extremes from west (W) and south-west (SW) in the Baltic Sea region during winter (DJF) based on a regional climate reconstruction (HiResAFF) over the period from 1850 to 2009. Extreme winds occur mostly and are strongest in the winter season. Although on average all wind directions are quite frequent over the Baltic Sea, extremes are very focused on W and SW directions.

In this Chapter extreme winds are defined as the exceedance of the 95$^{\text{th}}$ percentile of wind speed. Trends in the frequencies of extremes from W/SW can be detected, namely a positive trend from 1960 to 1990 and a negative trend since then. A correlation between the sum of W (SW) frequencies and corresponding intensities shows significant values. This means that years with more (less) W/SW winds show higher (lower) wind velocities. For the other directions, there is no such high correlation. After identifying eight circulation types, 4 patterns show relations to frequencies of W/SW winds above the 95$^{\text{th}}$ percentile. Three of these patterns show clear similarities in the temporal evolution compared to extreme W/SW wind frequencies.

Chapter 4

This Chapter aims at the variability of the probability distribution of daily wind speed in wintertime over Northern Europe in a series of global and regional climate simulations covering the last centuries, and in reanalysis products covering approximately the last 60 years. The focus of the study lies on identifying the link between the variations in the wind speed distribution to the regional near-surface temperature, to the meridional temperature gradient and to the North Atlantic Oscillation. The changes of the wind speed distribution is analysed with the help of the standard deviation and the 50$^{\text{th}}$, 95$^{\text{th}}$ and 99$^{\text{th}}$ percentiles.

The main result is that the link between the daily wind distribution and the regional climate drivers is strongly model dependent. It is concluded that no clear systematic relationship between the mean temperature, the temperature gradient and/or the North Atlantic Oscillation, with the daily wind speed statistics can be inferred from these simulations for Northern Europe.

In addition, for two global simulations a long-term tendency of the probability distribution of daily wind speed to widen can be connected to the land-use-change forcing used in these simulations.

Chapter 5

This Chapter validates a new wind proxy introduced with the collaboration of geologists, which is based on the relationship between a migrating coastal dune system and its driving wind conditions. The dune system is located at the Baltic Sea coast of Poland and is migrating from west to east along the coast. The analysed dunes show a layered structure, in some sense comparable to tree rings, and these layers could be used to determine the migration velocity per year. This migration velocity was used to investigate the influence of atmospheric parameters like precipitation, temperature and wind on the dune movement. The main driving factor is found to be the wind. Its relationship to the dune layer thicknesses allowed for statistical methods to identify a linear regression model linking layer thickness and wind speed. To validate this proxy a regional reanalysis data set is used. The linear model is based on the correlation between the frequency of winds from W and SW wind directions that surpass a predefined speed threshold and the dune migration velocity. A cross-validation with the leave-one-out-method reveals reliable correlations

between predictor and predictand similar to the values commonly excepted for the tree ring-temperature relationship. Thus, this Chapter verifies that this type of dunes can be validated as a wind proxy.

2 Variability of wind direction statistics of mean and extreme wind events over the Baltic Sea region.[1]

It is not clear to what extent the variations of seasonal mean winds and of seasonal extreme winds are related. This chapter investigates this relationship for the Baltic Sea area by analysing two regional climate gridded data sets, coastDat2 and HiResAFF, for the period 1948-2009 and 1850-2009, respectively. Both data sets are based on regional climate simulations incorporating information from observations with the aim of reproducing the observed trajectory of climate variables. Although the main aim of this study is the comparison of changes in wind direction statistics of mean and extreme winds the study also assesses the general comparability of the wind variable of both data sets.
The main part of the study compares mean and extreme wind events, with a focus on wind direction, in three aspects: direction distribution, regional differences and seasonal variability. The analysis reveals differences between mean and extreme winds in all three aspects. Hence, the overall conclusion is that the hypothesis that the statistics of mean wind can serve as a proxy for statistics of extreme wind is rejected, at least considering the Baltic Sea region.

2.1 Introduction

The inter-annual variability of winds, in terms of magnitude and direction, has been analysed much less than the variability of seasonal mean winds. In this study, the inter-annual variability of extreme daily winds in the Baltic Sea region and its relationship to the variability of seasonal means is investigated. Specifically, the hypothesis that the variability of directions and speed of daily wind extremes is similar to the variability of seasonal means is analysed. I address this problem by comparing mean and extreme wind statistics for (a) the distribution of wind intensity and direction, (b) regional differences in these distributions and (c) the temporal evolution of seasonal variability.
Changes in wind directions of mean and extreme wind statistics can be of importance for the possible economic and societal impacts of weather conditions (e.g. Jaagus and Kull, 2011). For European winter, a rule of thumb has been suggested according to which westerly winds bring warm and moist air from the Atlantic and easterly winds bring cool and

[1] Bierstedt, S.E., Hünicke, B. and Zorita, E. (2015): Variability of wind direction statistics of mean and extreme winds over the Baltic Sea region. Tellus A, accepted for publication.

dry air from the Asian continent (e.g. Jaagus and Kull, 2011). For other seasons this rule is not as clear, but atmospheric parameters are known to be strongly connected during the whole year, thus long-term changes in wind directions can cause major changes in the regional climate system, for example in precipitation patterns and cloudiness (Rutgersson et al., 2015). Rutgersson et al. (2015) emphasise the need for understanding and specifying potential long-term changes and variability of atmospheric parameters, e.g. wind, due to their potential impacts on hydrological, oceanographic and biogeochemical processes in the Baltic Sea region. A comprehensive understanding of changes in the wind climate is also necessary for the geomorphological analysis of Baltic Sea coastal stability and aeolian erosion processes (Clemmensen et al., 2014).

Changes in wind climate can also have strong impacts on coastal environments, either through high wind speeds of limited life span or sustained periods of above average mean winds. Extreme weather and climate events, such as storms (and accompanied extreme winds speeds), can lead to socio-economic and natural disasters. During storm events, extreme wind speeds occur often in combination with heavy precipitation. Storm events are linked to wind and pressure anomalies causing coastal flooding and severe wave action due to extreme sea level heights driven by storm surges and higher wind waves over sea, affecting the coastal erosion processes, especially at sandy coastlines. At the Baltic Sea coast, however, sandy coastlines and connected dune environments can be directly affected by changes in wind climate due to sand transport changes (Reimann et al., 2011). For these coastal dune environments, sand transport is found to be more strongly determined by long-lasting winds with above average wind speeds than by short lived extreme winds. Therefore, information about the variability of wind statistics are of increasing importance for risk management. Historical wind climate information, for instance, is needed for decisions concerning offshore wind logistics for the installation of offshore wind farms (Weisse et al., 2015).

Addressing these needs, previous studies of wind statistics over North-European regions have focused on changes in mean winds (e.g. Kent et al., 2013; Siegismund and Schrum, 2001) and/or extreme wind statistics (e.g. Nilsson, 2008; Raible et al., 2007), but only few have addressed the variability of wind direction (e.g. Keevallik, 2011; Jaagus and Kull, 2011).

The Baltic Sea region, situated in the north-eastern part of Europe, is one of the most investigated seas in the world (Reckermann et al., 2011), however, to date, little is known about long-term changes in wind direction statistics, the impact on the wave climate, and the consequences for coastal stability (Seneviratne et al., 2012). Recent studies on the Baltic Sea wave climate show different trends in average and extreme wave conditions for different regions and it is assumed that these changes are induced by systematic changes in wind directions (Rutgersson et al., 2014). The Baltic Sea Region is characterised by extremely variable weather conditions due to its position in the extra-tropics, lying between arctic and subtropic air masses. It is strongly influenced by the atmospheric circulation in the North Atlantic European sector, which is steered by two pressure systems, namely the

Icelandic Low and the Azores High, which define the North Atlantic Oscillation (NAO) (Hurrell, 1995). Due to the meridional pressure gradient between these two systems, westerly winds generally prevail over the Baltic Sea area. However, other wind directions are frequently registered (Rutgersson et al., 2014).

Existing studies for the Baltic Sea region regarding variability of wind directions are limited to the focus on changes in frequencies of wind directions, specifically for Estonia (Kull, 2005; Keevallik, 2008; Jaagus, 2009; Jaagus and Kull, 2011). For example, Jaagus and Kull (2011) investigated data from 14 Estonian stations covering the period from 1966 to 2008 and found an increasing trend in winds from south-west (SW) during winter. Comparable results for the whole Baltic Sea from 1958 to 2009 were described by Lehmann et al. (2011). Their study concluded that during winter (DJF) the frequency of westerly wind events increased, while at the same time easterly wind events decreased.

Different data sets, covering different periods, have been used to assess past wind and storm activity. Time series of wind observations can be inhomogeneous, due to, for example, station relocations (e.g. Krueger and von Storch, 2011) and/or changes of surface roughness because of land use changes (e.g. McVicar et al., 2012). Therefore, many studies have resorted to mean sea level pressure measurements to derive geostrophic wind speed, which can be then used as a proxy for surface wind speed (e.g. Alexandersson et al., 2000; Krueger and von Storch, 2011).

An alternative to station data are reanalysis data sets and reconstructions. In areas with a dense observational network, as in Europe, this kind of data set has a large advantage due to its temporal and spatial homogeneity (Weisse and von Storch, 2009). However, most reanalysis data sets cover only the last six decades and are too short to allow for a conclusive discrimination between any long-term trend and interdecadal variability (Bärring and Fortuniak, 2009). The longest reanalysis that exist (e.g. 20CR Compo et al., 2011) are affected by changes in the observations such as station density or measurement techniques especially before 1948 (Krueger et al., 2013).

In this study two gridded data sets are used, both based on the output of regional climate models that also incorporate information from observational data: (1) the regional reanalysis coastDat2 (Geyer, 2014), which covers the period from 1948 to the present and is based on a dynamical modelling approach and (2) the regional reconstruction HiResAFF (Schenk and Zorita, 2012), which spans the period from 1850 to 2009 and is based on a hybrid statistical-dynamical approach. Although, the coastDat2 data set begins only in the mid 20^{th} century, I decided to include this product in the study because in 2014 it was the longest regional reanalysis with such a high spatial ($0.22°$) and temporal (hourly) resolution Geyer (2014). Weisse et al. (2009), for example, emphasised that coastDat1 is well suited for the analysis of regional changes, especially in data sparse regions such as coasts or offshore, due to its higher resolution. Moreover, (Weisse et al., 2014) found that the validation of wind speed for coastDat1 and coastDat2 showed comparable qualities. The second data set, HiResAFF, combines the advantages of a high spatial resolution and a temporal coverage longer than the last 16 decades, but as it was recently introduced, it

has yet to be thoroughly analysed. Rutgersson et al. (2014) found that the variations of wind speed in HiResAFF shows comparable results to a geostrophic wind analysis. Due to the lack of validation studies for HiResAFF a comparison of coastDat2 reanalysis with the long-term HiResAFF reconstruction is included.
This paper has the following structure: Chapter 2 presents the data sets used in this study, introduces the frame of the investigation area and applied subdivisions, and describes the applied statistical methods. Chapter 3 presents a comparison of both data sets in terms of changes in wind direction and speed for mean and extreme wind events. Chapter 4 includes the main results of this study. Chapter 5 presents a discussion and conclusions.

2.2 Data

For this study daily mean wind data at a height of 10 m (hereafter surface wind data) over the past decades is analysed. Wind information from two recent data sets are used. Both are based on a combination of observational and model simulation data, but differ in their approaches to combining the two sources of information. Whereas one (coastDat2) is the result of a dynamical model approach, the other (HiResAFF) is a result of a hybrid statistical-dynamical approach. Due to this difference, the latter data set spans a much longer time period (around 150 years) and therefore allow an extended analysis of long-term trends and variability in wind direction changes from decadal to centennial time scales.

2.2.1 coastDat2 1948-2009

For the main investigation, wind data from the regional reanalysis data set coastDat2 (Geyer, 2014) is used. This data set originates from a regional climate simulation with the non-hydrostatic operational weather prediction model COSMO in CLimate Mode (COSMO-CLM, Rockel and Hense, 2008) driven by meteorological initial and boundary conditions from NCEP/NCAR Reanalysis 1 data (1948-present; T62 (1.875° $\approx$ 210 km), comprised of 28 levels, Kalnay et al., 1996; Kistler et al., 2001). The simulation was conducted, including spectral nudging (after von Storch et al., 2000), on a regular grid in rotated coordinates with a rotated pole at 170.0°W 35.0°N. It has a spatial resolution of 0.22° and the output is available on an hourly temporal resolution. I use daily mean wind data because of the comparability with HiResAFF, which is only available on a daily time scale.
The data set coastDat2 is the successor of coastDat1 (Weisse et al., 2009), which was originally conducted for a study of the statistics of extreme events and their long-term changes, and has been more thoroughly analysed. coastDat1 was based on a different regional model (REMO, Jacob and Podzun, 1997). The quality of wind fields in coastDat1

is found to be comparable to coastDat2. However, coastDat2 provides a better representation of high wind speeds (Geyer, 2014). Moreover, coastDat2 is driven by NCEP, which is an often analysed and commonly accepted data set. In the period and region covered by coastDat2 the changes in the quality and coverage of the observational data have been relatively small.

2.2.2 HiResAFF 1850-2009

In order to investigate the longer-term variability, HiResAFF, presented by Schenk and Zorita (2012), is used. Schenk and Zorita (2012) introduced the High RESolution Atmospheric Forcing Fields (HiResAFF) data set. This data set is based on a two-pronged approach that combines historical station data of daily mean Sea Level Pressure (SLP) and monthly mean 2 meter Temperature (T2m), available from the year 1850, and a shorter high-resolution regional climate simulation with the atmosphere-ocean coupled model RCAO (Rossby Centre regional Atmosphere Ocean model) over the period 1958-2007 (Doescher et al., 2002). This model data set has a horizontal resolution of $0.25° * 0.25°$ (≈ 25 km).
The HiResAFF daily atmospheric forcing fields for Northern Europe covers the period from 1850 to 2009 and is the result of a reconstruction by the application of the Analog-Method (AM, Lorenz, 1969; Kruizinga and Murphy, 1983; van den Dool, 1994). This method is a non-linear up-scaling method in which the historical observations (predictor) at day d_{obs} are compared to the corresponding data (predictand) simulated by the climate model RCAO for each day throughout the simulation period. The simulated day in which the modelled field displays the closest similarity with the station data at day d_{obs} is identified as the analog day, and all fields simulated in this analog day are taken as the reconstructed fields for day d_{obs}. Thus the AM can be essentially seen as a resampling of the model days in a way that has a better fit to the sequence of past observed station data.
As the AM does not assume any specific shape for the probability distribution of the variables, it can reconstruct non-normally as well as normally distributed variables. Hence, the AM reconstruction can, in principle, capture the extremes (magnitudes, frequencies), the probability distributions of the variables and the variability reasonably well on the daily scale (Schenk and Zorita, 2012). Schenk and Zorita (2012) also tested the sensitivity of the AM to the size of the analog-pool and found good agreements for all tested pool-sizes. They also investigated the influence of a reduced number of station data and reported a high level of confidence in a realistic reconstruction of wind.

2.2.3 Study area and definitions

The investigation area covers the Baltic Sea region in the geographical window $10° - 25°E$ and $51° - 61°N$. To investigate differences in Baltic Sea subregions wind roses at 9 points

(subjectively chosen to cover the whole region) scattered across the investigation area (Fig. 2.1) are analysed. The results of these 9 wind roses (not shown) could be regionally grouped into four groups, each one representative of a subregion. This result supports the decision to subdivide the area into four smaller regions. The subdivisions represent the south-western (SWR, 10°-18° E; 51°-56° N), south-eastern (SER, 17°-26° E; 51°-56° N), north-western (NWR, 10°-19° E; 56°-61° N) and north-eastern (NER, 17°-28° E; 56°-61° N) Baltic region (see Fig. 2.1).

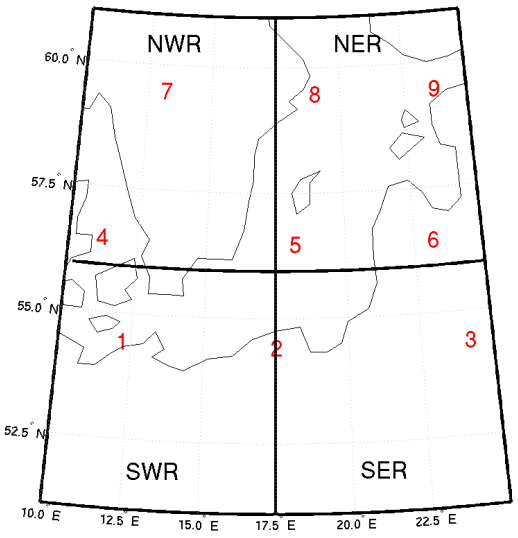

FIGURE 2.1: Area of study showing nine points which were used to illustrate the geographical subdivisions. The black lines demonstrate the area subdivisions (SWR, SER, NWR, NWR) used in section 2.4.2

The study is based on a seasonal analysis with seasons defined as: Winter (December, January, February - DJF), Spring (March, April, May - MAM), Summer (June, July, August - JJA) and Autumn (September, October, November - SON). Autumn and winter are typically the seasons with the highest wind speeds over the Baltic Sea (also found in this study).

Two definitions for mean wind are used. Definition (1) considers the three events per season which are closest to the 50^{th} percentile of wind speed (hereafter named: "median wind events"). Note that this definition is not the statistical "median", because the three events closest to the 50^{th} percentile of wind speed are used. This measure is used to ensure comparability with the definition of extreme events, which also includes not more than three events per season. Definition (2) considers the average of available daily data in the time period of interest (hereafter named: "average wind events"). This definition is only used for the Empirical Orthogonal Function (EOF) analysis in section 2.4.3. A different "mean" for the EOF analysis is used to increase the sample size and ensure robustness of

the EOF patterns, which would be smaller with only three events per season. Nevertheless, the analysis was also conducted with the "median wind events" definition and obtained similar patterns, but without any significant trends.
The extreme winds are defined by choosing a percentile threshold. In section 2.4.1 the three strongest events per season are defined as "extreme wind events". For the monthly analysis of wind direction frequencies in section 2.4.2, the threshold to define the extremes was the 90^{th} percentile. Applying a higher percentile would reduce the number of extreme events per month compromising the robustness of this statistic. Hence, every month includes approximately 3 extreme events. For the EOF analysis in section 2.4.3 the 98^{th} percentile is used.

2.2.4 Statistical methods

One statistical method applied in this study is the principal component analysis, also known as the Empirical Orthogonal Function (EOF). This analysis derives the dominant patterns of variability (von Storch and Zwiers, 1999). Note that the EOF analysis is applied to anomalies, i.e. deviations from the long-term mean.
Rogers' (1990) analysis of European sea level pressure with the EOF-method enables the determination of four main pressure patterns. He used this method to capture most of the variability of the daily pressure fields with just a few patterns.
In section 2.4.3 this method was used to identify and compare seasonal wind field patterns for mean and extreme wind events. In case of the mean wind events, monthly anomalies of the zonal (u) and of the meridional (v) wind component are determined based on the available daily data. The gridded fields of the wind components u and v are concatenated into one field, resulting in twice the dimension of the original fields. The EOF analysis is applied to this augmented field.
In case of the extreme events, the seasonal 98^{th} percentile of wind speed is calculated for the field mean of the Baltic Sea region. The u and v components on days above these percentile values are averaged, as the EOF analysis is applied to anomalies. These averages are used to determine the anomalies of u and v by subtracting them from the seasonal extremes, and hence the anomalies are not calculated by subtracting the long-term mean of the entire sample of winds.
The complex correlation coefficient is a method to determine the co-variability between two vector fields (von Storch and Zwiers, 1999). A 2-dimensional vector time series can be represented as a complex time series, where the real and imaginary components are given by the first and second dimension of the vector $m = u + iv$. Given two 2-dimensional vector time series $\vec{m} = (u_m(t), v_m(t))$ and $\vec{e} = (u_e(t), v_e(t))$, the complex correlation r_c is defined as the complex Pearson correlation between the two complex time series:

$$r_c = \frac{\sum (m_t * e_t^*)}{\sqrt{\sum (m_t * m_t^*)}\sqrt{\sum (e_t * e_t^*)}} \tag{2.1}$$

Where the superscript * denotes the complex conjugate. The result r_c is again a complex number. The complex correlation coefficient can be characterised by its magnitude, which describes the strength of the linear relationship between the magnitude of the vectors, and by a phase angle, which describes the average direction difference between both vector time series. This phase angle is the advantage of the complex correlation compared to a normal correlation, allowing the determination of the directional relationship between two vectors. Kundu (1975) applied this method to investigate the Ekman veering in the Pacific Ocean at the coast of Oregon (USA). In this case, the complex correlation is calculated between the monthly mean winds $\vec{m}$ and the monthly extreme winds $\vec{e}$, and thus provides a measure of the coupling of the variations in magnitude and direction between mean winds and extreme winds.

2.3 Comparison of coastDat2 and HiResAFF

In the following, the wind characteristics in the two data sets are compared in their overlapping period from 1948 to 2009. Although the overall aim of this study is the comparison of changes in wind direction statistics, the comparison of both data sets will also be focused on statistics of wind speeds. This section provides a general assessment of the comparability of the wind variable of both data sets.
Mean wind events (50^{th} percentile of wind speed, section 2.2.3) and extreme wind events (98^{th} percentile of wind speed) per season were determined. As illustration, Fig. 2.2 shows the differences between mean wind speeds of coastDat2 and HiResAFF (negative values indicate higher values for HiResAFF) for the 50^{th} and 98^{th} percentile in winter, displaying larger differences for the 98^{th} percentile. These differences appear in all seasons, which leads to the conclusion that HiResAFF produces higher extreme wind speeds than coastDat2 during all seasons.
For winter, summer and autumn, HiResAFF systematically presents higher values with respect to coastDat2 for mean and for extreme winds. In spring, the mean winds in HiResAFF are weaker, but extreme winds are stronger than in coastDat2. All seasons show higher deviations of HiResAFF with respect to coastDat2 in extreme wind events. Fig. 2.3 shows this comparison for the winter season.

The standard deviations (STD) for the 98^{th} percentile are higher than for the 50^{th} percentile for all seasons and in both data sets. The coefficient of variation (STD/mean) of the two data sets coastDat2 and HiResAFF is almost the same ($\simeq 0.47$).
Subsequently, several tests were conducted to compare the data sets more quantitatively. These comparisons between both data sets are conducted to document the main differences

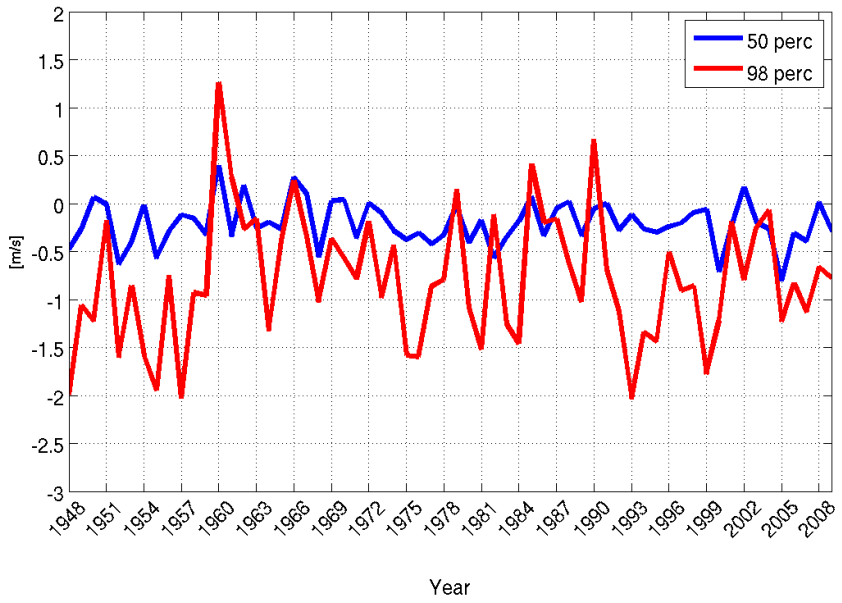

FIGURE 2.2: Difference of the 50th percentiles (blue) and 98th percentiles (red) of wind speed between coastDat2 and HiResAFF data sets during winter (DJF). The figure displays the mean over the area shown in Fig. 2.1.

found in this analysis of the wind and illustrate the uncertainty stemming from the use of different gridded products. The comparisons are not meant as a thorough critical analysis of the advantages or deficiencies of one data set over the other, which would require a comparison between the two underlying regional models, CCLM and RCAO that were used to produce these data. This is beyond the scope of the present study. For instance, the distribution of extremes probably deviates from a normal distribution and therefore a more sophisticated test than the F test would be required. Nevertheless, these tests can provide useful guidelines for further studies.

First, a student t-test, which tests the hypothesis that two samples have equal means, is conducted. This hypothesis of equal means could be rejected at the 95% level of significance for most parts of the area, both for the 50th as well as for the 98th percentile. Second, the ratio of variances is tested with a F-test. The hypothesis of equal variances can be rejected in about half of the area for the 50th percentile wind at the p=0.05 level and cannot be rejected in most areas for the 98th percentile. Third, a Kolmogorov-Smirnov test, which tests the hypothesis that two samples are drawn from the same continuous distribution is applied. This hypothesis of equal distributions is rejected at the p=0.05 level for all seasons. This test is repeated after subtracting the mean, and this reveals that, in this case, the Null-hypothesis of same continuous distributions cannot be rejected ($p \approx 0.3$). This indicates that both data sets preponderantly differ in their means but not in their distribution. However, differences between both data sets are not surprising, as

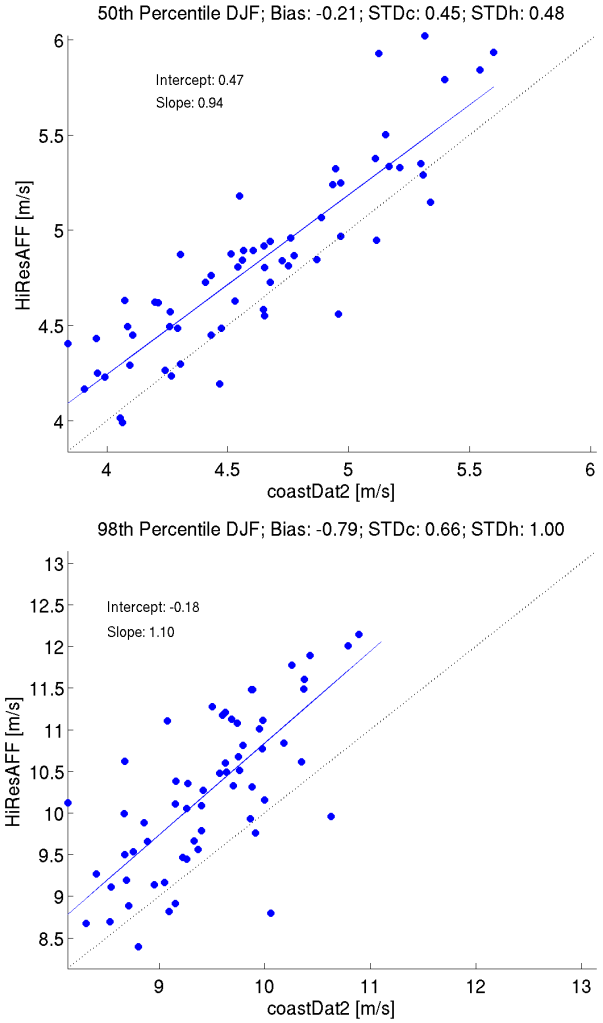

FIGURE 2.3: Scatter plot of the 50$^{\text{th}}$ (upper) and 98$^{\text{th}}$ (lower) percentile of wind speed of each winter for coastDat2 and HiResAFF for the period 1948–2009. The blue line represents the linear regression and the light grey line the one-to-one-correspondence line. The figure shows the mean over the area displayed in Fig. 2.1. (STD=Standard Deviation; c=coastDat2; h=HiResAFF)

both data sets are based on different dynamical models, each with their own systematic biases.

Both data sets incorporate information from observations and aim at replicating the observed time evolution of winds. Therefore, they can also be compared by the mutual (complex) time correlation (see section 2.2.4). The magnitude of the complex correlation coefficient of the area-averaged wind is, for all seasons, significant and higher than 0.7. This demonstrates that the variations in wind magnitude are coherent in both data sets. Furthermore, the phase angle of the complex correlation is always below 0.05°, meaning that the time variations in the wind directions are coherent in both data sets.

2.4 Comparison of mean and extreme wind statistics

2.4.1 Differences in directions

The distribution of wind intensity and wind direction is analysed by wind roses for each season in order to investigate differences between wind directions of median and extreme wind events (following the definitions in section 2.2.3). The results are summarised in Figure 2.4. The analysis here is based on coastDat2 wind data (1948-2009), with the main differences obtained in the analysis of HiResAFF presented later.

For median wind events, the main wind direction varies across the seasons: In wintertime (Fig. 2.4a), median winds are clearly dominated by SW wind. Spring (Fig. 2.4c) shows two main directions, namely E and NE with a secondary maximum for SW directions. In summer (Fig. 2.4e), the wind tends to blow from W, NW and SW. In autumn (Fig. 2.4g), the wind mostly blows from SW with a second maximum from SE.

The distribution of extreme wind directions (Fig. 2.4b, d, f, h) deviates from the distribution of median wind directions. All seasons are dominated by SW winds, and only in spring (Fig. 2.4d) is there a tendency of more frequent W winds and a weak secondary maximum from north-north-east (NNE). Thus, according to the analysis of seasonal wind roses, median wind directions seem to have a much more isotropic distribution than extreme wind directions. Extreme wind directions are focused mainly on SW and W directions during all seasons.

The analysis is repeated with the HiResAFF data set in the overlapping period (1948-2009). In the case of median winds, the results obtained with HiResAFF also display, as in coastDat2, a much more isotropic distribution of wind directions. The result confirms that the distribution of extreme wind directions is skewed to the south-western directions. The analysis of the longer period 1850-2009 in HiResAFF shows more isotropic median wind events, with bins forming almost a circle. These wind roses are smoother due to the higher number of events included in the analysis of 160 years (instead of 65 years). For extreme wind events, stronger westerly than south-westerly winds are found (not shown).

The co-variation is analysed between median and extreme wind directions by the complex correlation coefficient between both (calculated as described in section 2.2.4). The result shows no significant temporal correlation ($r \leq 0,25$) for all seasons, which points to a small co-variation between median and extreme wind directions. In conclusion, it does not seem possible to simply infer information of anomalous directions of extreme wind directions from the anomalous directions of median wind.

2.4.2 Regional differences

So far the distributions of median and extreme winds are compared as averages over the whole Baltic Sea region. In this section the possibility that these relationships may be

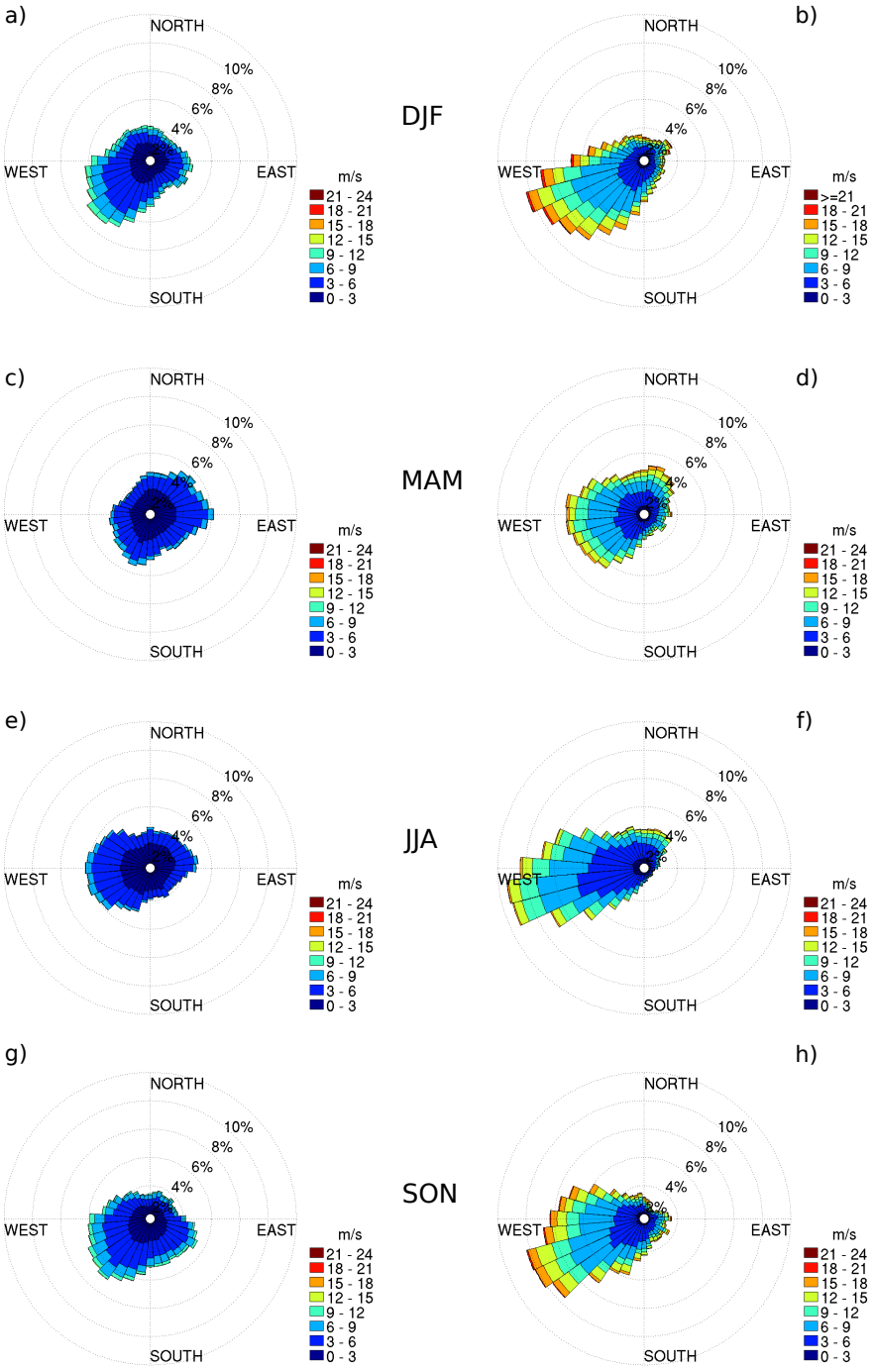

FIGURE 2.4: Wind roses of median (left: a, c, e, g) and extreme (right: b, d, f, h) wind in coastDat2 (1948-2009). The colours show the intensity (in m/s) and the bins show the direction from which the wind blows. Median events are defined as the three wind events per season which are closest to the 50^{th} percentile of wind speed. Extremes are determined as the three strongest wind events per season.

spatially heterogeneous is explored by investigating differences in Baltic Sea subregions. These subregions are hereafter indicated as south-western (SWR), south-eastern (SER), north-western (NWR) and north-eastern (NER) (see Section 2.2.3 for geographical information). Again, firstly the main results obtained with coastDat2 wind data (1948-2009) are shown. To reasonably separate the area into subregions wind roses (not shown) at 9 points scattered across the area (Fig. 2.1, see also 2.2.3) are compared.
Percentile calculations are separately applied to each month of coastDat2 (1948-2009) (see also section 2.2.3). As explained below, for median wind events (50^{th} percentile), differences among the subregions can rather be found between North and South than between East and West. For extreme wind events (three strongest days per season, see also section 2.2.3) there are no spatial differences in autumn and winter, where all 9 points are dominated by SW and W winds. Spring and summer again show mainly differences between North and South. This analysis thus supports the choice of subdividing the investigation area into North and South. However, I decided to subdivide the whole region into four equal subregions so as to capture possible minor differences between East and West (Fig. 2.1).
For median wind directions there is a notable absence of a seasonal cycle in all subregions. Figure 2.5 shows the annual cycle of the eight main wind directions for median wind events for the south-western region as illustration for the behaviour of all other regions.
Figure 2.6 shows the annual cycle of the eight main wind directions (N, NE, E, SE, S, SW, W, NW) for the extreme wind events, averaged over each of the four selected subregions (Fig. 2.1). In all four subregions, W and SW are the dominant wind directions for extreme wind events in all seasons, with SW winds being more frequent in winter and autumn and less frequent in spring and summer. SE and S wind frequencies have only little variations across all four regions. Beyond this, the regions display some specific characteristics. The southern regions (Fig. 2.6c,d) show high frequencies of W wind during spring and summer. The northern regions, in contrast, feature a different main direction in spring, with dominant N and NE winds (Fig. 2.6a,b).
The analysis for median and extreme winds is also conducted with the HiResAFF data set in the overlapping time period (1948-2009) to test the robustness of the results based on coastDat2 wind data. Median winds in HiResAFF show directions with almost the same frequency in all subregions (comparable to coastDat2 Fig. 2.5) and there is very little intra-annual variation. Extreme wind events in the eastern regions (NER, SER) also show a predominance of SW directions, whereas extreme winds in the western regions (NWR, SWR) show slightly lower (5-7 %) frequencies for SW winds compared to coastDat2. In these western regions, extreme winds from W show higher frequencies in the order of 10-15%. Nevertheless, for HiResAFF, extreme winds from W show highest frequencies in all regions. Thus, HiResAFF shows a stronger zonal component.

Summarising, the southern regions display higher frequencies of extreme winds for SW and W winds and lower frequencies for N, NE and NW than the northern regions, whereas

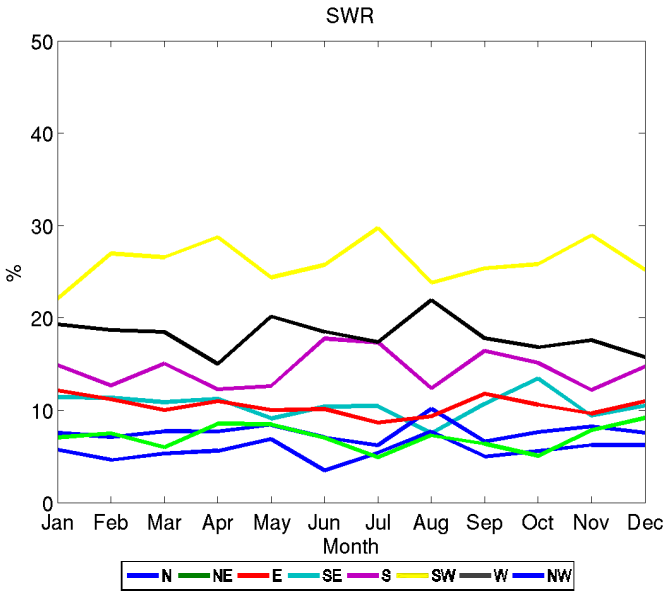

FIGURE 2.5: Annual cycle of the eight main wind directions of coastDat2 (1948-2009) for the south-western Baltic Sea region (SWR in Fig. 2.1). This figure only includes the three wind events per month with intensities closest to the 50th percentile of wind speed per month. Units are monthly mean frequency in %.

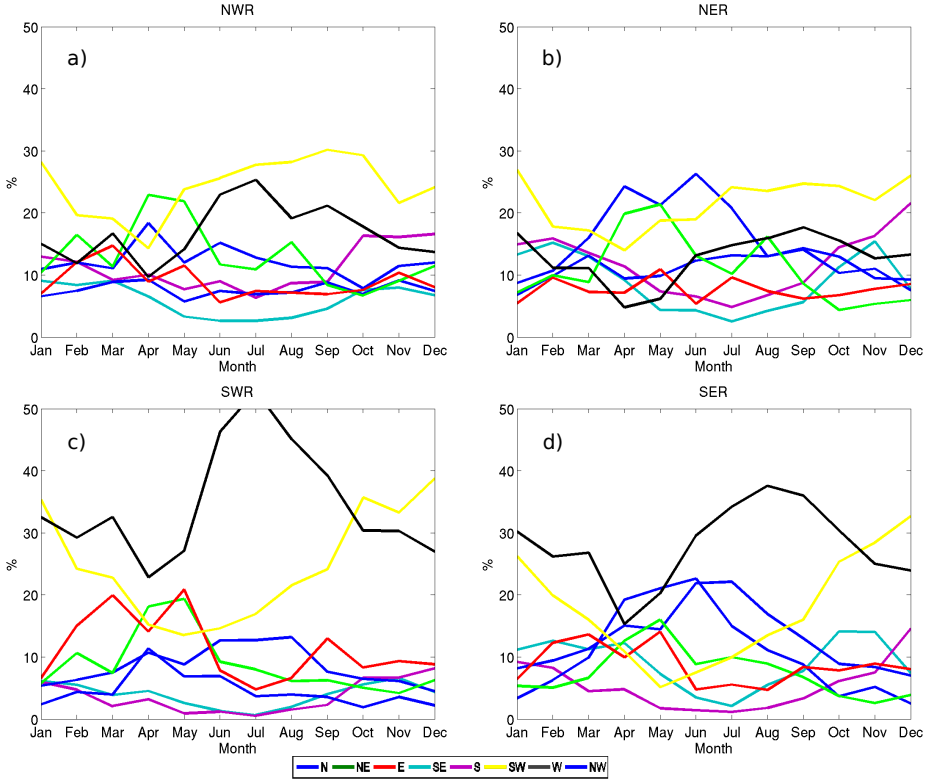

FIGURE 2.6: Annual cycle of the eight main wind directions for extreme events of coastDat2 (1948-2009) in a) north-western (NWR), b) north-eastern (NER), c) south-western (SWR) and d) south-eastern (SER) Baltic Sea (see Fig. 2.1). Extremes are defined by the 90th percentile of wind speed per month. Units are monthly mean frequency in %.

median winds generally display a more isotropic distribution than extreme winds in all subregions.

2.4.3 Seasonal patterns

As an example, Figure 2.7 displays the two leading EOF patterns together with their principal component (PC) time series for average and extreme wind events (see section 2.2.3 for definitions) for the winter season of HiResAFF (1850-2009). The corresponding explained variances are displayed in Table 2.1. In this section, the spatial co–variability of the wind directions is analysed by means of an EOF analysis. This analysis yields the main spatial patterns of anomalies that tend to evolve coherently in time. To conduct the EOF analysis, the zonal wind (u) and meridional wind (v) components are merged into one field with a doubled number of grid-cells. The patterns are based on anomalies of monthly mean wind speeds for the average wind statistics and on anomalies of the 98$^{\text{th}}$ percentile for extreme wind statistics (see section 2.2.4). The EOF analysis is applied to coastDat2 and HiResAFF in their overlapping period (1948-2009) and on longer time scales back to 1850 to HiResAFF.
For the period 1850 to 2009 the leading three EOF patterns for both average and extreme wind explain at least $\approx 82\%$ variance for all seasons. The explained variances per season and data set can be found in Table 2.1.

TABLE 2.1: Explained variance in % of the three leading EOF patterns for each season derived from HiResAFF (1850-2009 and 1948-2009) and coastDat2 (1948-2009). Results for monthly mean wind are shown as plain text and results for wind events exceeding the 98$^{\text{th}}$ percentile in **bold**.

HiResAFF 1850-2009	EOF 1	EOF 2	EOF 3	EOF 1+2+3
DJF	65 **41**	25 **31**	6 **11**	96 **82**
MAM	58 **38**	28 **32**	7 **12**	93 **82**
JJA	50 **48**	30 **29**	9 **8**	89 **86**
SON	54 **46**	33 **27**	7 **11**	95 **84**
HiResAFF 1948-2009				
DJF	64 **46**	25 **25**	6 **11**	96 **82**
MAM	59 **45**	29 **31**	6 **8**	93 **84**
JJA	50 **39**	29 **33**	10 **11**	89 **83**
SON	61 **43**	27 **28**	7 **11**	95 **82**
coastDat2 1948-2009				
DJF	63 **39**	22 **35**	8 **9**	93 **83**
MAM	56 **43**	24 **29**	8 **11**	88 **83**
JJA	56 **47**	18 **25**	13 **11**	87 **83**
SON	55 **39**	27 **36**	9 **14**	91 **89**

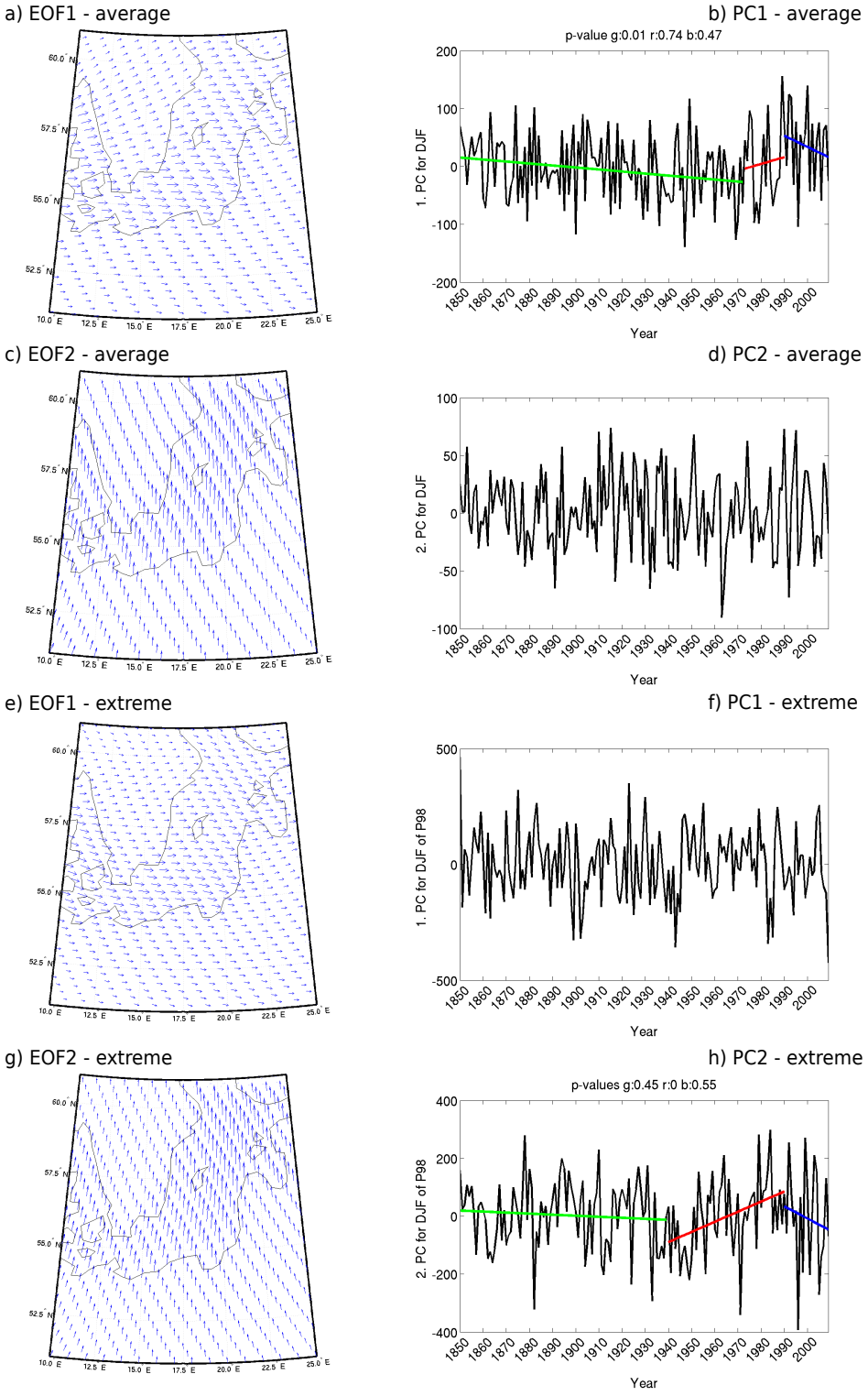

FIGURE 2.7: First leading EOF patterns together with their PC time series for average wind (upper four panels: a–d) and extreme wind (lower four panels: e–h) events of the HiResAFF data set (1850-2009). The left hand side panels show the pattern of variability of the combined u and v EOF analysis (see section 2.2.4). Arrows are not scaled for the sake of clarity. The right hand side panels show the corresponding principal component time series. The colored lines in b) and h) show trends on different time scales. The significance values (p-values) for the green (g), red (r) and blue (b) line are shown above the figures. Explained variances are indicated in Table 2.1.

EOF patterns:

In the following the resulting EOF patterns are described for each season and time period for HiResAFF (1850-2009), HiResAFF (1948-2009) and coastDat2 (1948-2009). For sake of clarity, this description is based on one polarity of the patterns, although it should be noted that the opposite polarity (the spatial pattern multiplied by -1) would represent the same EOF.

In winter (DJF), the first EOF derived from HiResAFF explains 65% of the average wind event variation over the period 1850 to 2009 (Table 2.1) and is defined by west (W) wind anomalies (Fig. 2.7a). Although the W wind pattern is similar for extreme events (Fig. 2.7e) the explained variance of 41% (Table 2.1) is lower.

The result for extreme wind patterns are generally confirmed by the analysis of HiResAFF for the period 1948 to 2009 (not shown) with a slightly higher explained variance of 46%. Mean wind events indicated a shift to more south-westerly winds in the period 1948-2009. This result is confirmed in the analysis of coastDat2 (1948 to 2009; not shown). This data set results in a similar direction of wind anomalies as HiResAFF in 1948-2009, both for average and extreme wind patterns. The use of coastDat2 exhibits a predominance of SW anomalies and slightly lower explained variances of 63% for average winds and 39% for extreme winds when compared to HiResAFF.

For spring (MAM; not shown), the EOF patterns of average winds in all data sets show predominantly SW anomalies, with an explained variance of approximately 56%. For extreme winds, the results differ between each data set: whereas the HiResAFF pattern exhibits a preponderance of westerly wind anomalies (W) for the period 1850-2009 and south-easterly anomalies (SE) for the period 1948-2009, the pattern resulting from the coastDat2 data results, as in the case of winter season, in south-west (SW) anomalies.

The summer season (JJA; not shown), for average and extreme winds, displays a SW pattern of wind anomalies for all data sets and all periods. Autumn (SON; not shown) reveals a similar pattern of anomalies of main wind directions as for winter: the HiResAFF pattern obtained in 1850-2009 mainly indicates W wind anomalies for averages and for extremes. For the time period 1948-2009, average and extreme wind anomaly patterns are characterised for both data sets (HiResAFF and coastDat2) by SW wind anomalies. Thus, autumn and winter display very similar patterns of wind direction variability, for both the average and extreme events. Note that this does not necessarily mean that the temporal evolution of their variability is correlated.

The second EOF of HiResAFF (1850-2009) displays a pattern of southerly wind anomalies for both average and extreme wind patterns, in all seasons (illustrated here for winter: Fig. 2.7c+g), with a slightly easterly component in summer. The dominant southerly direction of wind anomalies, for average and extreme winds, is also prominent in HiResAFF for the shorter period 1948-2009 (not shown). However, some seasons slightly deviate from this general rule: JJA average wind and SON extremes have an additional easterly component

and extremes for MAM an additional westerly component. CoastDat2 (not shown) average wind anomaly patterns show southerly winds and westerly extreme winds with a northern component for MAM and JJA and a southerly component for SON. For all data sets and periods, the explained variances of the second EOF for extreme events are higher than for average events (Table 2.1). The difference between the variance explained by the first and second EOF explained variances is much smaller for extremes than for the average winds. Hence the second pattern is, in relative terms, more important for extreme events than for average events.

The third EOF (not shown) is dominated by a cyclonic rotation over the Baltic area with a centre close to the Island of Gotland. The amount of explained variance lies between $\approx 6\%$ (MAM) and $\approx 12\%$ (JJA) for average and extreme events in all seasons. Because these values are quite low and the EOF patterns are physically not clear, it can be assumed that these patterns are dominated by noise.

Principal component time series (PC):
Another result of the EOF analysis is the principal component (PC) time series, which describes the variations of the amplitude of the spatial patterns through time. The PCs give information about long-term trends in the spatial patterns just described, and also about possible correlations in time of these patterns.
For average winds the HiResAFF data set (1850-2009) shows significant trends in winter, summer (not shown) and autumn (not shown) for the first PC. There is a significant negative trend in winter (negative for the polarity shown in Fig. 2.7b) and also a negative trend in summer from 1850-1973, followed by a non-significant increase until 1990. These trends are also visible in the period 1948-2009 (not shown) in HiResAFF and coastDat2, however, they are not statistically significant. In autumn, there is a significant increase from 1990 to 2009 for HiResAFF (1850-2009) and HiResAFF (1948-2009), coastDat2 shows a similar trend but without statistical significance.
It is important to note that no significant trends for extreme winds could be detected for the leading PC time series in any season or data set. For the second PC there is a significant positive trend in winter season from 1940 to 1990, which is only visible in HiResAFF (1850-2009)(Fig. 2.7h).

Additionally the seasonal correlation is calculated between the PC time series of average winds and the PC time series of extreme winds. This correlation shows low values for all seasons between r=-0,23 and r=0,18 for both data sets (coastDat2, HiResAFF) and both periods (1948-2009, 1850-2009). This suggests that changes of average winds can not be used to estimate changes of extreme winds. This is also shown in section 2.4.1 with the

help of the complex correlation between average and extreme winds.

The North Atlantic Oscillation is one of the leading patterns of seasonal climate variability in this region, especially in winter. It is thus expected that the link between the NAO and the variability of average wind speed is strong, but its link to the variability of extreme wind speeds has not been thoroughly investigated. The seasonal correlation between the leading PC and the NAO index shows comparable results for both time periods and data sets. Therefore, the following correlation coefficients are only shown for HiResAFF (1850-2009): Average wind events exhibit an expected high correlation for DJF of 0.64. However, for the other seasons the correlations have much lower values (MAM 0.28; JJA 0.17; SON 0.22), indicating that in seasons other than winter the NAO is not the main factor that modulates the average wind speed. For extreme wind events the correlations are low for all seasons (DJF -0.13; MAM -0.07; JJA 0.01; SON 0.04). This somewhat unexpected result indicates that the link between the variability of average wind speed and the variability of extreme winds is not strong.

The comparison of PCs and their corresponding EOF patterns leads to the following conclusions:
The first EOF of average wind describes the most important direction of wind variability. The analysis of the longer period 1850 to 2009 indicates that the main direction of variability of average winds is the zonal direction (W–E), whereas the analysis of the period from 1948 to 2009 (HiResAFF and coastDat2) reveals that the main direction of variability has turned in the recent decades with an additional meridional component (SW–NE).
The EOFs of extreme winds are derived from the anomalies relative to the average extremes, the patterns describing variations relative to the average of the high percentile winds. Thus it describes variations in time within the population of extreme winds. The analysis of the period from 1850 to 2009 indicates that the main direction of extreme wind variability is from W–E however, for the period from 1948 to 2009, the direction has turned to SW–NE. Therefore, concerning the long-term variation of wind directions, average and extreme winds have changed in a similar way over the last decades relative to their long-term mean.

This raises the issue of whether an anomalous direction of winds in a particular season contains information about the expected direction anomalies in the following seasons. The correlation between the seasonal PCs of average winds in adjacent seasons is found to be small. The correlation between the leading autumn PC with the leading winter PC in the same year shows only small values ($r \leq 0.3$) for all data sets and periods, suggesting that the intensity of the main pattern of wind direction variability does not tend to persist from one season to the next. This also happens for extreme wind events. Thus, it does

not seem possible to statistically predict (with linear methods) seasonal wind conditions from wind information from a previous season in the same year.

The comparison between EOFs derived from HiResAFF and coastDat2 explains a similar amount of variances, but the EOF patterns derived from HiResAFF tend to display a more zonal direction than in the other data sets (also seen for the wind rose analysis in chapter 2.4.1).

2.5 Discussion and conclusions

The study focused on the question of whether the variability of mean (median and average) and the variability of extreme wind statistics over the Baltic Sea region are comparable. An assumption could be made that changes in mean wind statistics could be used to approximate extreme wind changes. This study refuses this hypothesis, at least regarding wind direction over the Baltic region.
The study analysed two regional data sets in the time periods 1850-2009 (HiResAFF) and 1948-2009 (coastDat2) as well as their overlapping time period 1948-2009. Two data sets were utilized in this analysis (HiResAFF and coastDat2). As these two data sets had not previously undergone systematic analysis, the first task necessary was to compare the wind statistics in the common time period. Data collection of each data set differed and different models were used to produce the data sets. However, for the common period of time were both consistent concerning wind directions.
The second part of this study compared mean (median and average) and extreme wind statistics, with a focus on wind direction. The main conclusions are:
1. Median winds show a very isotropic distribution for all directions with a different maximum in each season. Extreme winds are much more constrained to SW directions for all seasons except spring where a second maximum can be found in NE direction.
2. A very weak co-variation of the anomalies of median and of extreme wind over the Baltic Sea region is found. Anomalous direction of median winds in one particular season and year are thus not indicative of extreme winds displaying the same anomalous direction.
3. A subdivision into four parts of the Baltic Sea region shows regional differences in the behaviour of median and extreme events. Median wind events have quite similar frequencies of direction in all four regions. These frequencies also stay relatively stable across all seasons. Extreme wind events show differences between northern and southern regions. The stormy seasons (DJF, SON) tend to be dominated in all four regions by SW winds. In spring and summer the northern regions are dominated by north-easterly winds and the southern regions by westerly winds.
4. The question of whether there is a persistent annual pattern of wind direction anomalies that persists through adjacent seasons is addressed. The temporal evolution of the patterns

of seasonal variability, derived from an EOF analysis of the seasonal anomalies, do not show significant correlations between adjacent seasons. Thus it is not possible, within a linear framework, to infer information about the anomalous winds in one season from the anomalous winds in the previous seasons.

Additionally, the long-term evolution of the leading PCs also displays a different behaviour for average and extreme winds. For the first PC (mainly zonal direction) I only found significant long-term changes over time for average wind events, but not for extreme winds, suggesting that whereas the zonal pattern of variability of average winds showed a trend, it showed no changes for extreme winds. Conversely, the second leading PC representing variability in the meridional direction did not change for average winds, but indicated a trend for extremes. The second pattern is more important in terms of explained variance for extreme events than for average events. An increasing trend for the first PCs of average wind is visible for shorter time scales (1948 to 2009) for both data sets. When analysing the longer time series (1850 to 2009) it becomes clear that this trend is not present over the whole period. The same effect was found, in numerous studies, for trends of wind speed. Over Europe, many studies found an increase in storm intensity, and therefore also higher wind speeds, between the 1960s and the mid 1990s (Gulev and Hasse, 1999; Gulev et al., 2001; McCabe et al., 2001; Paciorek et al., 2002; Wang et al., 2006). Whereas Bärring and Fortuniak (2009), on longer time scales, show that there is rather interdecadal variability than clearly defined long-term increasing or decreasing trends.

Moreover, it is found that the connection between the North Atlantic Oscillation (NAO) and the average winds differ from extreme events. The seasonal correlation between the first PC of extreme wind events and the NAO index is very weak. This is in contrast to the correlation between the NAO and the average winds in wintertime. It is known that the NAO has a large influence on the wind conditions over the Baltic Sea, especially during winter (Feser et al. 2014, Rutgersson et al. 2014), so this correlation is not surprising. However, in the other seasons there seem to be other atmospheric driving mechanisms for the variability of average wind speed. Extreme wind events do not show high correlations to the NAO in any season. It is concluded that the NAO is not the main driver for extreme winds.

The results provide insight on the issue of whether, and how, changes in mean wind statistics can be related to changes in extreme wind statistics (Seneviratne et al., 2012). The matter of the existence of long-term trends in extreme winds is also addressed (Donat et al. 2011; Krueger et al. 2013). In a review by Feser et al. (2014), it is stated that trends in storm activity crucially depend on the time scales considered. As storms produce extreme winds, this issue is also related to the present study. The results concerning wind direction support the statement that trends are dependent on the time span. The extreme events over the longer period in HiResAFF showed the highest frequencies for W winds, whereas for the shorter period covered by both HiResAFF and coastDat2 the distribution of wind direction showed a maximum of SW wind. This result is in agreement with previous studies based on different data sets and without regional subdivisions; for

example Jaagus and Kull (2011) also found a shift towards SW in the wind directions, albeit on shorter time periods (1966-2008). Therefore, when analysing differences in wind statistics between data sets, it is important to ensure that the time periods are the same. Moreover it is important to keep in mind the different data set uncertainties. Probably, the biggest difference between HiResAFF and coastDat2 is the spectral nudging which is only applied for coastDat2. This method is known to improve reconstructions and lower the difference relative to observations. It is argued that the analog method contains a higher level of uncertainties. The uncertainties include model uncertainties, noise in the used observations (e.g. measurement errors) - also present in reanalysis data sets -, dependencies on the analog pool size and the link between real and simulated predictors (Schenk and Zorita, 2012).

Furthermore, there are uncertainties due to the different models used to conduct the two reconstructions. Neither the regional model CCLM nor the RCAO model is perfect, but the aim of this study was not to identify the better data set. However, although both data sets have different uncertainties due to different models and methods, both show comparable results regarding the variability of wind direction statistics of mean (median and average) and extreme wind events.

Comparing coastDat2 and HiResAFF the reader should also keep in mind the impact of e.g. the bias on the EOF analysis. A difference in the mean would change the distribution and hence the variability, as lower mean values in wind speed would induce a more skewed distribution. Although both data sets already showed comparable results, a bias correction could lead to even more similar results, because the different means were identified as the main differences in both data sets.

As mentioned above, both data sets, HiResAFF and coastDat2 showed similar results. However, in the overlapping period (1948-2009) there are differences between both data sets regarding the frequencies of the SW and W wind directions for extreme winds. HiResAFF exhibited higher frequencies for W winds in all Baltic Sea regions. I suggest that this stronger zonal component may be an artefact of HiResAFF, due to the uncertainties mentioned above, but this question requires further study.

The overall conclusion of this study is that the hypothesis that the statistics of mean wind can serve as a proxy for statistics of extreme wind is rejected for the Baltic Sea region.

3 Long-term winter variability of western and south-western wind extremes over the Baltic Sea and its relation to pressure variability.

In Chapter 2 extreme winter winds from SW and W are identified to be strongest and can therefore be assumed to have the highest damage potential. Therefore the following chapter focuses on these specific wind events and tries to make connections to responsible large-scale pressure patterns.
Daily wind extremes from west (W) and south-west (SW) in the Baltic Sea region during winter (DJF) are analysed based on a regional reconstruction (HiResAFF) over the period from 1850 to 2009. In this study daily extreme winds are defined as the exceedance of the 95$^{\text{th}}$ percentile of the daily wind speed distribution. After identifying eight circulation types, four patterns show relations to frequencies of W/SW winds above the 95$^{\text{th}}$ percentile. The temporal evolution of three of these patterns show clear similarities to extreme W/SW wind frequencies.

3.1 Introduction

This study aims at identifying the link between daily winter extreme west (W) and south-west (SW) wind events to weather circulation patterns over the Baltic Sea area. The method is based on using the objective algorithm of K-means clustering coupled with principal component analysis (PCA) applied to daily fields of mean sea-level pressure (SLP). This helps clarifying the variability of these patterns as well as their relationship with W/SW wind extreme variability on an inter-annual time scale.
Recently, severe wind-storms have been responsible for large damages and substantial economical losses in several countries in Europe. These damages are partly dependent on the occurring wind direction. For example Sweden experienced most damages during NNW to SW winds, and by winds from NNE (Nilsson et al., 2004).
For the Baltic Sea region, wind storms are the natural hazards with the highest damage potential (Rutgersson et al., 2015). Hence, it is of great interest if changes in wind speed and wind direction are caused by natural variability or due to anthropogenic influences. Many studies have identified an increasing trend in wind speeds or storm numbers for the time period from the 1960's to the 1990's (see review by Feser et al., 2015). Nevertheless,

a long-term trend in wind storms has not been found yet. Studies about storm numbers in southern Sweden showed that these numbers present a minimum around 1960 but that the above mentioned trend is rather due to natural variability. It was stated that the analysed time period plays a crucial role for analyses trying to disentangle natural variability and climate change (Bärring and Fortuniak, 2009; Bärring and von Storch, 2004; Nilsson, 2008).

The Baltic Sea is a semi-enclosed basin, which is highly dynamic and strongly influenced by large-scale atmospheric circulation over the North Atlantic European sector (Hünicke, 2008; Lehmann et al., 2011). The winter climate of the Baltic Sea is steered by large-scale pressure systems (Lehmann et al., 2011), which control the air flow over Europe. One is the North Atlantic Oscillation (NAO), a system dominated by two opposing pressure systems; the Icelandic Low and the Azores High. The other one is the winter high and summer low over Russia. The NAO is the most important index to define the atmospheric circulation variability over the Baltic Sea (Lehmann et al., 2011). It strongly influences the climate of Europe especially during winter (Hurrell and van Loon, 1997). It is commonly known that winters with a positive/negative NAO index are associated with changes in cyclone activity in the North Atlantic region (Gulev et al., 2002; Hurrell, 1995). For example Alexandersson et al. (2000) reported a correlation between $95^{\text{th}}/99^{\text{th}}$ percentiles of geostrophic wind speeds and the NAO for North Atlantic storms and storms over the Baltic Sea.

Wind directions and their variabilities are also related to large-scale atmospheric circulations. Northern hemispheric SLP changes where found in the last half of the 20^{th} century (Serreze et al., 2000). The observed changes are described by significant decreasing SLP over the Arctic region and increasing SLP over South-Europe. Consequently, the pressure gradient intensified which induced stronger westerlies. Trends in the NAO, which is correlated with wind over the Baltic Sea, represent this intensification as well (Jaagus and Kull, 2011). The study of Bárdossy and Caspary (1990) investigates atmospheric circulation patterns over Europe from 1881 to 1989 and shows that the frequencies of some circulation types have changed over the last years. These changes could be detected for yearly and seasonally frequencies. That study showed an increase for zonal circulations since 1973 for December and January and a decrease for April and May. In contrast, easterly winds decreased especially during winter since 1980.

Such studies often use 'Großwetterlagen' after Hess and Brezowsky (1969). Kysely and Huth (2006) compared this subjective classification method to an objective classification method by which used the sea-level pressure. They found that both methods exhibit the same main changes regarding atmospheric circulation patterns over Europe in the last 40 years. Moreover, they showed that overall there are more changes in atmospheric circulation patterns in winter than in summer. Kyselý (2008) stated that the persistence of the circulation patterns increased since 1980 which is true for most circulation types in all seasons.

Studies analysing changes in mean wind and storms often rely on proxy data because wind

observation data are commonly known to be inhomogeneous. These proxy data are usually based on geostrophic winds and focus mainly on Northern Europe than specifically on the Baltic Sea and show different trends in e.g. storm numbers or intensities (Feser et al., 2015).
Another possible data set might be meteorological reanalysis data, but these data sets are limited in time since they require observations, which are only available in a reliable quality since 1948. Nevertheless, the close relation to observations is also a clear advantage. Therefore, I choose an observation-based data sets, namely HiResAFF (High-Resolution-Atmospheric-Forcing-Fields). This data set is a product of the analog method, a reconstruction method based on observations and regional climate modelling, and is explained in more detail in Chapter 2.2.2. The biggest advantage is its high spatial resolution, comparable to regional reanalysis data, and the long time period from 1850 to 2009. In this study, temporal changes in frequencies of extreme winter winds from W and SW are investigated. These changes can be related to changes in the occurrence of special circulation weather types. Four major circulation patterns, associated with W/SW wind, are classified from daily sea level pressure fields derived from HiResAFF over the Baltic Sea. Although there already are some studies regarding this relationship, it is argued that this study extends these to more general circulation types than only the NAO and it is more focused on the Baltic Sea.
This Chapter is structured as follows: The first subsection describes the applied methods, which is followed by the explanation of the results. The Chapter closes with a discussion and conclusions.

3.2 Data and methods

For this study daily mean wind data at a height of 10m and mean sea-level-pressure (SLP) data are analysed. The analysed data set, HiResAFF, is the result of a hybrid statistical-dynamical approach applied to a combination of sea-level-pressure and near surface temperature observations and model simulation data. This data set cover a time period from 1850 to 2009 and thus allows for long-term analysis. HiResAFF is described in more detail in Section 2.2.2.

3.2.1 Statistical methods and definitions

This analysis is based on winter (DJF) extreme west (W) and south-west (SW) wind events over the Baltic Sea region. Extreme winds are defined as the events which exceed the 95^{th} percentile of daily mean wind speed. In this case I use a little lower threshold than the 98^{th} percentile, used in Chapter 2, to increase the 'sample size'. In this analysis the Baltic Sea area is again separated into four subdivisions (see Fig. 2.1) south-west

(SWR), south-east (SER), north-east (NER) and north-west (NWR) but also the whole area visible in Figure 2.1 is considered. The wind directions are defined the same way as in Chapter 2.
The main focus of this study lies on the relationship of the extreme W/SW winds and predefined pressure patterns. In order to identify these weather circulation patterns affecting the Baltic Sea area, the K-means clustering algorithm coupled with PCA analysis is adopted. The PCA analysis is used to condense information of daily SLP fields and to reduce the number of variables during K-means clustering. The aim of the K-means algorithm is to identify groups that minimise the total within-cluster distance between the members of its cluster and maximise the distance between the centres of the clusters. Starting from a random classification of the daily SLP fields among the clusters, the Euclidean distance between each daily SLP field and the and the mean of each cluster is calculated. The iterative algorithm proceeds by permuting at attribution of the daily SLP fields and accepting this permutation when the within-cluster distance becomes smaller and the across-cluster means becomes larger. The algorithm stops when no optimisation is possible. The method requires the prescription of the number of clusters k and in this case I choose k to be eight. The K-means algorithm is described in more detail by Hartigan and Wong (1979).

3.3 Results

In Chapter 2 winter is identified as the season with strongest extreme wind events with prevailing directions from W and SW. Although on average all wind directions are quite frequent over the Baltic Sea, extremes are very focused on these directions (Fig. 2.4b). This section is dedicated to the temporal variability of those wind events and their relation to the variability of large-scale sea level pressure (SLP) patterns. In the following subsections I will analyse the frequency trends of W and SW winds and the correlations to circulation types identified with a cluster analysis described in Section 3.2.1.

3.3.1 Trends in wind speed and direction

A correlation between the five year running sum of W (SW) frequencies and the corresponding five year running mean wind speed shows for the whole Baltic Sea region a statistical significant value of 0.54 (0.25). For the other directions there is no such high correlation ($r<0.08$). This suggests that years with more (less) W/SW winds show higher (lower) wind velocities. This is also apparent after the separation of the Baltic Sea into four regions. For winds from W the correlation between the amount of west wind events and the mean wind speed of these events lies between 0.43 (SWR, Fig. 3.1a) and 0.68 (NER, Fig. 3.1b). For SW winds this correlations are a bit higher from 0.59 (SER, Fig.

3.1c) to 0.67 (NER, Fig. 3.1d). This illustrates that the identified connection of westerly winds with stronger wind speeds occurs over all Baltic Sea subregions.

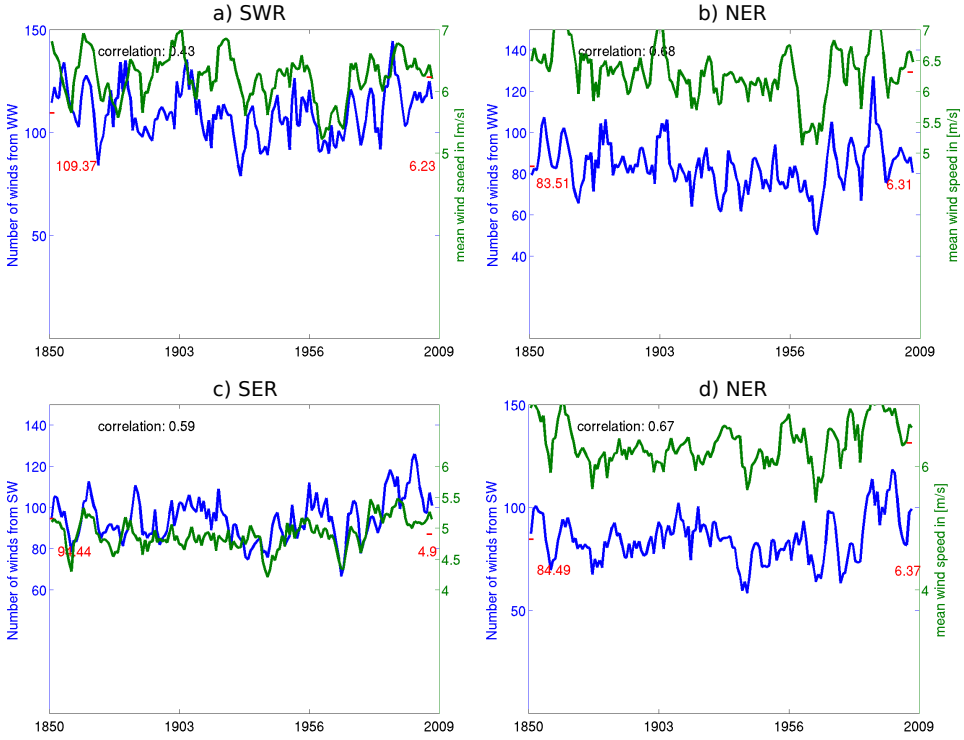

FIGURE 3.1: Five year running mean time series of W and SW wind event frequencies (blue) and the wind speeds of these events (green). The red marks on the y axes and the red numbers are the corresponding mean values. These plots are exemplary shown for the Baltic Sea regions with the weakest and strongest correlations, respectively, for W winds (upper two panels): south-west region (a-SWR) and north-east region (b-NER) and for SW winds (lower two panels): south-east region (c-SER) and north-east region (d-NER).

To investigate the temporal evolution of the extreme wind speeds in more detail Figure 3.2a+b show the time series of the frequencies of the 95$^{\text{th}}$ percentile exceedances as a sum over all grid points. These time series exhibit no long-term trend for the number of winds from W or SW. However, there is an increasing trend for both wind directions for a shorter time period from the 60's to the early 90's.

3.3.2 Relationship with circulation weather types

In a next step these findings are to be compared with circulation patterns, classified from daily sea level pressure fields based on the K-means clustering algorithm coupled with principal component analysis (see Sect. 3.2.1). To identify the most influential patterns the correlations between the frequency of occurrence of each cluster and the frequency of wind exceedances for winds of different directions are calculated, for yearly and five year

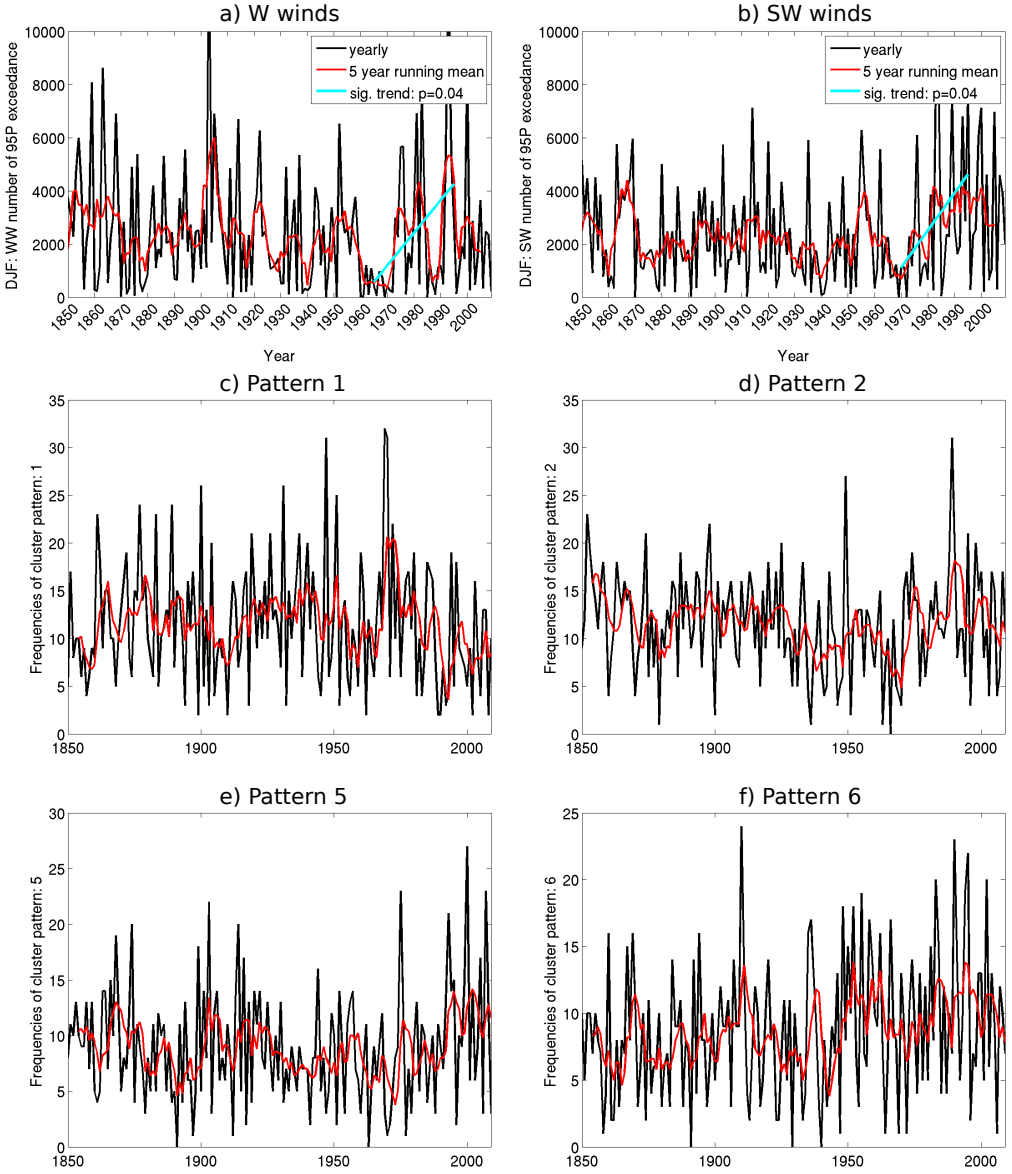

FIGURE 3.2: Field sum of frequencies per wind direction for the Baltic Sea area. a) westerly winds; b) south-westerly winds. The black line shows yearly frequencies, the red line demonstrates the 5 year running mean and the cyan line shows a significant trend. In both cases the significance value is p=0.04. c-f show the corresponding time series related to circulation patterns (Fig. 3.3) as yearly (black) and five year running mean (red) values.

running mean values for the whole Baltic Sea and the four subdivisions. The results for the whole Baltic Sea can be taken from Table 3.1. These correlations are comparable in all four subdivisions with some differences between the northern and southern parts (not shown).

The yearly correlation coefficients reveal four main driving patterns which are shown in

Figure 3.3. Pattern 1 is negatively correlated with W and SW wind above the 95th percentile over the whole region and all four subregions, it shows mostly meridional isobars which induce a flow from south to north with a tendency to north-west in the southern Baltic region.

TABLE 3.1: Correlation coefficients for the relationship between eight circulation pattern frequencies and the exceedances of the 95th percentile of wind speed of west (W) and south-west (SW) winds over the whole Baltic Sea region (shown in Fig. 2.1) for yearly (y) and five year running mean (5y) values.

whole Baltic	1	2	3	4	5	6	7	8
W y	-0.39	0.31	-0.19	-0.09	0.68	0.15	0.05	-0.37
W 5y	-0.33	0.43	-0.14	-0.05	0.65	0.30	-0.09	-0.16
SW y	-0.45	0.34	-0.18	-0.16	0.59	0.41	-0.05	-0.32
SW 5y	-0.52	0.47	-0.14	-0.04	0.65	0.50	-0.11	-0.23

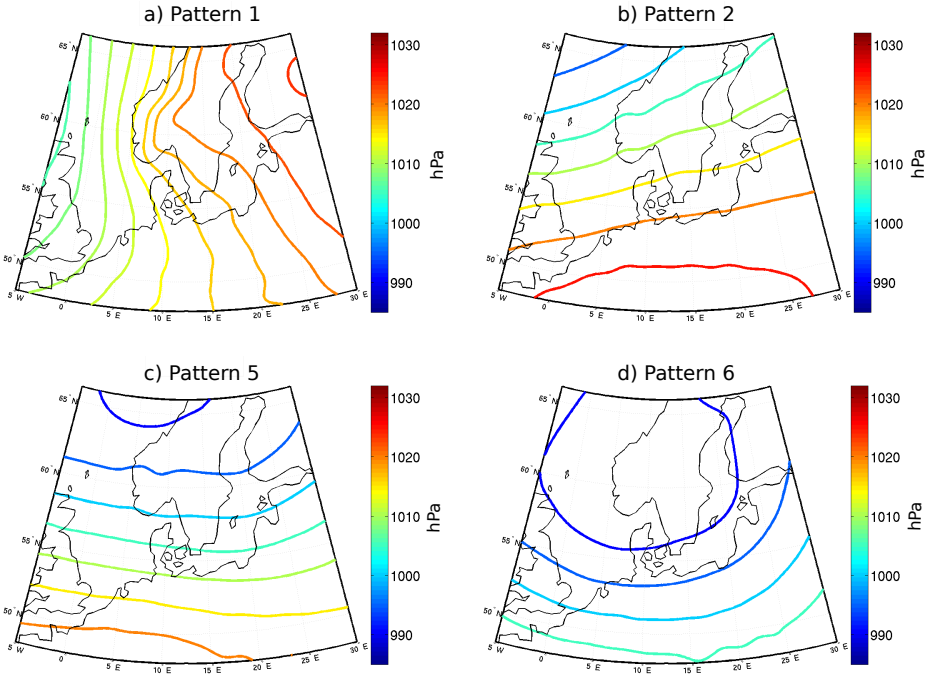

FIGURE 3.3: Four patterns derived from a k-mean cluster analysis whose time series (see Fig. 3.2) showed high correlations (see Table 3.1) with the frequency of W/SW wind which exceed the 95th percentile of wind speed.

Pattern 2 shows highest correlations for SW winds especially in the northern regions (NWR, NER). This pattern shows a strong SW flow which fits to the correlation results (Table 3.1).

Pattern 5 has the highest correlations for both W and SW winds in all four regions. This pattern is dominated by a low pressure system over north-west Norway, which induces a

strong westerly flow.
Pattern 6 shows highest correlations for SW winds in the southern regions (SWR, SER). This pattern exhibit a low pressure system over Scandinavia and hence shows a cyclonic rotation which induces a westerly and south-westerly flow over the Baltic Sea. These results show that the variability of the identified circulation patterns (1, 2, 5, 6) seem to be responsible for large parts of the variability of extreme winds from W and SW.
The five year running mean correlations showed that pattern 5 is most important for W winds in all regions and for SW winds only in the northern regions. SW winds in the southern regions show highest correlations for pattern 6. Pattern 2 has a big influence especially for SW winds in the northern regions. Hence, extreme SW wind frequencies show a difference between the northern and southern regions. Extreme W winds mainly depend on the variability of pattern 5.
The corresponding time series for these four patterns are shown in Figure 3.2c-f which can be compared with the percentile exceedances in Figure 3.2a+b. This comparison shows great similarities for pattern 5 (Fig. 3.2e) and W winds (Fig. 3.2a). Pattern 2 (Fig. 3.2d) and 6 (Fig. 3.2f) show a comparable temporal evolution to SW winds (Fig. 3.2b). Note that two of these patterns (2 & 5) are comparable to the NAO pattern, with only slight shifts of the centres of action to west or east. This subjective comparison agrees with the above explained correlation coefficients and leads to the conclusion that pattern 2, 5 and 6 are the prevailing pressure patterns during strong westerly or south-westerly winds over the Baltic Sea.

3.4 Discussion and conclusions

This Chapter compares winter winds from west (W) and south-west (SW), which exceed the 95$^{\text{th}}$ percentile of wind speed on a grid-cell scale, with pressure patterns. First results showed that more winds from these directions per year induce a higher mean wind speed per year. These results could be verified for the whole Baltic Sea as well as for the analysed four subdivisions.
The analysis of the 95$^{\text{th}}$ percentile exceedances showed no long-term trend but an increasing wind speed from the 60's to the early 90's. This increase was also found for storm frequencies over different regions of North-Atlantic and Europe by many studies (see review by Feser et al., 2015, and references therein). However, many studies showing this trend focus on relatively short time periods due to the usage of reanalysis data. Other studies based on geostrophic winds, derived from pressure proxies, cover longer time periods (Alexandersson et al., 2000; Bärring and Fortuniak, 2009; Bärring and von Storch, 2004). They also reported an increasing wind speed for the second half of the 20$^{\text{th}}$ century but also stated that on longer time scales no trend could be verified, but rather natural variability. This study supports this statement.
Furthermore, this study detected temporal changes in frequencies of extreme winds from

W and SW. These changes could be related to changes in the occurrence of four circulation weather types. Three of these types could be identified to mainly influence the W/SW wind variability and two of those are very comparable to the NAO pattern.
This is also in good agreement with other studies (e.g. Alexandersson et al., 2000; Lehmann et al., 2011). Lehmann et al. (2011) investigated the relation of cyclone intensification and a shift of the NAO centres of action, which also was connected to increasing westerly winds over the Baltic Sea. Moreover, Alexandersson et al. (2000) reported a correlation between $95^{\text{th}}/99^{\text{th}}$ percentiles of geostrophic wind speeds and the NAO for North Atlantic storms and storms over the Baltic Sea.
Thus, the results verify those studies for more regionalised pressure patterns, which are not just limited to the NAO, analysed with an observation-based data set covering the period 1850–2009 for the Baltic Sea region.

4 Variability of winter daily wind speed distribution over Northern Europe during the past millennium in regional and global climate simulations.[1]

Sea level pressure, as analysed in Chapter 3, is not the only influencing factor regarding wind variability. The following analysis also considers thermal indices. The study tries to identify large-scale factors which drive changes in the probability distribution of wind speed in winter over Northern Europe based on a series of global and regional climate simulations covering the last centuries, and reanalysis products covering approximately the last 60 years. The considered atmospheric drivers are the mean temperature, the meridional temperature gradient and the North Atlantic Oscillation. The overlaying question is whether and how the wind speed distribution may change during varying climate conditions and hence whether these conditions may provoke more and/or stronger wind speed extremes.
The main conclusion is that no clear systematic relationship between the mean temperature, the temperature gradient and/or the North Atlantic Oscillation, with daily wind speed statistics can be inferred from the simulations. The understanding of past and future changes in the distribution of wind speeds, and thus of wind speed extremes, will require a detailed analysis of the representation of the interaction between large-scale and small-scale dynamics.

4.1 Introduction

Anthropogenic climate change is expected to cause an increase of various types of extreme events, such as heat waves, but its effects on extreme winds is less clear. Indeed, Chapter 3 of the Intergovernmental Panel on Climate Change (IPCC) special report 'Managing the Risks of Extreme Events and Disasters to Advance Climate Change Adaptation' states that there is only low confidence in projections of changes in extreme winds (Seneviratne et al., 2012). One way to reduce this uncertainty is to compare the output of paleoclimate simulations over the past centuries with empirical evidence of past wind conditions, for instance derived from historical evidence or natural proxies (Costas, 2013). While there

[1] Bierstedt, S.E., Hünicke, B., Zorita, E., Wagner, S. and Gómez-Navarro, J.J. (2015): Variability of daily winter wind speed distribution over Northern Europe during the past millennium in regional and global climate simulations. Clim. Past Discuss. 11, 1479-1518.

is still a dearth of proxy records reflecting past changes in wind speed, new types of proxy records are being developed (Costas, 2013). A precondition for this comparison is to test whether different climate models provide a consistent picture of past changes in wind speed distribution. In this study several simulations with global and regional models are analysed and it is investigated to what extent they provide a consistent picture of the relationship between the variations in the wind speed distribution and large-scale drivers. The study focuses on Northern Europe in wintertime as this region and season are particularly prone to storminess.

Hypotheses put forward to explain changes in storminess are related to the general physical consideration that warmer periods provide more humidity and consequently more (latent) energy for possible storms. However, warmer periods are generally characterised by a weaker meridional temperature gradient due to the stronger warming of the high latitudes with respect to the tropics, and thus a weaker baroclinicity, which should lead to weaker or less storms (Li and Woollings, 2014; Yin, 2005). In addition, the North Atlantic Oscillation (NAO), as the main pattern of troposphere dynamics over the North Atlantic-European sector, is also related to the inter-annual variability of seasonal mean winds in this region. It is thus very plausible that the NAO is also involved in the variations of the distribution of daily wind speeds, e.g. Wang et al. (2011) state that NAO variations show a relationship with the 99^{th} percentile of wind speed. The NAO itself could also be related to changes in European near-surface winter temperature (Rutgersson et al., 2015). In this regard, scenario simulations indicate a contradicting tendency of the NAO in a warmer future, depending on whether it is defined from the sea-level pressure (SLP) gradient or from the geopotential height at 500 mbar (Z500). Gillett and Fyfe (2013) showed that the meridional SLP gradient will tend to become steeper polewards. On the other hand Cattiaux and Cassou (2013) also found a positive trend of the SLP gradient but found a negative trend of the Z500 gradient. This study focuses on surface winds which are rather influenced by SLP variations. The link between the NAO and external climate forcing over the past centuries is, however, unclear in climate simulations (Gómez-Navarro and Zorita, 2013).

Thus, for Northern Europe, from the dynamical point of view it is not clear how the distribution of wind speed would respond to changes in temperature. The analysis of long-term trends in wind extremes and storminess in the observational record has so far yielded inconclusive results, probably due to the difficulty of constructing homogeneous series of wind speed, because of e.g. station relocation or changing measuring techniques. Furthermore, the covered period might be too short to realistically demonstrate trends in the rarely occurring extreme wind events. On the other hand, reanalysis products covering long periods (e.g. the 20th Century Reanalysis 20CR; Compo et al., 2011) may be inhomogeneous due to the assimilation of new types of data through the simulated period. There has been a considerable debate on the storminess trends in long-term reanalysis data sets (Brönnimann et al., 2012; Krueger et al., 2013; Wang et al., 2013). Krueger et al. (2013) stated that before 1950 the time series of 20CR and observational mean sea

level pressure are not consistent. They suggested that the increasing density of station data leads to these inconsistencies. Wang et al. (2013), on the other hand, argued that new measurement errors and changed sampling frequencies would produce these inhomogeneities. This debate has also been discussed by Feser et al. (2015), who concluded that the analysis of long-term reanalysis data, affected by changing station density, should be conducted with caution.

The analysis of the climate of the past centuries can shed light on the question whether external climate forcing has an effect on the intensity or frequency of wind extremes and whether or not the temperature variability is linked to variability in statistics of wind speeds. Unfortunately, proxy-based climate reconstructions in general still do not provide information about extreme wind statistics in the past, except for intense tropical cyclones (e.g. Donnelly and Woodruff, 2007). However, new types of proxy data that may record past wind speed are being retrieved. For instance, coastal dunes at the North Sea coast contain layered structures that can be analysed by ground-penetrating radar. The layered structures contain information about grain size distribution and, indirectly, about intensity or frequency of high winds in the past (Costas, 2013). These types of proxies can potentially be used to test the skill of climate models to simulate the relationships between extreme wind statistics and external forcing or between extreme wind statistics and low-frequency variability of the large-scale surface climate.

The evolution of temperatures of the past millennium in this region, as reconstructed from proxy and long-instrumental records, exhibits a generally warm period in the early centuries (the Medieval Warm Period) and generally colder centuries around 1700 AD (the Little Ice Age), with the subsequent warming leading to the current warm period (Esper et al., 2014; Luterbacher et al., 2004; PAGES 2k, 2013). This alternation of warm and cold periods has been likely caused by external climate forcings (Fernandez-Donado et al., 2013; Hunt, 2006), in particular the recent warm period and the Little Ice Age, and thus it provides a suitable test of whether the variability of extreme wind statistics may follow a similar alternation.

Climate simulations had been previously used to address the connection between winds and temperatures in the past (e.g. Fischer-Bruns et al., 2005; Schimanke et al., 2012). Fischer-Bruns et al. (2005) analysed two historical climate simulations with the global climate model ECHO-G covering the period from 1550 to 1990 AD. These authors found that storminess and large-scale temperature variations were mostly decoupled in these simulations. However, they reported a connection between storm track variability and temperature over the North Atlantic for one of the two simulations in two periods with extremely low external forcing, namely the Late Maunder Minimum (1675–1710 AD) and the Dalton Minimum (1790–1840 AD). Nevertheless, they found no evidence of a linear co-variation between the number of extra-tropical storms and temperature variations in the simulations analysed.

The spatial resolution of global climate models may not be adequate to realistically represent extreme events, especially over regions with complex coastlines. In this respect,

regional climate models, driven by the fields simulated by global climate models, should provide a better representation of small-scale processes, topographic influences and of the land-sea contrasts (Gómez-Navarro et al., 2013, 2015b; Hall, 2014), and thus they should be better suited for the simulation of extreme events. Nevertheless, despite the fact that regional models provide an added value (Feser et al., 2011) they are also bound by the circulation biases of the driving global climate model simulations (Hall, 2014).
In this study an analysis of the variability of daily wind speed statistics over Northern Europe over the past centuries as simulated by different regional and global climate models is presented. The study mainly focuses on the consistency among the different models in simulating the relationship between large-scale drivers and the statistics of daily wind speed with the goal of identifying robust patterns across models that can be later tested with proxy reconstructions.
This paper is structured as follows: Chapter 2 describes the analysed data sets separated into climate simulations of global circulation models, regional circulation models and reanalysis products. Chapter 3 defines the area of interest and outlines the applied methods and definitions. Chapter 4 presents the analysis of the relationship of large-scale drivers and wind speed variance, as well as the comparison of the evolution of the wind speed variance in the millennium simulations. A discussion of the results and conclusions closes the manuscript.

4.2 Data

This study focuses on the statistical relationship between spatial and temporal mean temperature/pressure and daily wind statistics. Monthly mean two-meter temperature (T2M) values, monthly mean values of mean sea level pressure (SLP) and daily mean 10-meter wind speed (WS) are used for this analysis. These values are taken from a set of five simulations performed with five different models, with different spatial and temporal resolution: two simulations with the Regional Climate Models (RCMs) MM5 and CCLM, and three simulations with the global General Circulation Models (GCMs) ECHAM4-HOPE-G, ECHAM5/MPI-OM and ECHAM6/MPI-OM. ECHAM4-HOPE-G and ECHAM5-MPIOM were chosen because they had been used as the boundary forcing for the two RCM simulations, respectively. Note that for the RCM simulations the same external forcings were applied as for their driving global simulations. ECHAM6/MPI-OM was chosen due to its higher spatial resolution similar to the resolution of the RCM simulations analysed, but also for being the next generation of the previous versions of ECHAM4 and ECHAM5. Additionally, the global reanalysis NCEP/NCAR version 1 and a regional reanalysis named coastDat2 are analysed. Table 4.1 summarises the information about spatial and temporal resolution and time periods of the data sets used.

TABLE 4.1: Overview of the analysed simulations/reanalysis and their simulation acronyms, underlying atmosphere and ocean models, boundary forcings (only for regional data sets) as well as the spatial resolution of the atmosphere models and time periods, as used for the analysis.

	Simulation	Atmosphere	Ocean	Boundary	atm. spatial res.	Vegetation	Period
GCM	ECHO-G	ECHAM4	HOPE-G		3.75°	constant	1001-1990
	ECHAM5	ECHAM5	MPI-OM		3.75°	time dependent	850-2005
	ECHAM6	ECHAM6	MPI-OM		1.875°	time dependent	850-2005
RCM	MM5	MM5		ECHO-G	0.5°	constant	1001-1990
	CCLM	CCLM		ECHAM5	0.5°	constant	1655-1999
Reanalysis	coastDat2	CCLM*		NCEP	0.22°	constant	1948-2012
	NCEP				2.5°	constant	1948-2012

* with spectral nudging

Figure 4.1 shows the land-sea-masks for all data sets. For the regional data sets (CCLM, MM5, coastDat2) the whole available domain is visible and the study area is marked by a red rectangle. In the following the different data sets are introduced in more detail and their main differences are described.

4.2.1 Global Climate Model simulations

The coupled GCM ECHAM4-HOPE-G, also denoted in previous literature as ECHO-G (Legutke and Voss, 1999) consists of the atmospheric component (AGCM) ECHAM4 (Roeckner et al., 1996) and the ocean-ice component (OGCM) HOPE-G (Wolff et al., 1997). ECHAM4 has a horizontal resolution of T30 (approx. 3.75°x3.75° $\approx$ 400 km x 260 km in high mid-latitudes) and 19 vertical levels and HOPE-G a horizontal resolution corresponding to T42 (approx. 2.8°x2.8° $\approx$ 300 km x 200 km in high mid-latitudes) and 20 vertical levels. Both sub-models have been developed at the Max Planck Institute for Meteorology (MPI-M) in Hamburg. The ECHO-G millennium simulation (1001-1990 AD) is part of an ensemble of simulations conducted by the Helmholtz-Zentrum Geesthacht (HZG). The simulation is forced with changes in total solar irradiance, the dimming effect of volcanic eruptions on solar irradiance, and changes in greenhouse gases (CO2, NO2, CH4). The simulation was started with a cold ocean initial condition taken from a previous simulation corresponding to a situation representative of the Little Ice Age (Hünicke et al., 2011; von Storch et al., 2004; Zorita et al., 2004).
The coupled GCM ECHAM5/MPI-OM consists of the atmospheric component ECHAM5 (successor of ECHAM4, Roeckner et al., 2003) and the ocean and sea-ice component MPI-OM (Marsland et al., 2003). ECHAM5 has a T31 resolution with 31 vertical levels. The MPI-OM component has a horizontal resolution corresponding to T42 and 23 vertical levels. The analysed simulation ECHAM5/MPI-OM (850-2005 AD) is part of an ensemble of

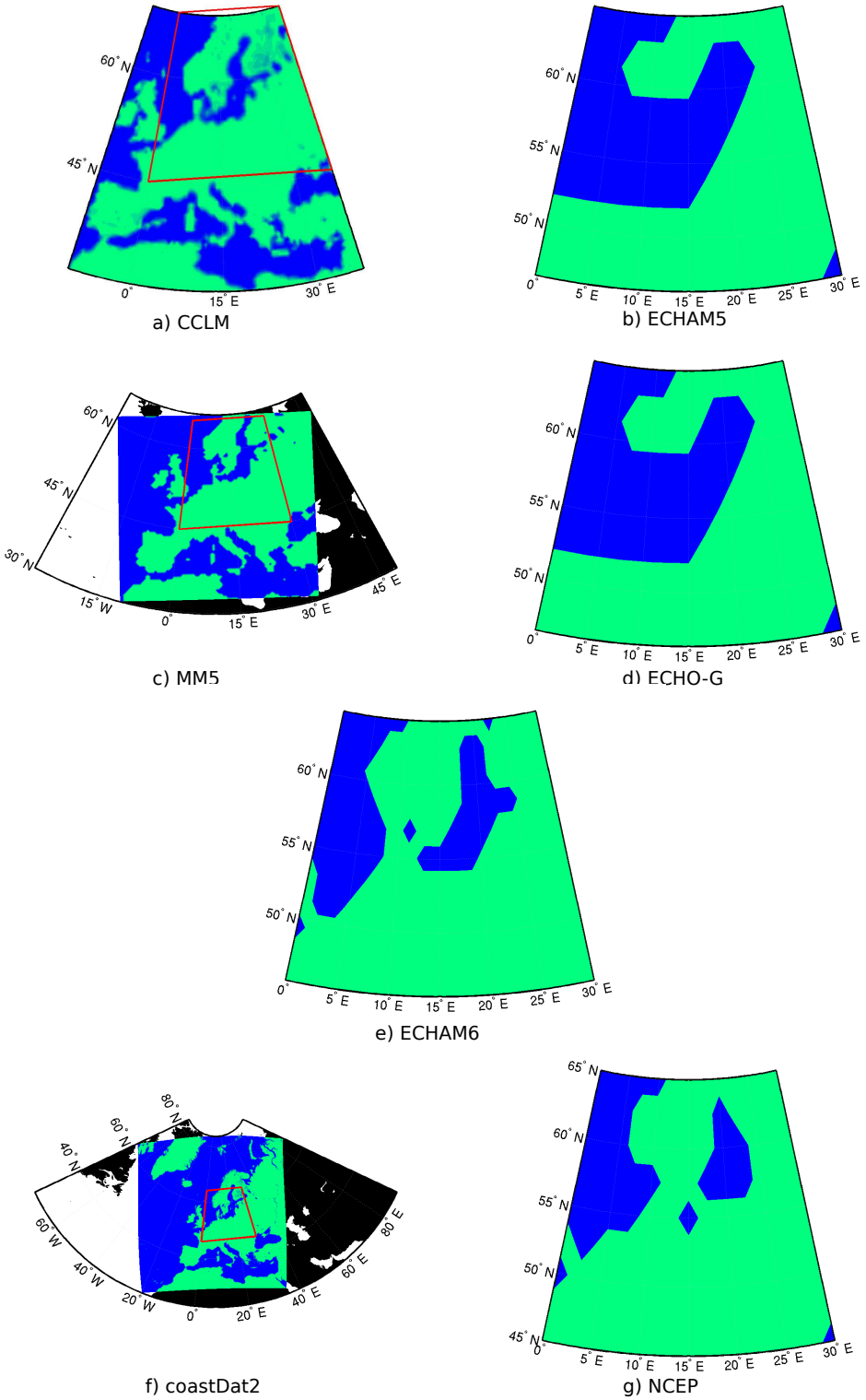

FIGURE 4.1: Land-Sea-Masks of the analysed simulations. Figures regarding global data sets (ECHAM5, ECHOG, ECHAM6, NCEP) only show the investigation area. Figures concerning regional data sets (CCLM, MM5, coastDat2) include the Land-Sea-Mask for the whole simulation domain and the investigation area is shown with a red triangle.

simulations conducted by the Max-Planck-Institute for Meteorology in Hamburg and will hereafter simply be named ECHAM5. It is driven by changes in solar irradiance (Bard et al., 2000), volcanic eruptions (Crowley et al., 2008), changes in Earth's orbital parameters, greenhouse gas and aerosol forcings. Additionally, land cover changes (Pongratz et al., 2008) are considered in this simulation. More details about the simulation setup and forcings can be found in Jungclaus et al. (2010).
The study includes a climate simulation with the model MPI-ESM with the P configuration (MPI-ESM-P, Giorgetta et al., 2013), which consist of the successor of ECHAM5 and the newest version of ECHAM, named ECHAM6 (850-2005 AD). The main differences between ECHAM6 and ECHAM5 are the higher vertical resolution (i.e., 47 instead of 31 vertical levels), increased horizontal resolution of T63 (1.875°x1.875° $\approx$ 200 km x 130 km in high mid-latitudes), the incorporation of new aerosol and surface albedo climatology and the use of a new short-wave radiation scheme in ECHAM6 (Crueger et al., 2013). The MPI-ESM-P simulation is part of the Climate Model Intercomparsion Project version 5 (CMIP5, Taylor et al., 2012). The boundary layer and turbulence parametrisation in ECHAM6 is based on the eddy diffusivity/viscosity approach (Stevens et al., 2013). The model was driven by changes in greenhouse gases and spectrally resolved solar irradiance, volcanic activity (Crowley et al., 2008), changes in Earth's orbital parameters and land use changes (Pongratz et al., 2008).

4.2.2 External forcings of the GCMs

Above the key-properties of the analysed global simulations are outlined. However, the differences in the external forcings used to drive the simulations play a crucial role in the analysis. Hence, additionally a comparison of these differences is provided. An overview can be found in Table 4.2. A more comprehensive comparison between ECHO-G and ECHAM5 was given by (Fernandez-Donado et al., 2013), however, it is summarised here and extended for ECHAM6.
While all three simulations include total solar irradiance (TSI), greenhouse gas (GHG) and volcanic forcing as external forcings, only ECHAM5 and ECHAM6 incorporate also anthropogenic aerosols and land use changes. There are various estimations of past TSI, which can be broadly divided into a strong (S; $>$ 0.2% TSI change since the Late Maunder Minimum (LMM)) and a weak (s; $<$ 0.1% TSI change since LMM) amplitude of variations (Fernandez-Donado et al., 2013). Strong (S) solar forcing is applied for ECHO-G and ECHAM5, in which ECHO-G uses higher values than ECHAM5. Weak (s) solar forcing is applied for ECHAM6. Estimations of changes in the main well-mixed GHG concentrations (CO2, CH4, N2O) are obtained from air bubbles enclosed in Antarctic ice cores. The CO2 concentrations were prescribed in ECHO-G after Etheridge et al. (1996), in ECHAM5 and ECHAM6 they follow Marland et al. (2003). The incorporation of the volcanic forcing into ECHO-G was done by including the net effect of stratospheric volcanic aerosols in

an effective solar constant in terms of a reduction in incoming short-wave radiation. For ECHAM5, latitudinally resolved changes in optical depth in the stratosphere were used. This might have an impact on climatic changes due to volcanic eruptions e.g. on the atmospheric circulation, especially over the extra-tropics during winter (see Fernandez-Donado et al. (2013) and included references). The orbital changes and land-use changes (only included in ECHAM5 and ECHAM6) are the same in both simulations. Orbital variations follow Bretagnon and Francou (1988) and vegetation changes Pongratz et al. (2008).

TABLE 4.2: Overview of the GCM forcings. The forcings are abbreviated as follows: S – strong solar forcing ($> 0.2\%$ change since LMM); s – weak solar forcing ($< 0.1\%$ change since LMM); G – greenhouse gas; V – volcanic; O – orbital; L – land-use change. The last column gives the references describing the experiments.

GCM	Forcings	Reference
ECHO-G	SGV	Zorita et al. (2004)
ECHAM5	SGVOL	Jungclaus et al. (2010)
ECHAM6	sGVOL	Schmidt et al. (2011)

4.2.3 Regional Climate Model simulations

The RCM MM5 model consists of a slight modification of the non-hydrostatic Fifth-generation Pennsylvania-State University-National Center for Atmospheric Research Meso-scale Model. Such modification allows this meteorological model to perform long climate simulations. This set-up has been used to conduct a long high-resolution climate simulation of the European climate during the last millennium, driven at the domain boundaries by the coupled GCM ECHO-G (Gómez-Navarro et al., 2013, 2015a). For the planetary boundary layer formation parametrisation, this simulation used the medium-range forecast (MRF, Hong and Pan, 1996) scheme. The RCM was driven by the same set of external forcing as the driving GCM ECHO-G (Sect. 4.2.1) to avoid physical inconsistencies. The domain of MM5 has a spatial resolution of 45 km. The model output is available on a daily scale and covers the period 1001–1990 AD. The analysed millennium simulation MM5-ECHO-G will hereafter be named MM5.

A second regional simulation was carried out with the non-hydrostatic operational weather prediction model COSMO in CLimate Mode (CCLM) (Rockel and Hense, 2008). The CCLM model was driven by initial and boundary conditions of the global ECHAM5 simulation. The regional model was, however, free to produce its own small scale spatial variability. The COSMO model uses a boundary layer approximation by implying horizontal homogeneity of variables and fluxes, which ignores all horizontal turbulent fluxes (Doms et al., 2011). The CCLM simulation over Europe had roughly the same spatial resolution as the MM5 simulation, but it covers only the period from 1655 to 1999 AD. The simulation CCLM-ECHAM5 will hereafter be abbreviated as CCLM.

4.2.4 Reanalysis data

The NCEP/NCAR reanalysis covers the period from 1948-present and has a spatial resolution of 2.5° (≈ 270 km x 175 km in high mid-latitudes) with 28 levels and is available at 6-hourly intervals (Kalnay et al., 1996; Kistler et al., 2001). In addition this study analyses the high resolution regional product coastDat2 (Geyer, 2014) resulting from a simulation with the regional model CCLM and driven by the global NCEP/NCAR reanalysis using a spectral nudging technique (after von Storch et al., 2000). The regional reanalysis coastDat2 covers Europe and the North Atlantic for the period from 1948 to present. It has a spatial resolution of 0.22° (≈ 25 km x 15 km) and the output is available on hourly time intervals.
All wind speed data were daily averaged to proceed with the analysis.

4.3 Methods and definitions

This analysis concentrates on the distribution of daily wind speed in wintertime (December, January, February - DJF) over central and northern Europe. The area of investigation has approximately the same extension from 45° to 65°N and 0° to 30°E for all data sets analysed.
The statistics of daily wind speed were evaluated over gliding time windows for the different simulation periods. These wind speed statistics include the standard deviation (STD) of the distribution, its 50^{th}, 95^{th} and 99^{th} percentiles (P50, P95, P99) and the differences P95 minus P50 (diffM) and P99 minus P95 (diffE) as a measure of the width of the distribution in the high wind ranges. The analysis of several percentiles and their differences allows the determination of basic changes in the characteristics of wind speed distributions, hence it is possible to investigate if it shifts with time with unchanged shape and/or whether its width changes. Thus, it can be discriminated between a change in the mean and/or in the extreme of the wind speed distribution. In this case 'extreme' means the tail of the distribution, which includes values above the 95^{th} percentile. For instance, increasing diffM and diffE values would show a broadening of the distribution which means higher extreme wind speeds. The three climate parameters analysed regarding their influence on wind speed are (1) mean seasonal near-surface air temperature (mTemp), (2) mean seasonal meridional temperature gradient (tGrad) and (3) the North Atlantic Oscillation index (NAO).
The temperature gradient is calculated as the absolute value of the difference between the northern (N) and the southern (S) half of the investigation area $tGrad = abs(N - S)$ for each model simulation. Due to the different resolutions the exact geographical domains of N and S differ. Therefore the border between both varies from around 53°N to 57°N.
The North Atlantic Oscillation (NAO) index is defined as the leading pattern resulting from principal component analysis (PCA) of the winter mean sea-level pressure (SLP)

field. This dominant pattern of variability is characterised by a low pressure system over Iceland and a high pressure system over the Azores (exemplarily shown for ECHAM6 in Fig. 4.2). As SLP field I used the GCM gridded pressure information of the North Atlantic and European area. This domain approximately spans from 70°W to 30°E longitude (from ≈ Boston to Istanbul) and from 70°N to 20°N latitude (from ≈ Tromsø to the southern part of Morocco). For computations conducted for the RCM simulations I used the NAO patterns derived from the driving GCM fields as well.

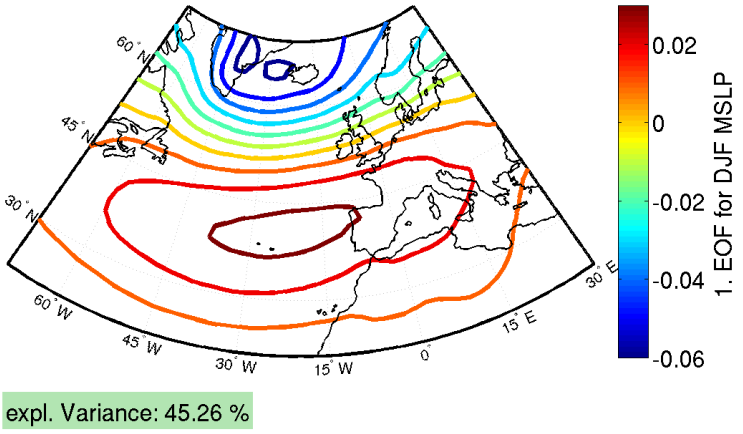

FIGURE 4.2: The NAO pattern exemplarily shown for ECHAM6 as the 1. EOF of mean sea level pressure (SLP). The corresponding principal components are used as the NAO index.

Because the aim of interest lies on the relationship between the slowly changing mean climate and the variability of the distribution of daily wind speed, the wind statistics are calculated considering gliding time windows over the respective time series for each model simulation before they are correlated with the running mean values of the atmospheric drivers. The climate parameters analysed are considered as means over the respective time windows and for Figures 4.3-4.8 these values are spatially averaged before the correlation computation with the wind statistics. For the long climate model simulations (ECHO-G, ECHAM5, ECHAM6, MM5, CCLM) I use 30-year running windows and for the shorter reanalysis data (coastDat2, NCEP) 5-year running time windows.

4.3.1 Test for significance: Random-phase bootstrap

A random-phase bootstrap method (Ebisuzaki, 1997; Schreiber and Schmitz, 1996) is applied to determine the significance of the correlation coefficients shown in Table 4.3 with

a significance level of p=0.05. This method allows us to take into account the autocorrelation structure of the series. For this method a Fourier transformation of the time series is conducted. The phases of the Fourier-transformed series are then replaced by random phases, and the result is transformed back to the time domain to obtain new surrogate time series. The surrogate time series has the same spectrum and autocorrelation as the original time series, but has a random time evolution. By generating a large number of surrogate time series, an empirical distribution of the correlation coefficient under the null-hypothesis (that the correlation is zero) can be constructed and used to determine the statistical significance of the correlation coefficient.

4.4 Results

As previously mentioned, this study is based on correlations between different parameters of the probability distribution of daily mean wind in wintertime and selected potential drivers: mean seasonal near-surface air temperature (mTemp), mean seasonal meridional temperature gradient (tGrad) and North Atlantic Oscillation index (NAO). Table 4.3 presents a summary of the statistical relationships derived from the different model simulations analysed. The presented time correlation coefficients are obtained by calculating the parameters of the daily wind probability distribution at grid-cell scale, followed by averaging over the whole spatial domain. The spatially resolved statistical analysis is presented for each model in the following sections. The significance of the correlation coefficients presented in Table 4.3 is tested as described in Sect. 4.3.1 by a random phase bootstrap method (Ebisuzaki, 1997; Schreiber and Schmitz, 1996) and marked as bold characters.
In the following, firstly the general findings for each of the climate drivers analysed (mTemp, tGrad, NAO) are presented by comparing all considered model simulations and reanalysis products. This is followed by a more detailed presentation of the results with focus on (a) the regional model simulations and their corresponding driving global models (b) the simulation with the global model ECHAM6/MPI-OM and (c) the reanalysis products. In addition, (d) the results for the overlapping time periods without reanalysis (1655-1990 AD) and with reanalysis (1948-1990 AD) data are compared and (e) for some of the long simulations a comparison of time slices is presented.

4.4.1 General comparison of all data sets

Relationship between mTemp and tGrad

A common characteristic shared by all analysed simulations is the negative correlation between the mean winter temperature (mTemp) and the mean meridional temperature gradient (tGrad). Hence, in warmer decades the northern regions warm more strongly

TABLE 4.3: Time correlation coefficients between the following parameters of the probability distribution of daily mean wind speed: standard deviation of wind speed (STD), the 50th, 95th and 99th percentile (P50, P95, P99) and the differences between P95-P50 (diffM) and P99-P95 (diffE) and some large-scale drivers: spatially averaged December-February air temperature (mTemp), the spatial air temperature gradient (tGrad) and the North Atlantic Oscillation index (NAO). The parameters of the probability distributions have been computed in 30 year sliding windows for the simulations and in 5 year sliding windows for the reanalysis products. The time series of the drivers have been smoothed with a running mean filter. Significant ($p<0.05$) coefficients (tested with a random phased bootstrap method) are written in **bold**.

	MM5	CCLM	ECHO-G	ECHAM5	ECHAM6	coastDat2	NCEP
tGrad – mTemp	**-0.47**	-0.56	**-0.35**	**-0.47**	**-0.53**	-0.25	**-0.52**
tGrad – NAO	**-0.60**	-0.23	**-0.40**	**-0.53**	**-0.70**	-0.31	**-0.54**
NAO – mTemp	**0.66**	**0.72**	**0.72**	**0.57**	**0.68**	**0.79**	**0.79**
mTemp – STD	**-0.76**	-0.26	0.34	-0.19	0.34	**0.40**	**0.36**
mTemp – P50	**-0.40**	0.15	**0.74**	0.04	0.43	**0.72**	**0.76**
mTemp – P95	**-0.79**	-0.18	**0.60**	-0.13	0.37	**0.53**	**0.52**
mTemp – P99	**-0.79**	-0.30	**0.54**	-0.13	0.34	**0.43**	**0.37**
mTemp – diffM	**-0.75**	-0.43	0.04	-0.33	0.26	0.01	0.05
mTemp – diffE	**-0.67**	-0.34	0.11	-0.13	0.18	0	**-0.38**
tGrad – STD	**0.45**	0.13	-0.01	-0.12	-0.38	0.23	-0.27
tGrad – P50	**0.40**	0.10	-0.13	-0.17	-0.42	-0.05	**-0.48**
tGrad – P95	**0.52**	0.21	-0.05	-0.12	-0.38	0.17	**-0.35**
tGrad – P99	**0.45**	0.15	-0.16	-0.12	-0.36	0.14	**-0.34**
tGrad – diffM	**0.44**	0.20	0.10	-0.05	-0.31	0.34	-0.08
tGrad – diffE	0.26	0	-0.28	-0.07	-0.18	0	0.01
NAO – STD	**-0.42**	0.12	**0.34**	0.32	**0.44**	**0.70**	**0.58**
NAO – P50	-0.12	**0.67**	**0.64**	**0.55**	**0.52**	**0.86**	**0.80**
NAO – P95	**-0.43**	0.28	**0.53**	**0.40**	**0.46**	**0.79**	**0.70**
NAO – P99	**-0.48**	-0.03	**0.50**	**0.39**	**0.43**	**0.70**	**0.57**
NAO – diffM	**-0.46**	-0.29	0.07	0.18	**0.36**	0.48	0.34
NAO – diffE	**-0.49**	**-0.50**	0.14	0.21	0.22	-0.06	-0.30

than the southern regions, and in colder decades the northern regions also cool more strongly than the southern regions. This 'high-latitude amplification' is also found in climate simulations for future scenarios. In those simulations, it is caused by several positive feedbacks that operate more strongly at high latitudes, such as ice-snow-albedo feedback (Hall and Qu, 2006) and black-body radiation feedback (Pithan and Mauritsen, 2014). European temperature reconstructions over the past centuries also indicate that in colder periods such as the Late Maunder Minimum (around 1700 AD) temperatures in higher latitudes cooled down more strongly than further south (Luterbacher et al., 2002).

Relationship between mTemp and wind speeds

The relationship between the mTemp and the median winds (P50) is positive in all analysed simulations and reanalysis products, with the exception of the regional simulation with MM5. The correlations, taken individually, are not always statistically significant

at the 5% level. These positive correlations imply that periods with higher winter temperatures than normal also tend to show higher median winds. Contrary to the rest of the simulations and also opposite to the link found in its driving global model ECHO-G, the particular behaviour of the regional model MM5 is not limited to this particular correlation between mean air temperature and median wind. Table 4.3 already shows that the MM5 simulation often behaves differently compared to all other simulations. The other regional model CCLM does show a positive correlation between air temperature and median wind, but this correlation is lower compared to the global simulations and in the reanalysis products.
Warmer air temperatures are also strongly linked to larger values of the high percentiles of the distribution of daily wind, P95 and P99, for most of the simulations. Again, the exceptions relate to the regional model simulations MM5 and CCLM. MM5 presents a negative correlation and CCLM a weak positive correlation.
Variations in the width of the daily wind distribution are described by the differences between the high percentiles, P95 or P99, and the median wind P50. The correlations between these measures of the distribution widths and mean temperature tend to be small for all simulations with the exceptions of the regional models MM5 and CCLM. For these two regional models the correlations are strongly negative, and more strongly so for the MM5 model, indicating that in periods with warmer air temperatures the wind distribution gets narrower at the same time that it shifts to lower values of wind speed, as indicated by the negative correlation with P50.

Relationship between tGrad and wind speeds

The correlation coefficients between the distribution of wind speeds and tGrad are summarised in the third block of Table 4.3. In general, the correlations tend to be weak, with some exceptions. In the MM5 simulations they are stronger and positive, whereas in the ECHAM6 simulation they are somewhat weaker but negative. Both reanalysis products also offer a contrasting picture. In the NCEP reanalysis the correlations between tGrad and the median wind P50 or the higher percentile winds P95 and P99 are negative and statistically significant, whereas in the coastDat2 product they tend to be positive but weak.

Relationship between NAO and wind speeds

The NAO is a large-scale winter circulation pattern that describes the mean strength of the seasonal mean westerly winds in the North Atlantic-European sector and therefore it is plausible that it is also related to the distribution of the daily wind speed in Northern Europe. The correlations between the NAO index across the different simulations yield, however, an incoherent picture. Most simulations display a positive and relatively strong correlation between the NAO index and the spatially averaged P50, with the exception of the two regional models, MM5 and CCLM.

Thus, the regional models behave again differently to their respective driving GCMs. In the case of MM5 the correlation between the NAO index and P50 correlation is strikingly negative whereas in the case of CCLM the correlation is weakly positive. A positive phase of the NAO is linked to stronger westerly winds over Northern Europe and hence a negative or weakly negative correlation of the NAO with P50 is surprising. It is later shown that the negative sign of this correlation in the regional simulations is caused by the behaviour of the regional models over land areas, whereas the sign of the correlation over ocean is the expected one.
The correlation between the NAO index and the width of the distribution (STD) of wind speed averaged over the study region tends to be also positive for most simulations, indicating that stronger mean westerlies tend to concur with a wider distribution of daily wind speed. However, there are exceptions. Again, the regional model simulation MM5 displays a strong negative correlation and the regional model simulation CCLM shows a positive but weak correlation. These negative (MM5) or positive but weak (CCLM) correlations also contrast with the link between the NAO index and the width of the wind speed distribution in their parent global models, ECHO-G and ECHAM5, respectively, both of which display positive and statistically significant correlations. Similarly to the global models, in both reanalysis products the NAO index is strongly and positively correlated with the width of the wind speed distribution.

Relationship between NAO and mTemp

It is well known that the winter NAO index is positively correlated with air temperatures in Northern Europe. The link between the parameters of the wind speed distribution on one side, and the NAO or the mean air temperature on the other side may thus be just a reflection of the same physical relationship. This is also supported by paying attention to how the correlations with the NAO and with the mean temperature vary across simulations (third line in Table 4.3). It seems clear that this line in the table displays a similar, though not identical, pattern of correlations across the simulations analysed. However, the spatially aggregated analysis does not allow to disentangle which of both factors, NAO or mTemp, is the physical driving factor for the variations in the distribution of wind speed.

Relationship between mTemp, tGrad and wind speed

The correlations shown in Table 4.3 are indicative of a simple relationship between mTemp or tGrad on one side and median wind speed or the width of its probability distribution on the other side. Certainly, there must be other underlying factors that require a more detailed analysis. For instance, the period covered by the different data products is different. The reanalysis products represent the last decades, when the anthropogenic warming is probably dominating temperature trends.

In the following subsections the study investigates in more detail the links between the large-scale atmospheric drivers and the distributions of daily wind at a grid-cell level, which allows us to better understand the spatially aggregated correlations included in Table 4.3. The following figures (Fig. 4.3-4.6) display the correlation patterns between the different large-scale climate indices and the parameters of the wind speed distribution at grid-cell scale. The upper two panels in the figures show the results derived from the regional models for direct comparison with their driving GCMs. The lower two panels include the results derived from the GCM ECHAM6 (not used to drive any regional model in this study) and the two reanalysis products.

4.4.2 Simulations of the regional models CCLM and MM5 versus their driving global models ECHAM5 and ECHO-G

In the CCLM simulation (1655-1999 AD) the relationship between P50 wind speed and mTemp (Fig. 4.3) in general shows a negative correlation or correlations close to zero, with the exception of a land area east of the Baltic where the correlation is positive. Hence, in this regional simulation, colder periods can be related to generally stronger winds. In contrast, the correlation between the mean temperature and P50 in the ECHAM5 simulation is positive in the northern part of the domain, with some regions showing negative correlations in the south, in-between correlations are around zero. The MM5 and the ECHO-G simulations also display a qualitatively similar, but even more clear, contrast. In the MM5 simulation, median wind speeds over land areas are clearly negatively correlated with mean temperature, whereas over oceanic areas P50 is positively correlated with mTemp. The ECHO-G simulation displays clearly positive correlations over the whole area, similar to the ECHAM6 simulation and the regional reanalysis products.
Concerning the link between mTemp and the width of the distribution (STD) the regional simulations and ECHAM5 the STD correlates negatively with the mean temperature (Fig. 4.4a,b and c), indicating that colder periods tend to be related with a wider distribution of wind speed over the whole area. This is also supported by the negative correlation between mTemp and the difference P99-P50 (not shown, Table 4.3). Since P50 in the regional models was also negatively correlated with mTemp, the regional models tend to be associated with broader wind speed distributions and with stronger mean winds.
The ECHO-G simulation (used to drive MM5) displays, in contrast, positive correlations in a region along the North and South Baltic Sea, straddled by regions of zero or negative correlations in Scandinavia and central Europe (Fig. 4.4d).
It is assumed that these results may be induced by a stronger meridional temperature gradient (tGrad; see Sect. 4.3). This assumption is strengthened by the negative correlation between mTemp and tGrad, which shows a spatially averaged value of -0.56 in the CCLM simulation and -0.47 in the MM5 simulation. This negative correlation indicates that lower mean temperatures tend to occur with stronger meridional temperature gradients

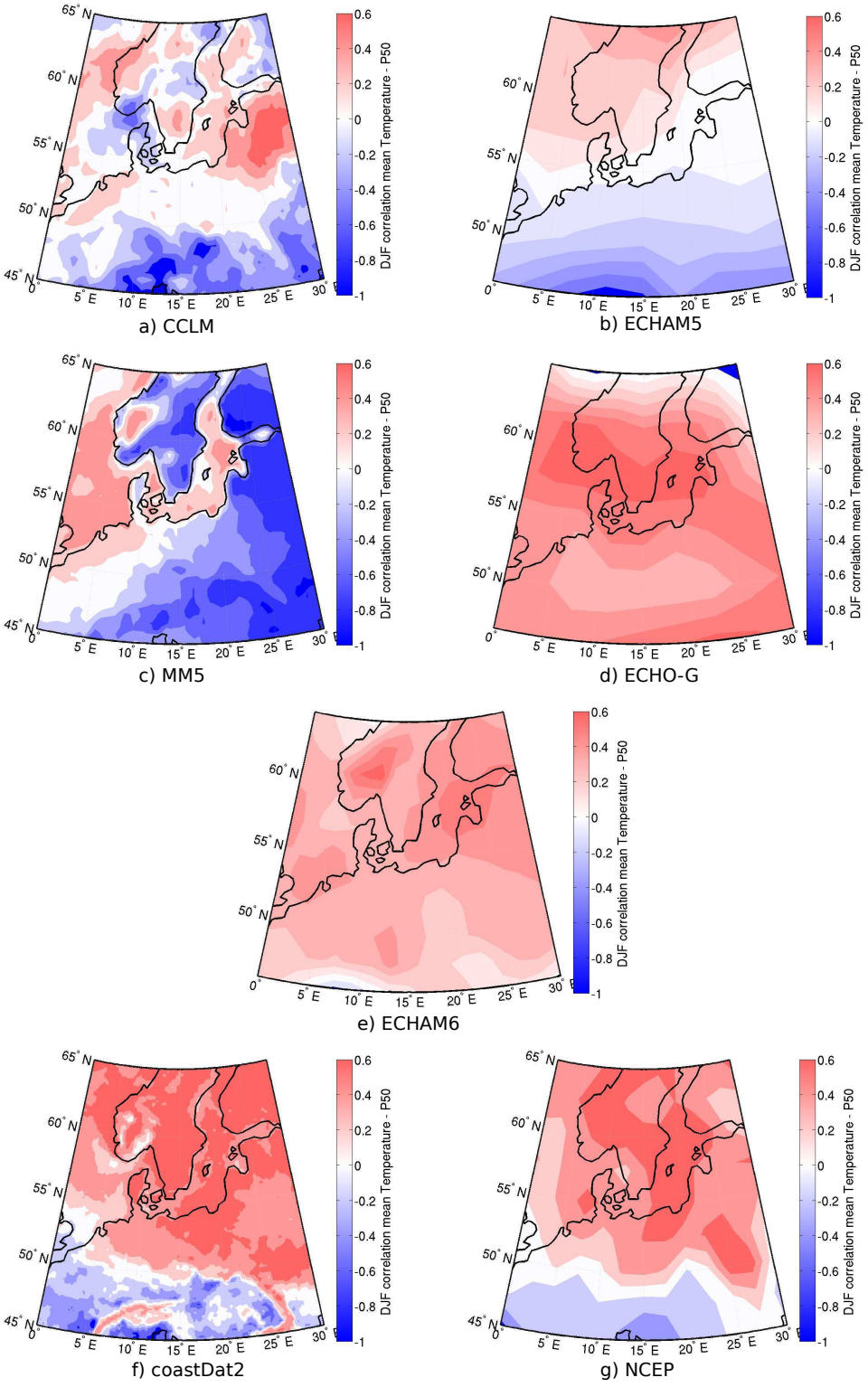

FIGURE 4.3: Correlation of field mean Temperature and 50th percentile of wind speed for 7 different data sets: a) CCLM (1655-1999 AD), b) ECHAM5 (850-2005 AD), c) MM5 (1001-1990 AD), d) ECHO-G (1001-1990 AD), e) ECHAM6 (850-2005 AD), f) coastDat2 (1948-2012 AD), g) NCEP (1948-2012 AD)

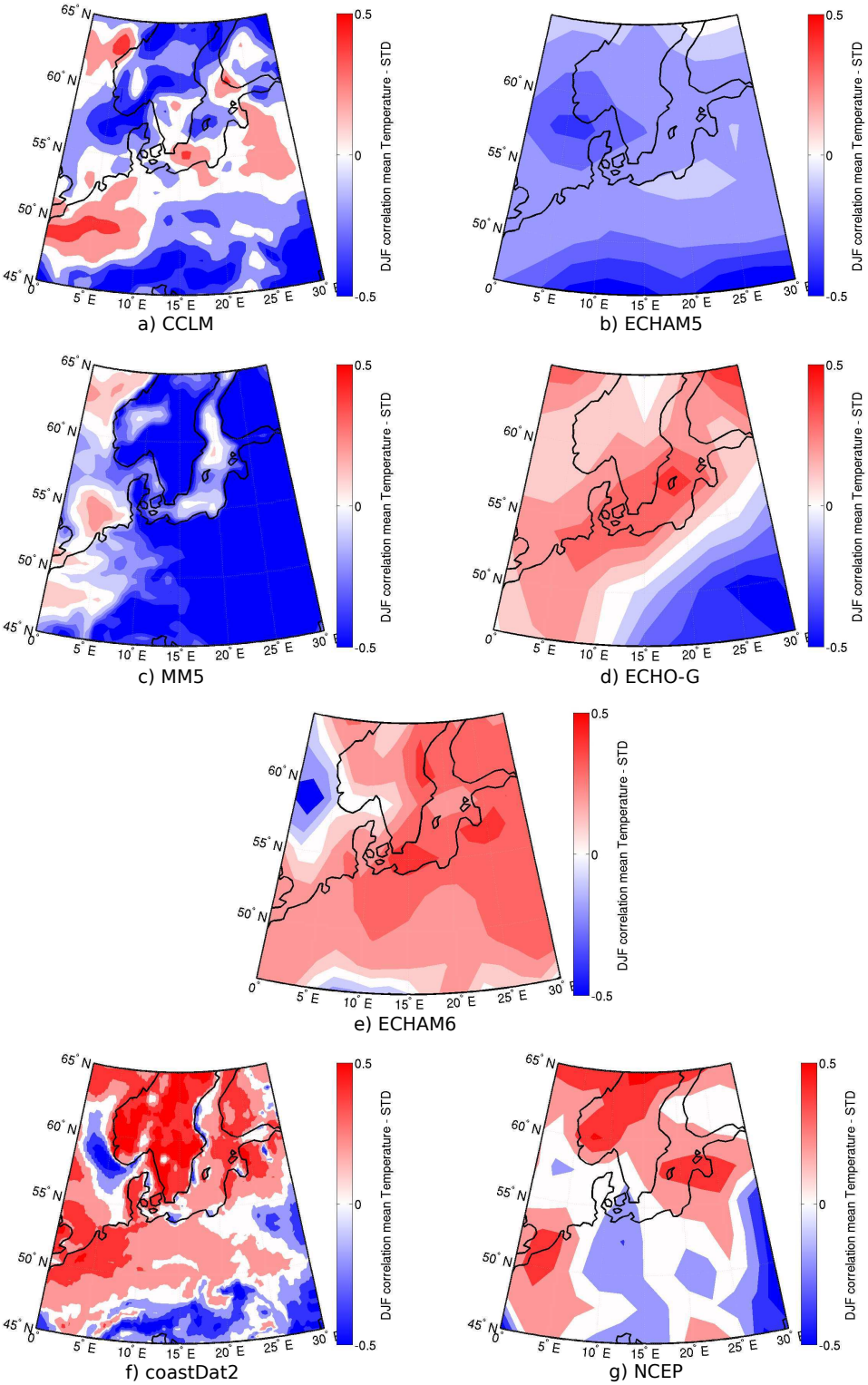

FIGURE 4.4: Correlation between field mean temperature and standard deviation of wind speed for 7 different data sets: a) CCLM (1655-1999 AD), b) ECHAM5 (850-2005 AD), c) MM5 (1001-1990 AD), d) ECHO-G (1001-1990 AD), e) ECHAM6 (850-2005 AD), f) coastDat2 (1948-2012 AD), g) NCEP (1948-2012 AD)

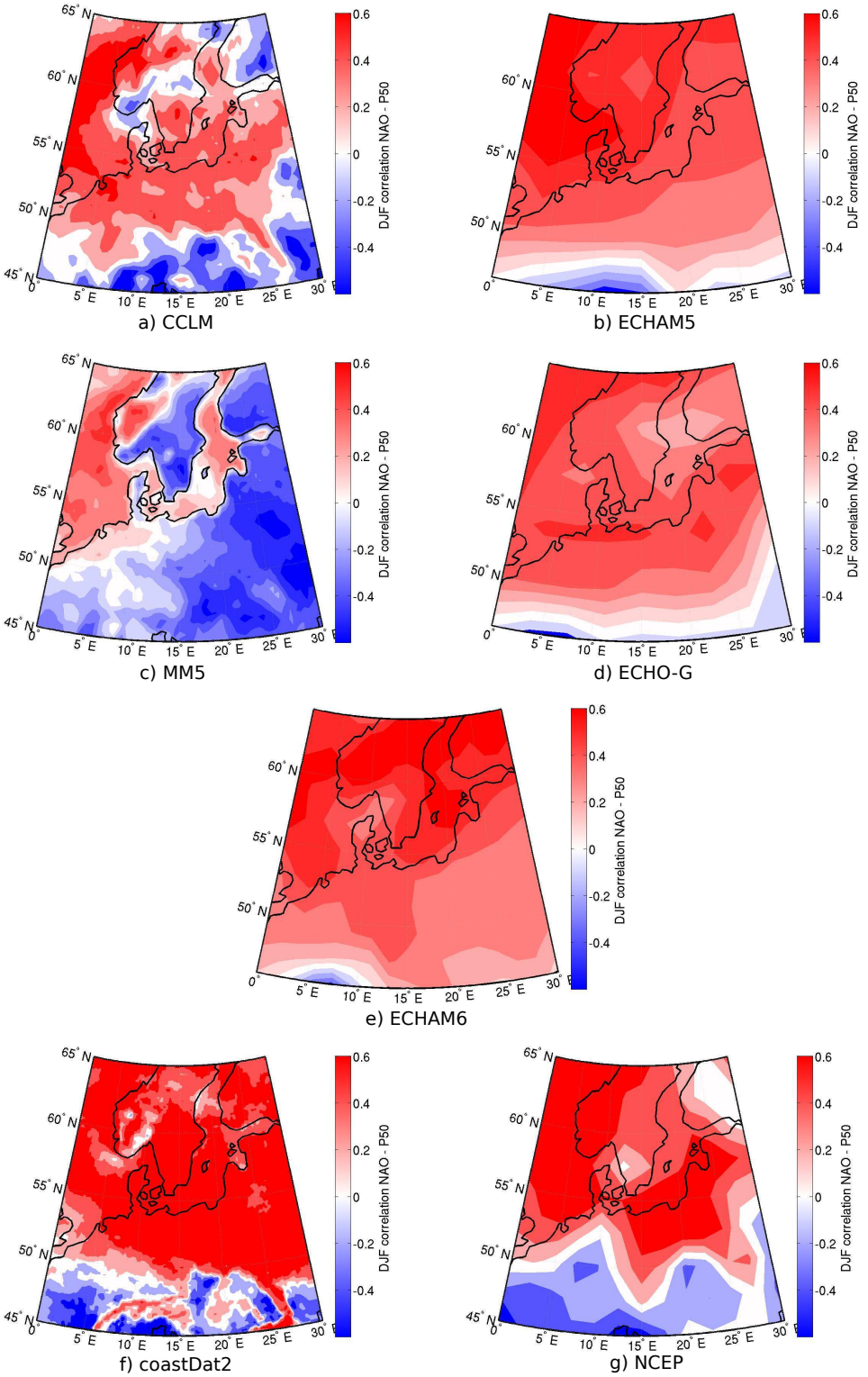

FIGURE 4.5: Correlation between NAO index and 50th percentile of wind speed for 7 different data sets: a) CCLM (1655-1999 AD), b) ECHAM5 (850-2005 AD), c) MM5 (1001-1990 AD), d) ECHO-G (1001-1990 AD), e) ECHAM6 (850-2005 AD), f) coastDat2 (1948-2012 AD), g) NCEP (1948-2012 AD)

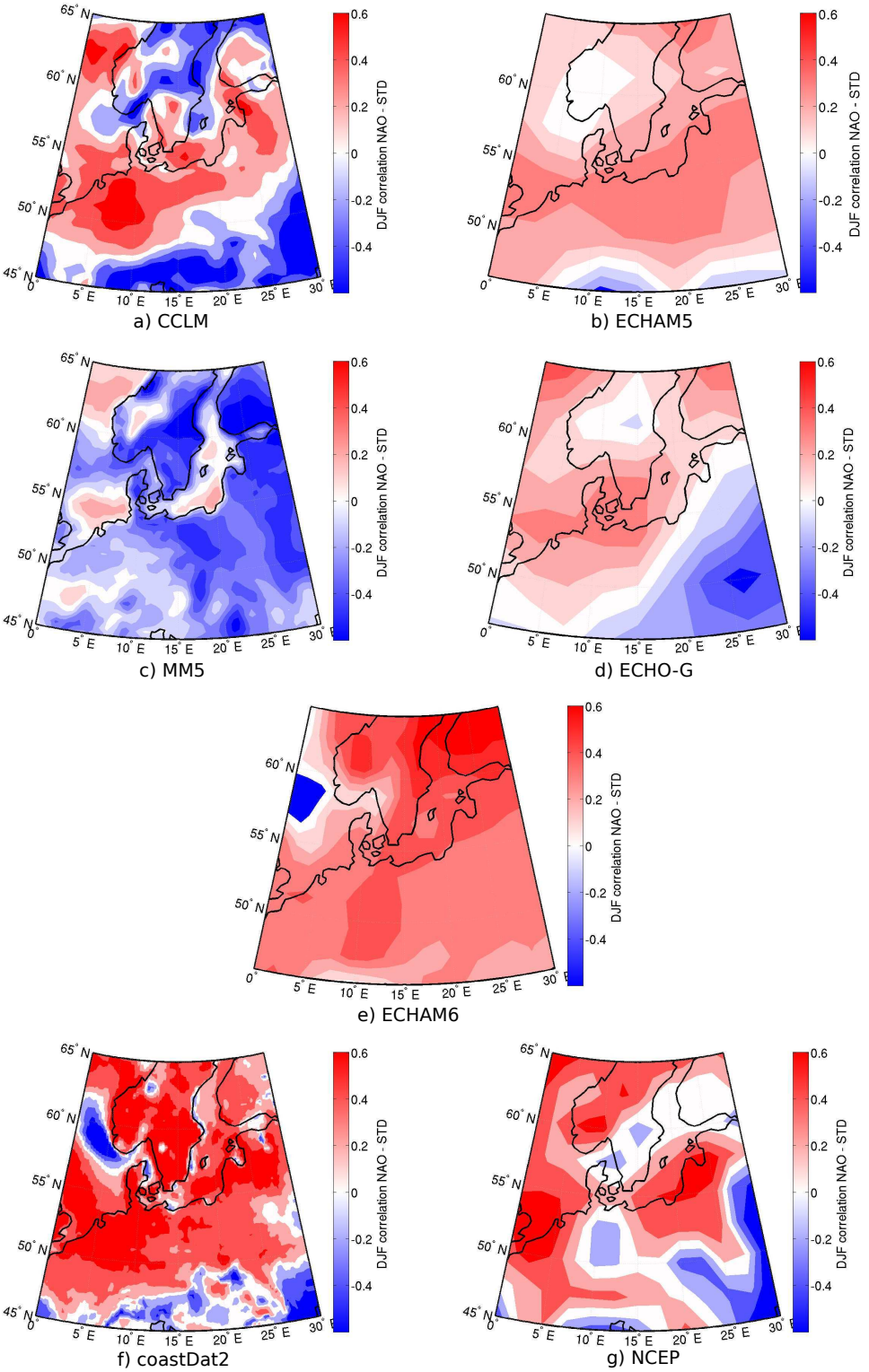

FIGURE 4.6: Correlation between NAO index and standard deviation of wind speed for 7 different data sets: a) CCLM (1655-1999 AD), b) ECHAM5 (850-2005 AD), c) MM5 (1001-1990 AD), d) ECHO-G (1001-1990 AD), e) ECHAM6 (850-2005 AD), f) coastDat2 (1948-2012 AD), g) NCEP (1948-2012 AD)

in these simulations, and thus, tGrad could be the primary driver for the changes in the wind speed distribution. Therefore, the study also analysed the relationship between the parameters of the wind speed distribution and tGrad (Table 4.3). This analysis reveals, however, contrasting results between both regional simulations: The correlations in the CCLM simulation are only minor and not statistically significant, whereas in the case of MM5 they are relatively strong for all parameters of the wind speed distribution, except for the difference P99-P95.

Additionally, the relationship between the mean NAO index and the distribution of wind speeds is investigated. The correlation coefficient between the NAO index (Sect. 4.3) and the median wind P50 displays clear similarities of the regional simulations and the driving global simulations, respectively (Fig. 4.5). However, the differences between the results provided by the regional models and those provided by the global models are profound. The correlation patterns derived from the regional models display positive correlations over oceanic areas, but in general negative correlations over land areas. This is reflected by a west-east correlation dipole (in the CCLM simulations the zero of this dipole does not coincide with the coast line). In contrast, the global simulations display positive correlations over the whole region (Fig. 4.5b,d,e). The idea that a positive NAO index should be associated with stronger winds in general is only confirmed in the global simulations. The regional models indicate that a stronger NAO tends to be linked to stronger winds only over the ocean and coastal areas, but not over Central and Eastern Europe. This difference may hint to an influence of the boundary layer parametrisation in regional models over continental areas.

The spatially averaged correlation between the NAO and STD is very low in the CCLM simulation (0.12), but much stronger and negative in the MM5 simulation (-0.42). This difference can now be explained by the different correlation patterns shown in Fig. 4.6. The spatially resolved map showing the correlation between the NAO index and the grid-cell STD in the regional models CCLM and MM5 and in the global model ECHO-G is remarkably similar to the correlation patterns between the mean temperature and the STD (compare Fig. 4.6 and 4.4). Again, the CCLM simulation shows positive correlations over North Western Europe whereas the correlations in MM5 are negative over the whole region. The global model ECHO-G tends to show higher positive correlations over the North Sea and the Southern Baltic Sea, straddled by negative correlations over Central-Eastern Europe. An exception is the result for ECHAM5, although the spatially averaged correlation between NAO and mTemp shows a high positive value of 0.57 (Table 4.3), the patterns for mTemp-STD and NAO-STD show completely different signs. A comparison with a different ECHAM5 simulation with a weaker solar forcing (Krivova and Solanki, 2008) showed rather comparable results between mTemp-STD and NAO-STD (not shown). Which leads to the conclusion that the external forcing of each simulation plays a crucial role for the relationship of mTemp and the wind speed distribution.

As already known by the scientific community NAO and mTemp are correlated, hence it is not surprising that in most simulations both show comparable relations to the wind speed

distribution. Nevertheless, due to internal model variability and different resolutions the global and regional models show different spatial fingerprints for the correlation maps.

4.4.3 The global model ECHAM6/MPIOM

In general the correlation patterns between the large-scale drivers and the parameters of the distribution of wind speed resemble those obtained with ECHAM5 and ECHO-G (ECHAM4/HOPE-G), but some clear differences exist. The higher spatial resolution of ECHAM6 does not, however, lead to correlation patterns that resemble those derived from the regional model simulations CCLM and MM5, pointing towards changes in the physical parametrisation (i.e. PBL -Planetary Boundary Layer- scheme) as the main factor explaining the differences in the simulations.
The correlation patterns between the median wind speed P50 and the mean temperature or the NAO index in ECHAM6 are indeed similar to the ones derived from ECHAM5 and ECHO-G, displaying generally positive, albeit weak, correlations between the median winds and temperature (Fig.4.3). The correlations between the median wind and the NAO index are positive and strong (Fig.4.5). However, the correlations of these two driving factors with the width of the wind speed distribution, represented by STD, differ in ECHAM6 from the other two versions of ECHAM (Fig.4.4 and Fig.4.6). ECHAM6 displays correlation patterns that are positive and spatially more homogeneous, whereas the ECHAM5 and ECHO-G simulations show higher correlations in the Southern Baltic surrounded by negative correlations in Scandinavia and Central Europe. Again, an exception is ECHAM5 correlation between mTemp and STD, which shows an over all negative relationship.
Physically, the relationship between mTemp and median wind is positive (but statistically not significant) in the ECHAM6 simulation. This indicates that warmer temperatures are accompanied by a shift towards higher wind speeds and by a slight tendency to a broader wind speed distribution (see also Fig. 4.4e). tGrad shows negative correlation with the median wind, consistent with the link between a decreased temperature gradient in warmer periods.

4.4.4 The reanalysis data coastDat2 and NCEP

The link between the large-scale drivers and the wind speed distribution for the two reanalysis products NCEP and coastDat2 is presented. It can be argued that these two reanalysis data sets should be closer to the real climate, because they both incorporate information based on meteorological observations. On the other hand, the reanalysis models are integrated over a relatively short period of time of about 60 years. Therefore the decadal-scale links between the large-scale climate drivers and the probability distribution of wind speed derived from these data sets is most likely afflicted with a higher degree

of uncertainty. The correlation patterns derived from NCEP and coastDat2 are based on gliding 5-year windows, instead of 30-year windows as for the longer simulations described before.
The correlation between mTemp and the parameters of the wind speed distribution for coastDat2 and NCEP shows generally significant positive values with P50, STD, P95 and P99, but no significant correlation for diffM and diffE. The spatially resolved correlation between mTemp and P50 (Fig. 4.3f+g) and the STD field (Fig. 4.4f+g) is also dominated by positive values, with highest coefficients over southern Norway, and weaker or slightly negative correlations in the southern regions of the domain. Therefore, the correlation patterns in the reanalysis data represent a shift of the wind speed distribution from low to high wind speeds during warmer periods, with a tendency to wider wind speed distribution in the northern and a small influence of temperature in the southern regions.
The relationship between tGrad and mTemp is negative (-0.25 for coastDat2, -0.52 for NCEP), again showing that colder periods are related to stronger meridional temperature gradients in agreement with all other models analysed here. Thus, the results obtained from the reanalysis products resemble more closely the ones derived from the global climate model simulations (ECHAM5, ECHAM6, ECHO-G) than from the regional simulations (MM5 and CCLM).
The correlation between tGrad and the distribution of wind speed is found to be predominantly weak in the coastDat2 data, with the only mentionable value (0.34) for the correlation tGrad-diffM. This result means that higher temperature differences between North and South are slightly correlated with a broader wind speed distribution. In contrast, for the NCEP reanalysis, the link is strong but opposite: weaker meridional gradients are linked to stronger median winds and wider wind speed distributions.
Regarding the link to the NAO, both reanalysis data sets display a consistent picture, with a positive NAO closely linked to stronger median winds and wider distributions (STD) in most of the domain. This link is stronger over the northern regions and becomes smaller and even negative over the southern fringes of the domain. Again, this spatial structure resembles more closely the structure provided by the global models and differs from the pattern provided by the regional models.

4.4.5 Results in the overlapping time periods 1655-1990 and 1948-1990

In this section the above explained results are compared with results for the overlapping time periods without (1655-1990 AD, 30y running mean) and with reanalysis data (1948-1990 AD, 5y running mean). Regarding the overlapping period 1655 to 1990 the main conclusions remain the same for both, Table 4.3 and figures 4.3-4.6. In Table 4.3 some correlations become higher (mTemp), whereas some stay at the same level (NAO, tGrad– beside ECHAM6 which shows values around zero) and some are lower (mTemp-tGrad).

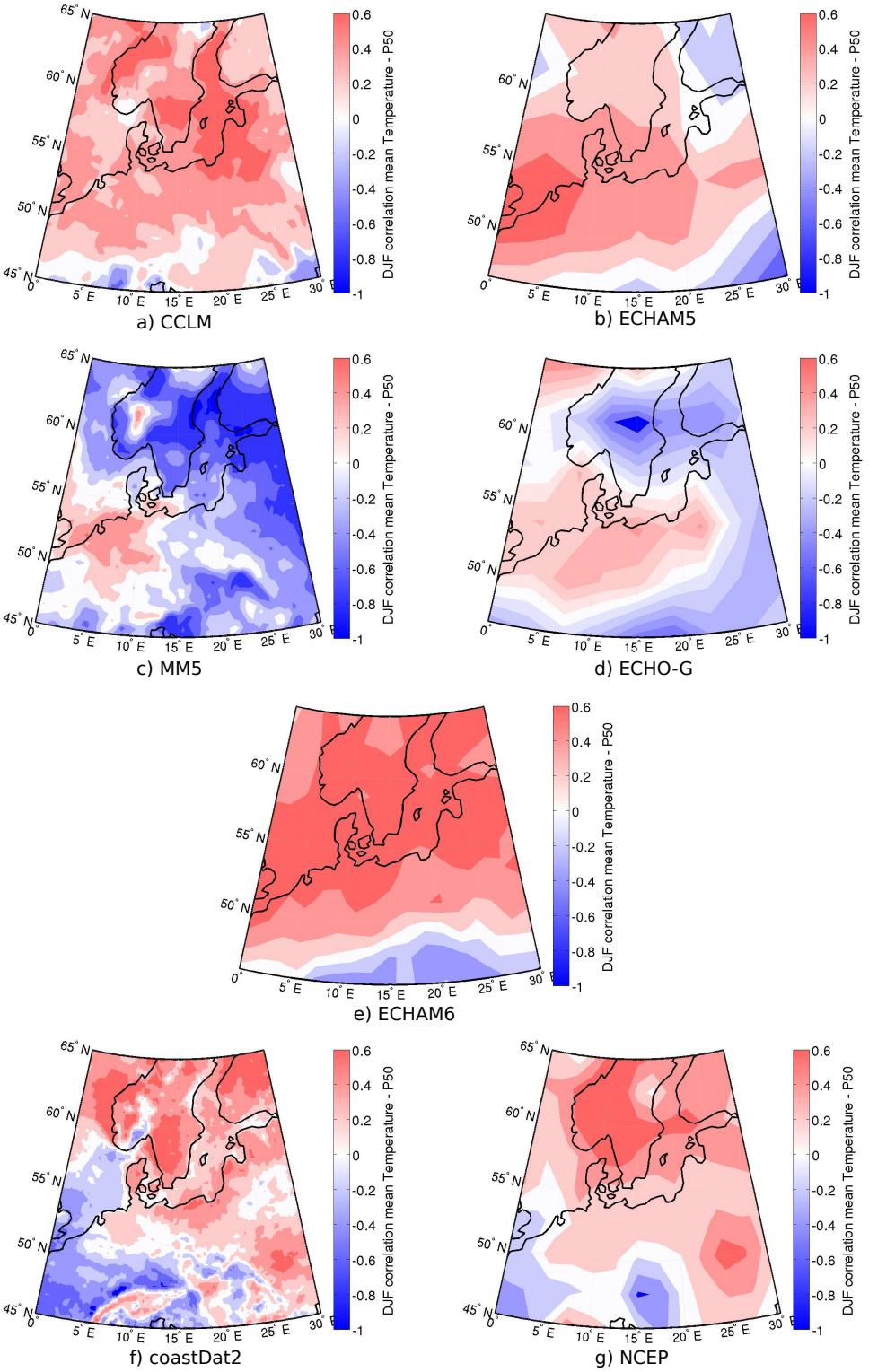

FIGURE 4.7: Correlation of field mean Temperature and 50th percentile of wind speed for 7 different data sets in the overlapping time period from 1948 to 1990: a) CCLM, b) ECHAM5, c) MM5, d) ECHO-G, e) ECHAM6, f) coastDat2, g) NCEP

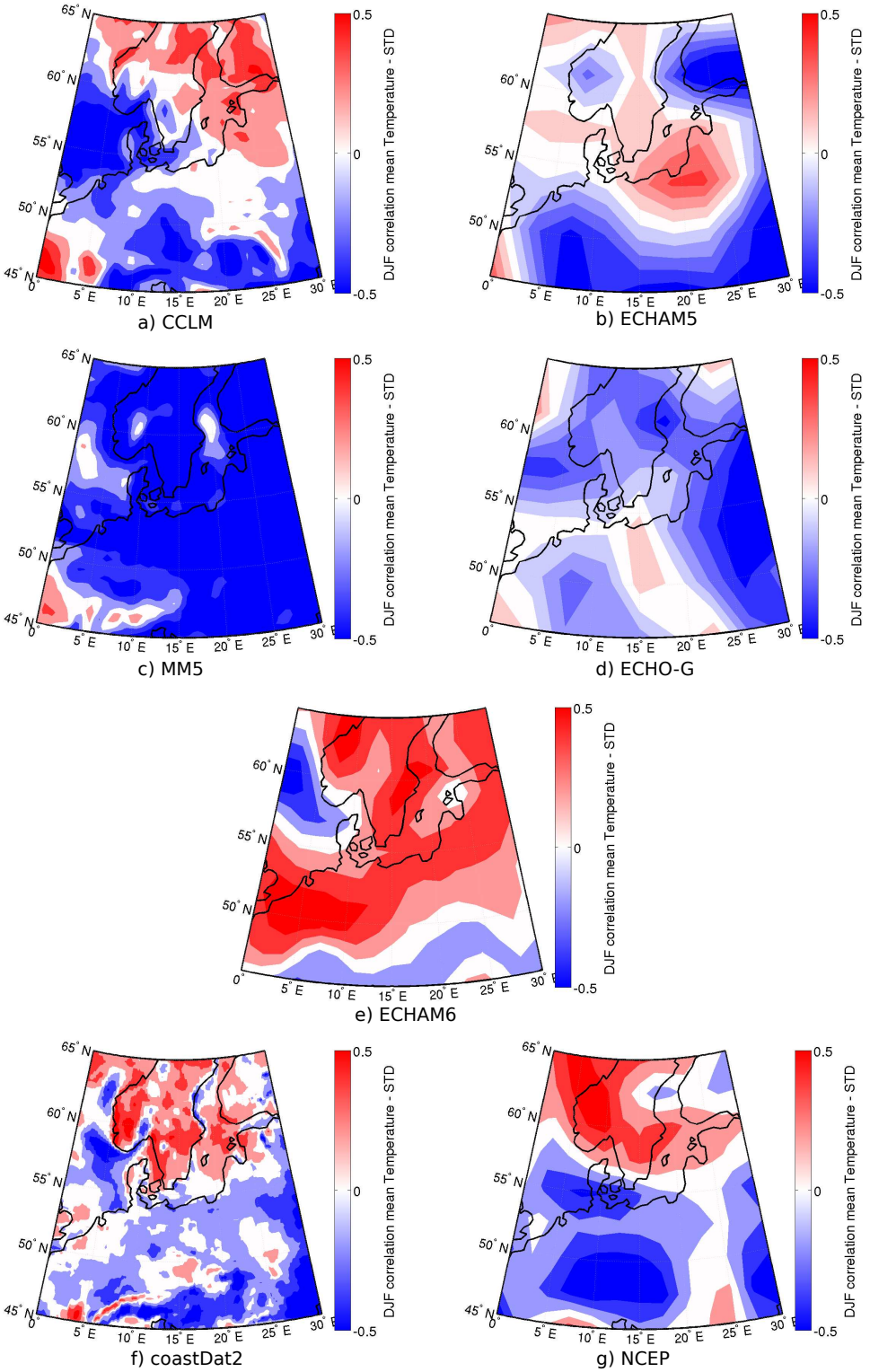

FIGURE 4.8: Correlation of field mean Temperature and STD of wind speed for 7 different data sets in the overlapping time period from 1948 to 1990: a) CCLM, b) ECHAM5, c) MM5, d) ECHO-G, e) ECHAM6, f) coastDat2, g) NCEP

The conclusions concerning the spatial correlation maps are also very comparable: Due to almost the same time period all four results for CCLM in the overlap show almost identical patterns. The GCM results are also very similar between both periods with slightly higher values for the overlapping period. Only MM5 shows a difference above western and central Europe where positive values occur for the overlapping period (1655-1990 AD) and negative or values around zero for the whole period (1001-1990 AD).
Regarding the overlapping period 1948 to 1990 the values and patterns change. Nevertheless each model simulation still shows different results, and they do not become more similar to the reanalysis data (Fig. 4.7+4.8). Figure 4.7 shows the correlation pattern of mTemp and P50 for the period 1948-1990 which shows more negative (positive) areas for MM5, ECHO-G, ECHAM6, coastDat2 (CCLM, ECHAM5) compared to the results of the whole available time periods. The results for NCEP change only marginally. For the correlation between mTemp and STD (Fig. 4.8) there are also more negative (positive) areas for MM5, ECHO-G, coastDat2, NCEP (ECHAM5). CCLM shows a shift from a positive region over the Benelux area to Scandinavia. ECHAM6 stays comparable in both periods. Note that for all data sets these results are less robust due to the fewer analysed values.

4.4.6 Centennial-scale evolution of the wind speed variance over the past millennium

In the previous sections the links between large-scale atmospheric drivers and the distribution of wind speed at decadal and multidecadal time scales are analysed. The time series of the width of the wind speed distribution over the past millennium indicate, however, that the slowly changing soil boundary conditions may also have a strong influence on the long-term evolution of the variability of wind speed in Northern Europe. Figure 4.9a shows the time series of the spatially averaged standard deviation of the wind speed distribution at each model grid-cell for the simulation conducted with the model ECHAM6. The most remarkable feature of the averaged STD is its almost continuous increase during the simulated period. This monotonous increase is also seen in the corresponding time series calculated with the output of the ECHAM5 simulation (not shown), but not in the data of the ECHO-G (based on ECHAM4) simulation (Fig. 4.9b). A suggestion about the origin of the increase in the standard deviation of the wind speed distribution can be obtained by comparing the spatially resolved STD in the last decades versus the initial decades in the simulation. Figure 4.10a shows the ratio between the spatially resolved standard deviations for the periods 1871-1990 AD (P1) and 1001-1091 AD (P2), respectively. The values of this ratio are higher than unity (STD larger at the end of the simulation) over the land areas of central Europe, with a maximum at about 25 degrees east. The standard deviation over oceanic grid-cells and over Scandinavia does not change significantly between these two periods in the simulations. Again, this spatial pattern of increase in the

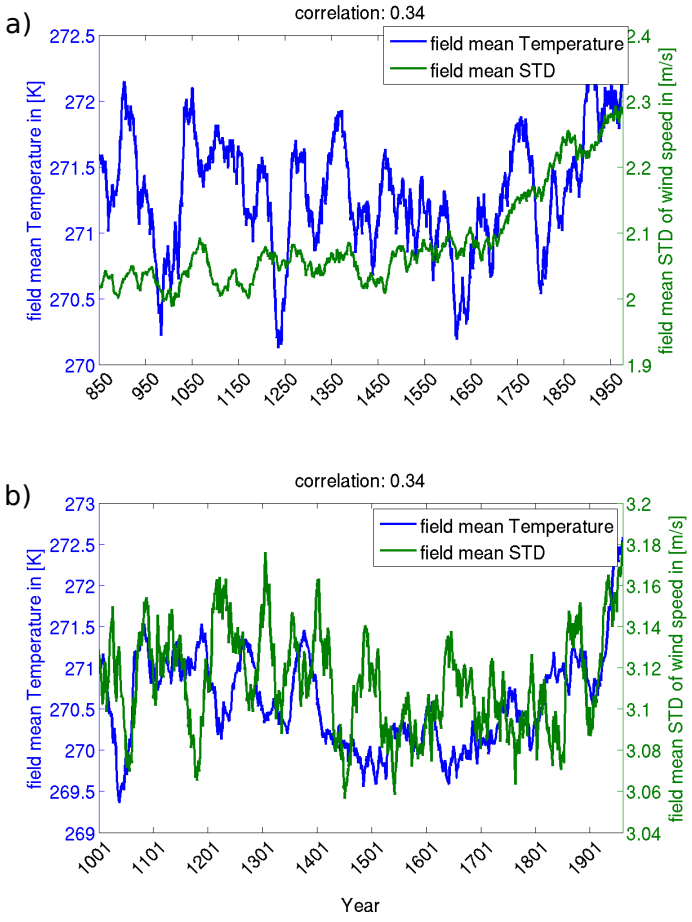

FIGURE 4.9: Time series of 30 year running mean values of mean temperature (blue) and the standard deviation (STD) of the wind speed (green) for the GCMs ECHAM6 (a) and ECHO-G (b). In both models the correlation between the blue and the green line is 0.34.

width of the wind speed distribution is also simulated by the ECHAM5 simulation (not shown), but not in ECHO-G where the ratio is scattered around 1 (not shown).

The spatial pattern of changes in STD between the beginning and end of the ECHAM6 and ECHAM5 simulation suggests that the increase in the width of the wind speed distribution may be related to surface-boundary processes. This suggestion is supported by the changes in forest cover in the course of the last millennium as reconstructed by Pongratz et al. (2008). This reconstruction was used to drive the models ECHAM6 and ECHAM5 (see Sect. 4.2). The difference in tree fraction in each model grid-cell between the periods 1871-1990 AD (P1) and 1001-1091 AD (P2) is shown in Figure 4.10b. The spatial agreement between the reduction in tree fraction and the widening of the wind speed distribution between the beginning and the end of the millennium is remarkable and strongly supports the hypothesis that the distribution of wind speed is mainly affected by land-use changes and related changes in surface roughness length.

This is supported by the analysis of a third time period from 1571 to 1690 AD (P3) which

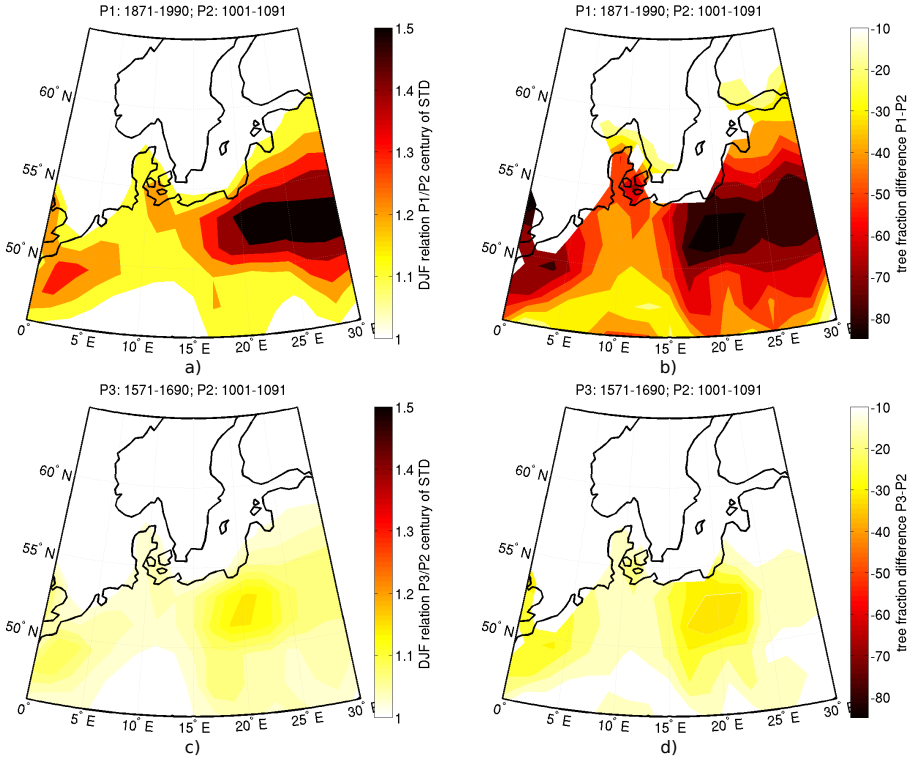

FIGURE 4.10: a) Relation between part 1 (P1: 1871-1990 AD) and part 2 (P2: 1001-1091 AD) standard deviation (STD) of wind speed (ECHAM6). b) Tree fraction difference of P1 minus P2 derived from Pongratz et al. (2008). c) Relation between part 3 (P3: 1581-1690 AD) and P2 STD for ECHAM6. d) Tree fraction difference of P3 minus P2 derived from Pongratz et al. (2008).

also shows a strong agreement for the STD ratio (P3/P2; Fig. 4.10c) and the tree fraction difference (P3-P2; Fig. 4.10d), albeit with less intense values presumably due to the less intense deforestation in period P3. Hence, it is concluded that a less extensive forest cover causes a widening of the wind speed distribution, and vice versa.

This is also visible for the time series in Figure 4.11a, which shows the temporal evolution of the tree fraction (black line) and the 30 year running mean STD for ECHAM6 (green line in Fig.4.9a multiplied by -1), both lines show a remarkable agreement in the long-term evolution. The simulation with ECHAM5 shows a comparable evolution for the STD (not shown). The simulation with the model ECHO-G, which was not driven by changes in land use, does not show a long-term increase or change in the width of the distribution of wind speeds (see green line in Fig.4.9b), supporting the strong influence of land cover changes on the distribution of wind speeds.

Therefore, at multi-centennial time scales the correlation between the wind speed distribution and temperature that was explored in the previous sections, for ECHAM5 and ECHAM6, could have been indirectly caused by land-use changes. At these time scales, anthropogenic deforestation and mean temperature exhibit a positive trend. Thus the expansion of the wind speed distribution and the increase of temperature in these decades

might be induced by physically different factors, leading to positive correlations in this analysis.

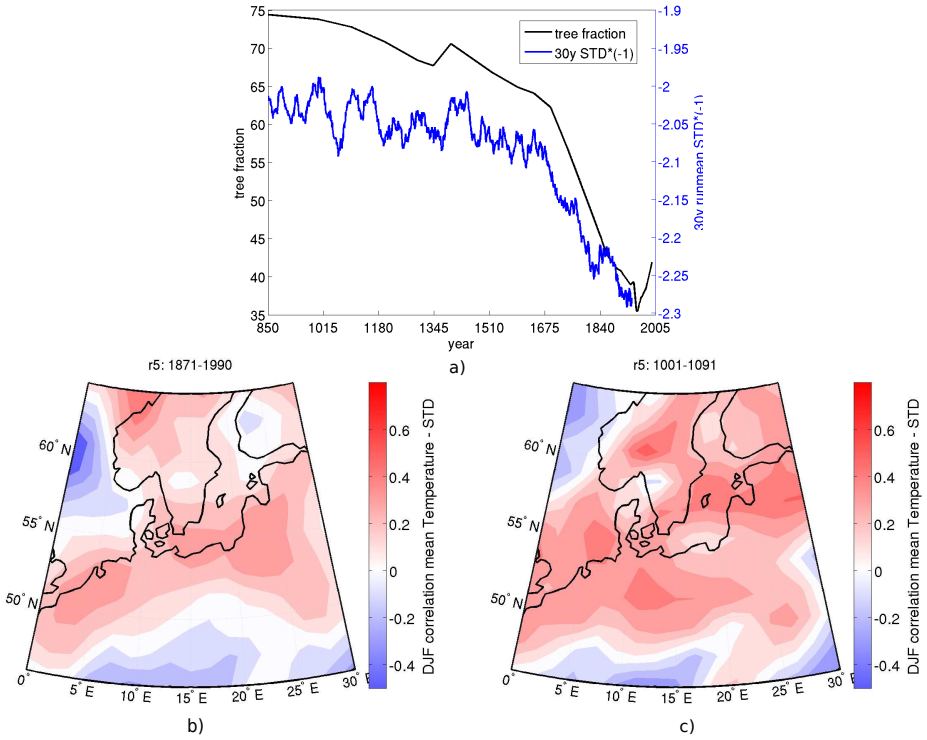

FIGURE 4.11: a) tree fraction after Pongratz et al. (2008) (black) averaged over the investigation area. ECHAM6 30 year running mean STD of wind speed (multiplied by -1) (blue). b) correlation between field mean temperature and STD for 1871-1990 with a 5 year running mean computation c) correlation between field mean temperature and STD for 1001-1091 with a 5 year running mean computation.

Figure 4.11a shows the temporal evolution of the tree fraction used to drive ECHAM5 and ECHAM6 (black line). This proves that on shorter time scales (e.g. 100 or 200 years) the effect of this surface-boundary process is negligible, especially before the 17^{th} century when the trend is very weak. Figures 4.11b+c exhibit the correlation between mTemp and the STD for the periods P1 and P2 calculated with a 5 year running mean. Hence, these figures show the relationship between mean temperature and the wind speed distribution independent of the deforestation effect. Therefore, this statistical effect can be disentangled by separating the analysis of these simulations into two time periods (TP1: years 850-1500 AD, TP2: years 1500-2005 AD).

The correlations between mean temperature and the width of the wind distribution does show a difference in the correlation. For TP1 of ECHAM6 mTemp-diffM is around 0 and mTemp-diffE -0.25, for P2 0.63 and 0.57, respectively. For TP1 of ECHAM5 mTemp-diffM is -0.26 and mTemp-diffE is -0.38, for TP2 0.26 and 0.12, respectively. Both time periods in the GCMs show different signs for the relation between mean temperature and the shape

of the wind speed distribution. These results suggest that specifically for ECHAM6 the correlation between the mean temperature and the width of the wind speed distribution is a statistical artefact mediated by deforestation.

4.5 Discussion and conclusions

This study investigates and compares different simulation data sets and reanalysis products, on time scales covering the last decades to the past millennium, regarding the probability distribution of the daily wind speed in winter time over Northern Europe. This investigation is aimed at identifying the large-scale factors that drive changes in this probability distribution. The study is based on correlations between different parameters of the wind speed distribution and different climatic indices related to mean temperature, meridional temperature gradient and the North Atlantic Oscillation. The overlaying question is whether and how the wind speed distribution may change during varying climate conditions and hence whether these conditions may provoke more and/or stronger wind speed extremes.

One prominent result is that the link between the thermal indices and the North Atlantic Oscillation appears physical consistent in all data sets, and thus all models are consistent in this regard. The relationship between the NAO and mean temperature over Europe is a known effect (Rutgersson et al., 2015), in wintertime this is also positive in all models. This effect is caused by the advection of maritime air masses by stronger westerly winds in a more positive NAO state (also discussed in Gómez-Navarro et al., 2015a). Also, the correlation between mean Temperature (mTemp) and the temperature gradient (tGrad) shows negative values for all models, indicating that warmer periods are linked to a weakened meridional temperature gradient. This might be explained by the fact that northern regions warm (cool) more strongly when the overall temperature is higher (lower). In climate change projections this is referred to as polar amplification, although it has been also identified in paleoclimate simulations and reconstructions over the past millennium (Luterbacher et al., 2002).

However, a second important result is that the correlation between the large-scale indices and the parameters of the wind speed distribution exhibit markedly different results among the data sets analysed and it is difficult to derive general conclusions on the effect of these large-scale drivers on the distribution of daily wind. Comparable difficulties are reported by Fischer-Bruns et al. (2005). They analysed two simulations of ECHO-G. One simulation showed a link between temperature and storm track variability over the North Atlantic Ocean, which also would have an influence on the wind speed over Europe, whereas the other simulation did not show such a connection. Furthermore, these authors conducted a literature review about climate change experiments with global climate models which lead to different conclusions. Some models therein indicated an intensification of North Atlantic storm tracks, whereas others showed no changes during a warming climate or

even a reduction of extreme winds in the North Atlantic area.
Nevertheless, in this study the three global simulations present similarities that warrant to place them in one group. Fig. 4.3 through 4.6 show patterns of correlations obtained in the global simulations that are generally similar. This can be expected to a certain degree because the three atmospheric models included in the GCM belong to the same ECHAM family. And further analyses with completely different GCM families would be necessary to reinforce these findings. Likewise, the correlation patterns obtained from the two regional models are also generally similar, although in this case both models, MM5 and CCLM, are structurally different.
The striking result is that the regional models do not seem to inherit the dynamical properties of their respective global models, but produce instead different correlation patterns between the large-scale drivers and the wind speed distributions. In the case of the link between the median wind and the large-scale drivers, the differences between each regional model and its driving global model mostly occur over land areas (see Fig. 4.3 and 4.5). However, in case of the link between the standard deviation of wind speed and the large-scale drivers, the differences seem spatially more complex (see Fig. 4.4 and 4.6). It is plausible that the higher resolution and the different parametrisation schemes of the boundary layer shape the link between the large-scale dynamics and turbulent processes that modulate the width of the daily wind distribution. As Hall (2014) and Gómez-Navarro et al. (2013) already stated the RCMs should provide a better representation of small-scale processes, topographic influences and of the land-sea contrasts, and thus should be better suited for the simulation of extreme events.
The comparison of the correlation coefficients in Table 4.3 shows differences in signs and statistical significance. Regarding statistical significance, it is noticeable that for tGrad and wind speed there are only significant values for MM5 and NCEP, although with different signs. CCLM as one of the regional model simulations is the only simulation which shows almost no significant correlations. Its forcing global model ECHAM5 only shows significance for the NAO - wind speed correlation. ECHAM6 as the successor of ECHAM5 also shows only significant values for tGrad - mTemp and for NAO - wind. ECHO-G and coastDat2 show significant values for wind speed values in correlation with mTemp and NAO.
The correlation between tGrad and wind speed shows significant values only for MM5 and NCEP but both data sets exhibit different signs. MM5 reveals positive correlations, which implies that stronger winds are associated with a stronger temperature gradient. This positive correlation is only appreciated for the regional data sets: MM5, CCLM and coastDat2. The global data sets, ECHO-G, ECHAM5, ECHAM6 and NCEP, show negative values, indicating stronger winds corresponding to weaker temperature gradients. Thus, only the regional data sets support the findings of Li and Woollings (2014), which say that weaker meridional temperature gradients induce weaker or less storms due to a weaker baroclinicity. These results demonstrate that the influence of the spatial resolution and especially the different boundary layer parametrisation may be a critical factor to

establish a link between climate change and changes in near-surface wind speeds.
Another indicator for the influence of the spatial resolution on these results might be the fact that only the regional simulations MM5 and CCLM show strong negative correlations between mean temperature and the width of the probability distribution as measured by diffM/diffE. These correlations suggest that colder periods are connected with stronger wind speed extremes. In contrast, the GCM data show no clear correlations between these parameters. This study does not allow us to provide a comprehensive dynamical explanation for the different behaviour of wind speeds in changing temperature or pressure conditions: the models show different results although each model seems to be dynamical consistent in itself. Therefore, a detailed analysis of each of the simulations, and maybe of the computer codes, becomes necessary to understand how the different correlation patterns arise.
On centennial time scales, I identified land-use changes as a very important factor modulating near-surface wind in the simulations. Note that anthropogenic changes in land-use are prescribed only in the ECHAM5 and ECHAM6 simulations, whereas for ECHO-G land-use is kept constant during the whole simulation. The analysis of the ECHAM5 and ECHAM6 millennium simulations reveals a strong increase of the standard deviation of wind speed for the last decades since the industrialisation, and in areas that coincide with larger deforestation along the last centuries. The impact of land-use changes on wind conditions was also shown by Pessacg and Solman (2013) in simulations with the regional model MM5 over South America for different idealised land-use scenarios.
The main conclusion that can be drawn from this study is that the link between large-scale climate drivers and the distribution of daily wind speeds in wintertime in this region is complex and not fully constrained by currently available simulations. All models analysed here have been individually profusely used in climate simulations and the data sets have been used in a number of other previous studies, and no gross deficiencies have been pointed out so far. This study is new because it employs recently available long high-resolution paleo-simulation, and compares all these models regarding a relationship between temperature and NAO conditions and wind speed. I conclude that, although climate models may be dynamically sound in the large-scale contest, the impact of climate change on variables like near-surface wind speed distribution possibly depends more strongly on the details of the physical parametrisation and changes in surface forcing, like deforestation, than on the large-scale dynamical drivers, such as large-scale temperature or sea-level-pressure changes.

5 A wind proxy based on migrating coastal dunes: statistical validation and calibration.

The previous chapters exhibited the need for more reliable data sets regarding the analysis of wind variability. One possibility might be presented by proxy data. Although for temperature and precipitation there already exist a number of proxies there still is a deficiency on wind proxies on annual temporal resolutions. In the frame of CLISCODE - the project this study is based on - Ludwig et al. (2015) presented a dune record for the analysis of annual and even seasonal wind-field variations based on a dune system located at the Baltic Sea coast of Poland.
The following analysis statistically validates this dune record and shows that it derives acceptable validation values as a wind proxy.

5.1 Introduction

Future climate change may induce changes in wind conditions at all time scales, ranging from multi-decadal trends to changes in the daily and seasonal variability including wind extremes. To analyse future wind changes it is essential to understand how changes in the external forcing influenced wind conditions in the past. In contrast to other meteorological parameters like temperature or precipitation, there is a dearth of wind proxy records capable of reflecting changes in past wind regimes. And any proxies, although possibly imperfect, can be very useful in this regard. Recently, Ludwig et al. (2015) presented a new proxy for annual wind-field variations based on a composite bar code, reflecting the width of different dune layers that are annually formed, of a dune system alongshore the polish Baltic Sea. This study aims at the statistical analysis of this new wind record.
Aeolian processes are the result of interactions between climatic factors like temperature, precipitation or wind and land surface, therefore it can be assumed that coastal dunes include information about changes of these atmospheric parameters (Lancaster, 1994). The analysed dunes migrate and are composed of alternating, varying sediment properties with homogeneous sand grains, which contain information about how the dune structure responded to past wind conditions during migration. These varying sediment properties can be seen as an analogous to tree ring width records, which also may include information about changing climate conditions (Girardi, 2005). This kind of dunes do not only exist at the Polish coast, but also e.g. at the Curonian spit (Lithuania) where the alternating

dune structure is also interpreted as a result of winnowing of lighter quartz grains due to higher wind speeds (Buynevich et al., 2007).
The potential of dunes to give information about storminess has already been analysed (Clemmensen et al., 2014; Costas, 2013; Reimann et al., 2011), but existing studies use the connection between dune structure and wind only on decadal or millennial temporal resolution. The novelty of the Ludwig et al. (2015) study lies in the focus on seasonal to annual resolution.
Proxy-based reconstructions of wind conditions may offer the advantage of a better temporal homogeneity than observational records, for which changes in the location of the measure device may result in very large stepchanges in the mean wind and wind variability. In addition, dune-based records may help fill spatial gaps in observational data sets, which might be of special interest for analyses of the changing wind climate. For example there are many wind analysis using pressure measurements as wind proxy, to take advantage of the better homogeneous properties of pressure readings over time (e.g. Alexandersson et al., 2000; Krueger et al., 2013), while others try to infer information of past wind events from documented damages on dikes (De Kraker, 1999) or forests (Nilsson et al., 2004).
Many studies have addressed past changes in wind climate (see review by Feser et al., 2015, and references therein) with many different approaches. Some analyse wind speed changes (among others: Alexandersson et al., 2000; Gulev et al., 2001; Krueger et al., 2013; Matulla et al., 2007; Wang et al., 2006) and some wind direction changes (e.g. Jaagus and Kull, 2011; Lehmann et al., 2011), both on different time scales and with different data sets. These studies include analyses of observations derived from instrumental records (Chaverot et al., 2008; Franzén, 1991), but these data sets are likely not totally consistent due to instrumental changes or relocations.
Some studies have used meteorological reanalysis, which should in principle overcome the inhomogeneity problem, instead of direct station observations (e.g. Gulev et al., 2001; Wang et al., 2006). Reanalysis is a method which uses a combination of weather information (e.g. surface weather stations, satellites) of past weather records which run through a meteorological forecast model to produce a gridded, homogeneous data set of many atmospheric and oceanic variables with a temporal resolution of a few hours (Dee et al., 2015). Due to their use of observations, this kind of data may span a limited period in which the records can be considered homogeneous. However, I use the connection to observations as an advantage and validate the possible dune archive with a regional reanalysis data set.
Here, the statistical links at inter-annual time scales between wind conditions in different seasons and the annual dune layers are studied, and the relationships between the reconstructed wind and wind characteristics with a focus on wind direction and strength are assessed. I include precipitation and temperature into this analysis to learn more about the dependencies of these three atmospheric factors and their influence on the dune system. The time series here was conducted with two dendrochronological methods, namely replication and cross-dating. This was done by Ludwig et al. (2015) to overcome missing

values and dune-to-dune variations inside the dune system, which consists of seven active dunes. Although the analysed dune archive covers only a short period from 1987 to 2012 this analysis can be considered relevant for the paleoclimate community because it verifies an attempt to apply dendrochronological methods to identify dunes as wind proxies. Hence, this analysis could be adopted to other dune systems which are bigger and or move more slowly, e.g. at the Curonian spit.
This paper is structured as follows: Chapter 2 describes the analysed data from the coastDat2 reanalysis and the Łeba dunes. Chapter 3 explains the used statistical methods. Chapter 4 presents the results. A discussion of the results and conclusions closes the manuscript.

5.2 Data and area

In the following the reanalysis product coastDat2, used in this study, is introduced and briefly discussed. Furthermore, the investigation area Łeba and its climatological and dune characteristics are described. An elaborated description about the analysed dune data can be found in Ludwig et al. (2015).

5.2.1 Meteorological data

For the main investigation, wind data from the regional reanalysis data set coastDat2 (Geyer, 2014) is used. Please note that meteorological reanalysis are the result of a model simulation, in which observations have been assimilated. The meteorological model is the same for the whole period of reanalysis - in contrast to the operational reanalysis used for real weather forecasts - in which the model has been continuously improved trough time. The number of observations assimilated in the reanalysis may change over time as well, but since one of the aims of meteorological reanalysis is to produce an homogeneous data set, the changes in the number and coverage of observations is usually kept to a minimum, at least over several decades. For reanalysis that span longer periods, like the 20CR product (Compo et al., 2011) covering the last 150 years, this condition cannot be fulfilled. In this case, the coastDat2 data set covers the period from 1948 onwards. And thus, it can be considered to be largely homogeneous.
Hence, this kind of data sets are supposed to resemble the reality and to be strongly related to observations. In this study, the analysed data set is coastDat2, a result of a regional climate simulation with the non-hydrostatic operational weather prediction model COSMO in CLimate Mode (COSMO-CLM, Rockel and Hense (2008)) driven by meteorological initial and boundary conditions from NCEP/NCAR Reanalysis 1 data (1948-present; T62 ($1.875° \approx 210$ km), 28 level, (Kalnay et al., 1996; Kistler et al., 2001)). The simulation was conducted, applying spectral nudging (after von Storch et al., 2000). It has a spatial

resolution of 0.22° and the output is available on hourly temporal resolution. However, the dunes cannot provide such high resolutions, hence, it is decided that daily averaged data is sufficient.
Weidemann (2014) compared the measured wind conditions at three German coastal stations (Kiel, Warnemünde, Kap Arkona) with the COSMO-CLM (used to generate coastDat2) model output. He reported a slight systematic overestimation of wind speed, but good agreement regarding daily mean wind speeds, generally acceptable results regarding the daily wind speed variability - notwithstanding an underestimation of high wind speeds - and comparable wind directions. He stated that some discrepancies might be introduced by the model COSMO-CLM, but that others might be due to in-situ measurement errors. A more detailed description of coastDat2 can be found in Chapter 2.2.1.
The relationship between wind and sand migration may additionally be dependent on other atmospheric parameters, like precipitation and temperature. Regarding temperature, the daily mean 2-meter temperature from coastDat2 is used. Regarding precipitation the daily sum of total precipitation, which includes convective and large-scale precipitation as well as snow is used. The results obtained with coastDat2 data were also confirmed with precipitation data provided by the Climate Research Unit (CRU; Mitchell and Jones, 2005). This gridded data set is the result of a spatial interpolation of station data. The obtained results were found to be comparable (not shown).

5.2.2 Łeba dunes

The active dune system in Łeba (Poland) covers an area of 5,5 km^2 and is situated on top of a barrier that separates the Lake Lebsko from the Baltic Sea. To the north, pine trees and foredunes prevent sediment supply from the beach to reach the proper dune system; hence, the material that forms the dune is self-contained with little contamination from outside the system and public entering is prohibited since 1967.
These barchanoid dunes are up to 600 m long and 27 m high. The material is fine-grained and well-sorted and the dunes attain an average migration velocity of around 10 m/yr. This dune system has been geologically analysed before by Borówka and Rotnicki (1995); Borówka (1980, 1979, 1995). They also mentioned some climatological characteristics of this area, which will be briefly recapped and compared to own results in the following subsection. Additionally, an overview about their results and results from Ludwig et al. (2015) regarding the relation of wind and this dune structure will follow.

5.2.2.1 Climatological characteristics

Due to its west-east alignment, the dune migration is strongly connected to westerly winds (Borówka, 1980), which mostly occur and are strongest during winter and autumn (see Chapter 2). Westerly winds transport the sand from the luv side (west) of the dune to

the lee side (east) of the dune and so contribute to the eastward movement of the dune (Fig. 5.1) due to sediment deposition on the eastern dune side. Hence, the more westerly winds the thicker are the dune layers, which also means a higher dune migration velocity. Additionally to wind, temperature and precipitation have an influence on the Łeba dune

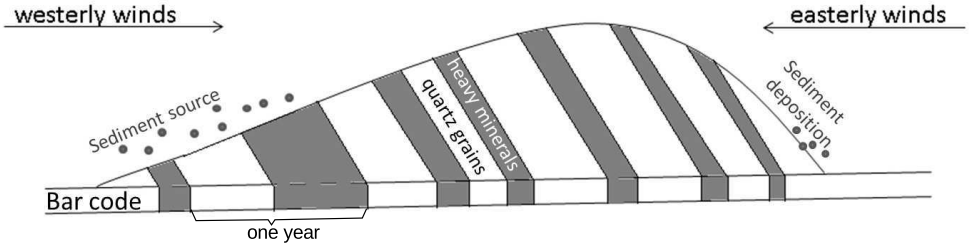

FIGURE 5.1: Schematic representation of the Łeba dune structure (adapted from Ludwig et al. (2015)), consisting of white (quartz grains) and black (heavy minerals) layers.

migration. Nevertheless, winds are the most important drivers of aeolian processes in general. Borówka (1980) reported the mean annual total precipitation amount in the research area to be about 700 mm with a maximum occurring in summer and autumn. Furthermore, he stated that the area undergoes only small annual temperature variations. From coastDat2, within the period 1948-2012, I calculated a mean annual precipitation amount of about 630 mm and seasonal mean temperatures for winter=−1.6°C, spring=5.4°C, summer=15.7°C, autumn=7.9°C averaged over the area shown in the right panel of Figure 5.2. These values change only slightly when considering the period covered by the dunes (1987–2012). The precipitation amount is then 627 mm and seasonal mean temperatures are: winter=−1.1°C, spring=5.8°C, summer=16.2°C, autumn=8.1°C.

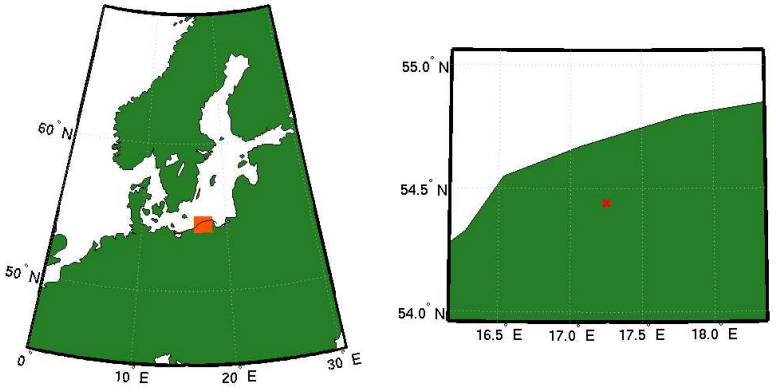

FIGURE 5.2: Location of investigation area. Left: Red box marks the area of the analysed gridded wind information from coastDat2 (1987-2012). Right: Analysed area with dune location (red dot) close to Łeba, Poland.

5.2.2.2 Archive of seasonal wind intensity

The homogeneous dune properties prevent grain size characteristics to be used as an indicator of wind speed. However, the dune sands are characterised by alternating changes in the sediment composition, which shows intervals dominated by light quartz grains and intervals with interspersed layers of heavy minerals. Both intervals are caused by seasonally changing wind conditions (Borówka, 1980; Ludwig et al.). The quartz layer (white colour) consists of quartz grains with some particles of heavy minerals (black colour). Both kinds of grains are mainly transported to the east by westerly winds. Furthermore, Borowka's observations of the Łeba dunes unveiled that winds from the east winnow quartz grains, leaving accumulated heavy minerals, hence a black layer develops.
Easterly winds are most frequent in spring, but the strongest winds occur during autumn and winter, when prevailing west winds dominate and quartz-dominated intervals in the dune layers develop. Ludwig et al. (2015) showed, that a quartz-dominated interval (white layer) and an interval with layers enriched in heavy minerals (black layer) represent a whole year. This alternating pattern is termed sedimentary bar code (Fig. 5.1), and it varies from year to year. Ludwig et al. (2015) compiled this bar code out of six different profiles from the dune system. These profiles differ from dune to dune. They applied two dendrochronological methods, namely replication and cross-dating, to overcome dune-to-dune variations and gaps in the sedimentary record.
Annual variations in the bar code thickness, and hence in the migration rates, correlate with changing west wind intensities. A comparison with wind data extracted from the reanalysis data set coastDat2 with the bar code thickness showed that during years with strong west winds the net dune progradation to the west is higher than during years with weaker west wind intensities. The bar code covers a time period of 26 years from 1987 to 2012. The above mentioned results from Ludwig et al. (2015) are statistically validated in this study.

5.3 Statistical methods

This study focuses mainly on the relationship between sand movement and wind conditions during different seasons: Winter (December to February; DJF), Spring (March to May; MAM), Summer (June to August; JJA) and Autumn (September to November; SON). The analysed wind conditions are defined based on wind speed thresholds. These thresholds, relevant for sand movement at the investigation side, are unknown, so that different thresholds have been used to find an optimal relationship between wind conditions and the dune bar code. The study also uses eight different wind direction subdivisions (North=N, North-East=NE, East=E, South-East=SE, South=S, South-West=SW, West=W, North-West=NW), 360 degrees are divided into eight equal sectors of 45 degrees each to derive conclusions on the dune driving wind directions.

The results used to develop the linear regression model are based on the Pearson correlation coefficient. Therefore, the number of daily wind means above predefined wind speed and direction with the migration velocity of white, black and both combined layers are seasonally correlated. In this way the leading relationships between the white and black bars (predictor–y) and different combinations of wind direction and wind speed (predictand–$\tilde{y}$) are identified. Afterwards a linear regression model (Eq. 1) is applied based on this relationship. This model is tested and validated with the help of cross-validation, namely the leave-one-out-method (Birks, 1995; Michaelsen, 1987). This validation technique is commonly used for dendrochronological analysis to investigate the linear relation between tree ring width and temperature when the temperature record is short.
The leave-one-out-method addresses the problem of a short record of observations that does not leave enough independent data for validation, once all data have been used to calibrate the statistical model. In the leave-one-out method to validate the statistical model, all observations except one are used to calibrate the statistical parameters. The calibrated statistical model is then used to estimate the value of the predictand for the first time step, which is then compared to the observation. A complete loop over all observations is then conducted in which at each step only one observation is not included in the calibration of the statistical model. In the end, a measure of the statistical skill is obtained as an average of the mismatch between estimated and observed values of the predictand at each 'left-out' time step. In this case, this means that successively one of the available 26 predictor values (bar thickness) is left out and the remaining 25 values are used to "predict" the corresponding days per wind direction over a pre-defined wind speed threshold (predictand). In the end there are 26 predicted wind condition values ($\tilde{y}$), which can be compared to the actual values (act(y)) derived from coastDat2. Both are compared with the help of the root-mean-square-error (rmse–Eq. 2), which can be used to determine the explained variance ($rmse^2$) and the correlation coefficient is calculated between predictand and actual values.
In addition, I try to find an optimal ratio between the number of westerly and easterly winds that better describe the thickness of the black layer. Thereby, a local regression is used - here local means that the regression is based only on a set of observational data points (x,y) - that lie within a certain limited region in a x-y plot. The value of the parameters of the statistical model thus depend on where the observations are numerically located. The statistical models that are used in this analysis are weighted linear least squares and a 2nd degree polynomial model. This regression is named 'loess' and it is equivalent to finding a smooth curve composed of linear of second-degree polynomials that better fit the (x-y) data points. The span for this filter is optimised with the lowest root-mean-square-error after the leave-one-out-method.

$$\tilde{y}_i = p1_i * y_i + p2_i \tag{5.1}$$

$$rmse = \sqrt{\frac{\sum_{i=1}^{n}(act_i(y) - \tilde{y}_i)^2}{n}} \tag{5.2}$$

5.4 Results

Before the linear regression model is applied to identify a relationship between dune migration and wind conditions, the connection between the dune movement and other atmospheric parameters is analysed. The following chapter is devoted to the correlation between the migration velocities of the white and black layers and temperature, precipitation and wind. Afterwards, I explain the results concerning the linear regression model between the migration velocity and wind for a specified direction and speed threshold.

5.4.1 Dune migration velocity and meteorological forcing

As mentioned above, the dunes in the area are formed of alternating layers with different sediment compositions, termed "bar-code". The white bars (layers), containing mainly quartz sands, have a mean thickness of 6.86 m. The black bars (layers) are characterised by heavy minerals and show an averaged thickness of 5.67 m. The dune migrates by the action of the wind as material from the rear part of the dune is transported over the dune all the way forward to the head of the dune. The nature of the transported material depends on the meteorological characteristics that prevail during the transport time, and thus on the seasonality. As it will be explained later, the succession of white and black layers corresponds to the annual cycle in the meteorological characteristics and this allows for the dating of each pair of layers. In this case, the time period covered by the layers formed in the dunes span the years 1987-2012.
The thickness of both type of layers varies, but not independently of each other: the thickness of the back and white layers correlates with 0.48 and the whole dune system is moving about 12.53 m per year on average. This dune migration is influenced by atmospheric parameters. These parameters are temperature, precipitation and wind. The most important parameter is obviously the wind as it transports the sand. Nevertheless the other factors have some influence:

Precipitation

The study investigates the relationship between bar thickness and seasonal precipitation. The amount of soil wetness influences the compactness of the top layers of the dune and their sensitivity to the wind drag. Statistically, this relationship appears to be different for the two bars. For the white bar the only noticeable correlation is found for autumn

(SON) with 0.24. The black bar shows a mentionable correlation only for spring (MAM), which is negative (-0.38). I assume that these contradicting correlations are in correspondence to the wind conditions during these seasons. In autumn, the wind is stronger and precipitation does not hinder the sand transport, especially for lighter white particles. In spring the wind speed is lower and therefore precipitation might prevent sand transport because wet grains are heavier and they may stick together. Hence, the quartz grains cannot be 'blown out' and therefore there are less concentrated black particles in the dune layer, which is the reason for a negative correlation with spring precipitation for the black layer.

Temperature

The temperature also shows relations to the white and black dune layer thickness. The white layer has slight correlation coefficients in spring (-0.27) and autumn (0.29) with contradicting signs. The black layer shows correlations in winter (-0.21) and autumn (0.45). The colder half-year apparently reveals a negative correlation between temperature and bar thickness. Therefore, dunes migrate less in colder winter and spring seasons. In summer the temperature does not seem to play any role or maybe the dunes are not migrating in this season, due to the weaker winds. In autumn, sand movement tends to be faster with higher temperatures.

The two meteorological parameters temperature and precipitation combined might play a role, especially during winter seasons. It is assumed that low temperatures, below zero, together with precipitation stabilise the dunes and thus hinder the sand transport. To consider this effect I analysed the correlation between wind conditions and sand movement by excluding or including days with frost and precipitation. The biggest differences can be seen in winter (compare Fig. 5.5a and 5.3a), some differences in spring (compare Fig. 5.5b and 5.3b) and none in summer and autumn (not shown). Winter and spring show with and without frost days the same correlation sign but some correlations are higher for days without frost and precipitation. In spring higher correlations can be seen for northern and eastern winds, but they are still quite low. For winter the correlation coefficients get higher without frost and precipitation especially for black bars and northern and eastern winds. Nevertheless, autumn still has the highest correlations between wind and bar thickness.

Wind

The analysis regarding the relationship between wind conditions and layers is based on wind intensity per wind direction. The latter is divided into eight subdivisions (N, NE, E, SE, S, SW, W, NW). The wind intensity is defined by applying two measures. One measure is the mean wind speed per wind direction calculated only in the days from a certain wind direction. The second measure is the number of days per wind direction.

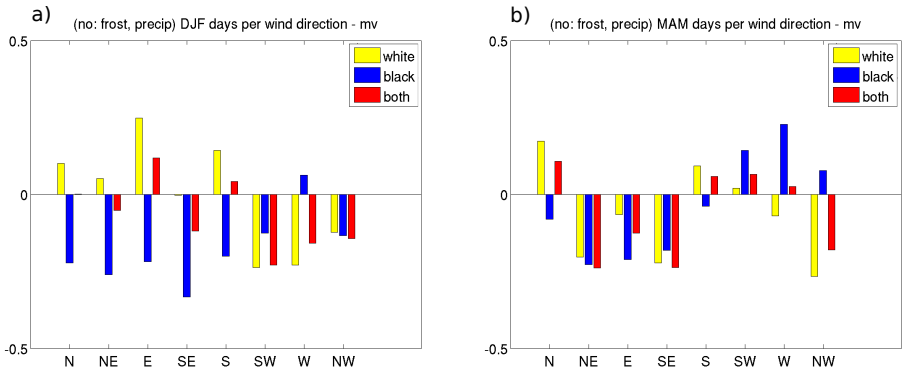

FIGURE 5.3: Correlation between the number of days per wind direction without frost and precipitation days and dune thickness (migration velocity–mv) of the white layer (yellow), black layer (blue) and both together (red). The correlations are shown for the seasons winter (DJF), spring (MAM) and for eight wind directions.

The correlations between white, black and combined bar thicknesses and these two wind intensity measures for the eight predefined wind directions are shown in Fig. 5.4 and Fig. 5.5, respectively. The correlation coefficients reveal winter and summer to be the least

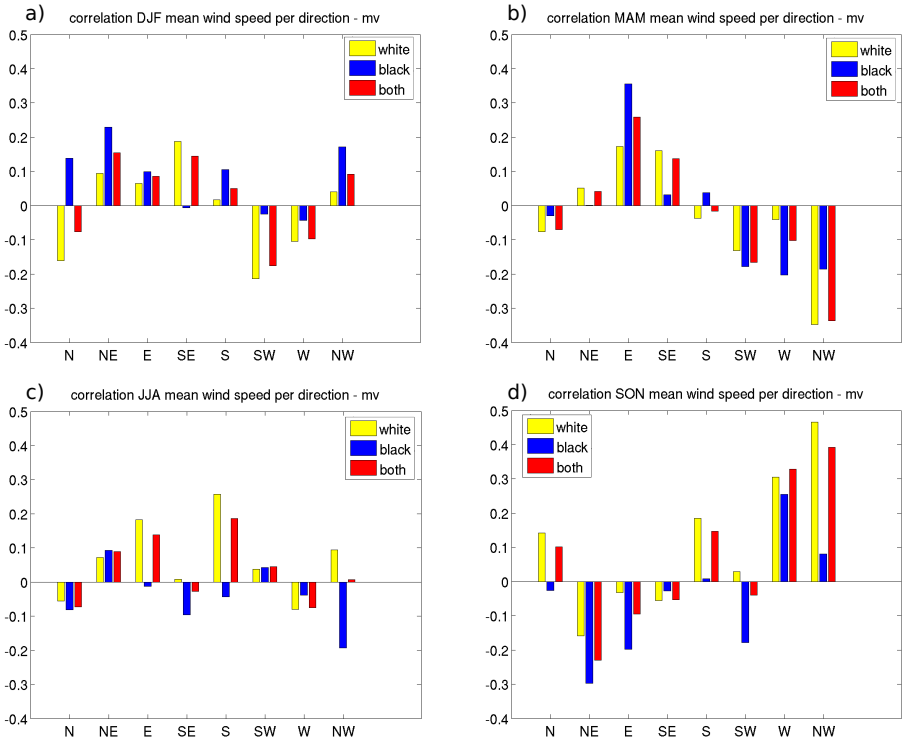

FIGURE 5.4: Correlation between mean wind speed and dune thickness (migration velocity–mv) of the white layer (yellow), black layer (blue) and both together (red). The correlations are shown for the seasons winter (DJF), spring (MAM), summer (JJA) and autumn (SON) and for eight wind directions.

effective seasons regarding sand transport regardless of the wind intensity definition. Only in spring does a noticeable difference exist between the two definitions, mean wind speed

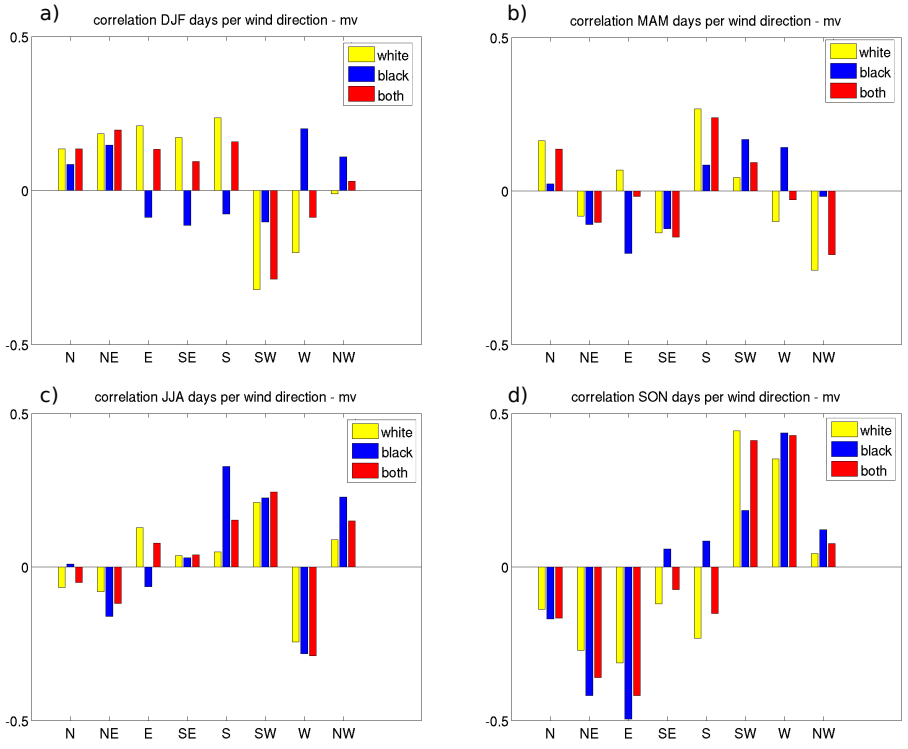

FIGURE 5.5: Correlation between the number of days per wind direction and dune thickness (migration velocity–mv) of the white layer (yellow), black layer (blue) and both together (red). The correlations are shown for the seasons winter (DJF), spring (MAM), summer (JJA) and autumn (SON) and for eight wind directions.

and days per wind direction. During this season, the mean wind speed from E apparently has an influence on the thickness of the black layer. The duration of wind directions seems to be less effective in spring. This is an interesting result as it is an indication for the winnowing of white and black grains as mentioned by Borówka (1979). Nevertheless, autumn is the season with highest correlations for both measures and both bars, pointing to this season to be the most important for sand transport. During this season the number of days per wind direction shows higher correlations with the bar thickness.

As a next step, days per wind direction with wind speeds over a predefined wind speed threshold are analysed to connect the two measures of wind speed and days per wind direction. The wind speed is binned into 10 groups ranging from 0 to >10 m/s. The only wind directions with mentionable correlation coefficients are W, SW, E, NE in spring (Fig. 5.6) and autumn (Fig. 5.7). The correlation coefficients in the other seasons and wind directions are predominantly low (not shown). The results regarding the following analysis focus on spring and autumn because the results show that these seasons are the driving seasons.

In spring there is a difference between the sign of the correlation coefficients of high (>7 m/s) and low (<4 m/s) wind velocities. For W and SW (Fig. 5.6a+b) wind directions the sign of the correlation is positive, and is especially stronger for the black layer regarding

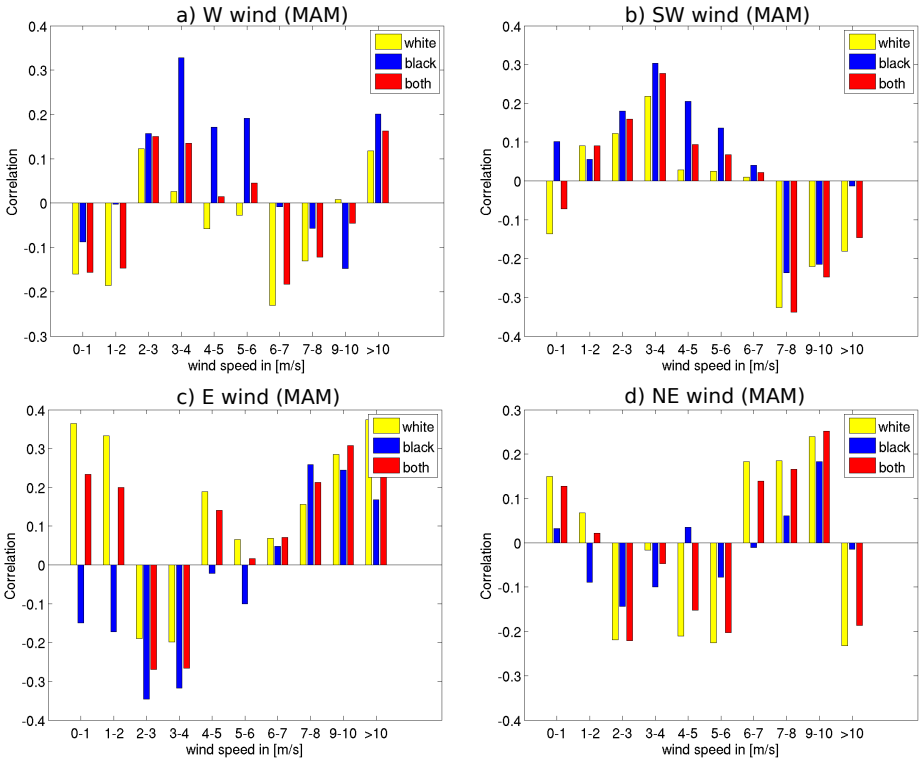

FIGURE 5.6: Correlation between the number of days per wind direction in a specified range of wind speeds and dune thickness of the white layer (yellow), black layer (blue) and both together (red). The correlations are shown for the seasons spring (MAM) for W (a), SW (b), E (c) and NE (d) wind directions.

low wind speeds. For SW winds the correlation to wind speed is negative, especially for the white layer, regarding high wind speeds. The opposite occurs for E winds (Fig. 5.6c). Low wind speeds correspond to a negative correlation for the black layer and high wind speeds show a positive correlation for both layers. NE (Fig. 5.6d) winds show only small correlations (<0.3) for all wind speeds.
In autumn there is no such separation between high and low wind velocities for the above mentioned wind directions. W winds show strong positive values for all wind speeds higher than 5 m/s (Fig. 5.7a). SW winds show also high positive correlation coefficients for wind speeds from 3 to 5 m/s for both layers (Fig. 5.7b). NE winds (Fig. 5.7c) and E winds (Fig. 5.7d) have negative correlations with both layers regardless of the wind speed.

5.4.2 Linear regression

The highest correlation between days per wind direction and the thickness of the white and black layer can be seen in autumn for W and SW wind directions, thus this season and directions are used to develop a linear regression model with the layer thickness as predictor and wind speed as predictand. For W winds correlations are highest for wind speeds >= 5 m/s (see Fig. 5.7a). For SW winds correlations are highest for wind speeds

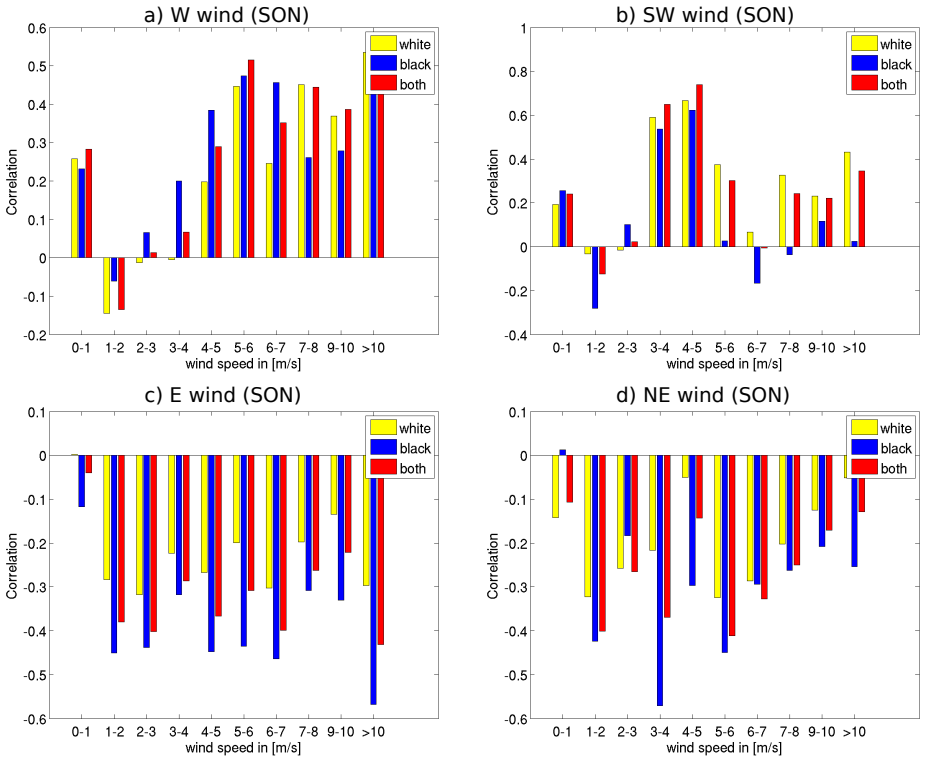

FIGURE 5.7: Correlation between the number of days per wind direction in a specified range of wind speeds and dune thickness of the white layer (yellow), black layer (blue) and both together (red). The correlations are shown for the seasons autumn (SON) for W (a), SW (b), E (c) and NE (d) wind directions.

from 3 to 5 m/s (see Fig. 5.7b). The linear relationship between days per wind direction with these predefined wind speeds and the migration velocity of black and white layer is tested with the leave-one-out-method (Sec. 5.3). I use the migration velocity (predictor), and its linear relation to the number of days with SW and W wind with the above mentioned wind speed (predictand). The leave-one-out-method allows for the validation of this relation by comparing the predictand with the actual number of days per wind direction. The correlation coefficients for predictand and actual values, the rmse and the explained variance of this analysis are shown in Table 5.1 for W (SW) winds.

The best results are obtained for SW winds, which is likely due to the stricter defined wind speed threshold. With this threshold values for the correlation between migration velocity and days per wind direction are higher (compare Fig. 5.7a,b). However, a stronger limitation applied for the wind speed (3-5 m/s), excludes a lot of observations, and therefore this result is less robust than the results obtained for W winds. Nevertheless, the validation of W winds shows comparable results to accepted validation values of dendrochronological analyses.

TABLE 5.1: Correlation, rmse and explained variance values (obtained with leave-one-out validation) used to compare predicted and actual number of days per wind direction. The prediction is based on dune thickness, which is identified to have a linear relation with W winds over 5 m/s and SW winds between 3 and 5 m/s.

		correlation	rmse	exp. variance
W	white	0.35	3.16	12.2%
	black	0.31	3.20	10.1%
	both	0.42	3.06	17.9%
SW	white	0.61	1.58	37.1%
	black	0.53	1.70	27.8%
	both	0.68	1.46	46.8%

There is a strong positive (negative) connection between the migration velocity of the black layer and W/SW (E/NE) winds. I assume that white and black sands are transported together eastwards by westerly winds. In days with easterly winds, which are usually weaker, only the white lighter particles are transported to the back of the dune, enriching the black layer. This idea of winnowing was already explained by Borówka (1979) for the Łeba dunes.

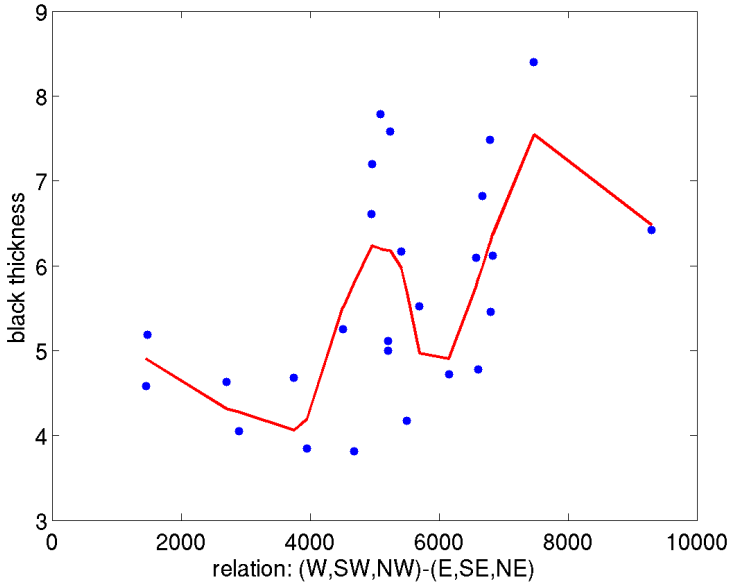

FIGURE 5.8: Scatter plot of the difference between westerly (W, SW, NW) and easterly (E, SE, NE) winds and the black layer thickness. The red line shows the smoothing with a loess filtering (see Sec. 5.3).

As already mentioned, westerlies transport white and black particles together to the east, where they deposit and build a new layer. Easterly winds on the other hand winnow only the lighter white grains and transport them backwards to the west, hence a black layer forms. This effect lead to the idea that there might be an optimal ratio of days with west

and east winds per year, which defines the black layer thickness.
To test this hypothesis I use a scatter plot of the difference between west (W, SW, NW) and east (E, SE, NE) winds during all seasons and the black layer thickness per year (see Fig. 5.8). The data points are smoothed with a loess filter (red line in Fig. 5.8). If an optimal ratio between east and west should exists, the smoothed curve would show a clear maximum. This result does not show this maximum and therefore no clear optimal ratio can be derived from these results. Nevertheless, there seems to be a minimum value of this ratio (≈ 4000) under which the black layer remains small.

5.5 Discussion and conclusions

This analysis validated migrating coastal dunes identified by a geological analysis of Ludwig et al. (2015) as a new wind proxy. The analysed dunes at the polish Baltic Sea coast are characterised by alternating white and black bars representing light quartz grains and heavy minerals. These bars might be regarded as analogous to tree ring width records. The analysis of the dune records composite was conducted similarly as with dendrochronological methods. Hence, the chosen validation technique is also a common tool to verify the relation between tree-ring width and temperature.
The study investigated the relationship between bar thickness and the atmospheric parameters: precipitation, temperature and wind. The focus lies on the relation to wind conditions because wind is assumed to actually transport the sand grains. However, precipitation and temperature also have an influence on dune migration:
Regarding precipitation, the results showed contradicting signs for the white and black bars for spring (MAM) and autumn (SON). The white layer showed a positive correlation for autumn. One reason for this result might be that in autumn the wind is stronger and precipitation does not hinder the sand transport. In fact some rain might improve the transport due to turbulence, which makes more sand grains available (Borowka 1980). In spring, the black layer showed a negative correlation with wind speed. This season is characterised by lower wind speeds and therefore precipitation might prevent sand transport because wet grains are heavier. The influence of precipitation on sand transport, and hence the dune processes, depends on the seasonal wind conditions.
A contradiction between seasons is also apparent regarding the temperature relation. The results showed that dune layers migrate less in the colder seasons winter and spring, probably due to stabilising effects during frost days. In the warmest season summer there is only minor migration visible due to weak winds. Hence, the dune primarily migrates in autumn, a season without frost but with strong winds.
Due to its west-east alignment the dune is most sensitive to westerly (W, SW) and easterly (E, NE) winds. This relationship with wind is seasonally dependent. In spring the influence is wind speed related. Low wind speeds correlate positive (negative) with westerly (easterly) winds and the opposite is true for high wind speeds. In autumn the influence is

strongly direction dependent, westerly winds correlate positively with dune layer thickness and the easterly winds correlate negatively, more or less independent from wind speed.
These results showed that the dune movement is most dependent on autumn and spring weather conditions. The black layer development, in particular, seems to depend strongly on the spring conditions, a season characterised by NE and E winds of less intensity. These results support the idea, put forward by Borowka (1979), of the winnowing of white particles. The less intense easterly winds in spring are only strong enough to transport the white particles backwards (westwards), thus, heavy minerals get concentrated and build a black dune layer at the lee side of the dune.
After analysing the influence of meteorological parameters on dune migration, the study focused on the linear relationship of the migration velocity and the frequency of days with SW and W winds surpassing a specific wind speed threshold. The derived linear relationships were validated with the leave-one-out method due to the limited length of the observational record. This linear model allowed to hindcast the wind speed from the migration of the dunes over the past decades. The correlations between the observed and reconstructed wind speeds lie between 0.31 and 0.68 and are comparable to the correlations typically obtained for other climatic proxies e.g. tree rings. As an example, Bräuning and Mantwill (2004) derived correlation values with leave-one-out validation of 0.41 to 0.78. This results lead us to the conclusion that alternating dune structures can be used as wind proxies also on annual time scales.
Dunes as wind proxies had already been used before as wind proxy (Clemmensen et al., 2014; Reimann et al., 2011), but only on decadal or millennial temporal resolution.
This study therefore, validates statistically the interpretation by Ludwig et al. (2015) of the dune layers and dune migration velocities as indicators of annual and even seasonal wind conditions. Although, the dune system analysed here covers only a period of 26 years, it is suggested that the analysis is of relevance for paleoclimate studies since it can be applied to other dune systems covering longer time periods.

6 Summary and conclusions

This thesis is dedicated to the study of wind variability, with a focus on wind direction, over northern Europe and the Baltic Sea, with special attention to strong winds. The analysis period ranges from a few decades, using different reanalysis data, to the past millennium, using different model simulations. Some of the conducted investigations cover all seasons, albeit others are focused on the winter, due to the higher wind speeds during this season.

In a first step, this study analyses the differences in the behaviour of mean and extreme winds in three aspects: direction distribution, regional differences and seasonal variability. In this part of the analysis two different data sets were employed to assure the robustness of the results. The study showed that there are differences between mean and extreme winds in all these three aspects. Each season exhibited a different prevailing wind direction, but the main wind directions of mean winds showed a much more isotropic distribution than extreme winds. For extreme wind a predominance of south-west winds during the whole year was found. Hence, stronger winds tend to occur from south-west during all seasons. Looking at the individual seasons, mean wind events showed comparable wind direction frequencies for the whole Baltic region, which showed little variations during a year. Extreme winds, in contrast, do show regional differences in some seasons. Northern and southern Baltic region display different characteristics for extreme winds during summer and spring. Winter and autumn, on the other hand, are dominated by south-west winds over the whole Baltic Sea.

The investigation of whether there are patterns of wind direction anomalies that persist over several subsequent seasons revealed no significant temporal correlations in the Baltic Sea region. Hence it is not possible, within a linear framework, to infer information about the anomalous winds in one season from the anomalous winds in the previous seasons. Furthermore, the zonal character of mean winds has strengthened over the past decades, which has not occurred for extreme winds. Conversely, the meridional pattern of variability has not changed for mean winds, but it shows a long-term trend for extreme winds in the Baltic.

This analysis enabled an answer to the first question posed in the Introduction: Are mean wind statistics a useful tool to draw conclusions on extreme wind statistics over the Baltic Sea? It could be demonstrated that changes in mean wind statistics cannot be used to approximate extreme wind changes over the Baltic Sea region.

Because extreme wind speed showed a tendency to occur from west and south-west during winter, the analysis was extended to investigate the link between these wind directions

and their relationship to air-pressure patterns. The investigation of winds from west and south-west which exceed the 95th percentile of wind speed lead to the conclusion that, in general, a higher mean wind speed from these directions occurs with a higher frequency of winds from these directions over the Baltic Sea.
Previous studies had showed an increase in wind speeds from 1960 to the mid of the 1990's, which could be also seen in the present study for the frequencies of extreme west and south-west winds. However, in general the analysis of the last 160 decades showed no long-term trend for wind speeds and wind direction frequencies.

The question: What pressure patterns drive extreme westerly winds over the Baltic Sea? could be answered with: The variability of extreme west and south-west wind frequencies can be related to three pressure patterns, two of which bear similarities to the NAO pattern.

Additionally to pressure patterns, there might be other large-scale factors influencing wind variability over Northern Europe. Therefore, the analysis is also aimed at identifying the large-scale factors that drive changes in the probability distribution of wind speed in winter over Northern Europe. The considered atmospheric drivers are the mean near-surface temperature, the meridional temperature gradient and the specific pressure pattern of the North Atlantic Oscillation. The overlaying question was whether and how the wind speed distribution may change during varying climate conditions and hence whether these conditions may cause more and/or stronger wind speed extremes.
As this relationship might be strongly influenced by external forcings and this influence may be noticeable on longer time scales than only on a few decades, the investigation was extended from reconstruction-based data sets towards model simulation data. However, the study also compared simulation results with reanalysis results, which are used as a ground truth to verify the model results. The analysed products cover time periods from the last decades to the past millennium.
The link between the temperature indices and the NAO appeared physically consistent in all data sets. However, regarding the relationship of these large-scale indices and the wind speed distribution the study revealed clear differences between the data sets. The three global simulations presented similarities, which could be expected as they are based on the same model family. On the other hand, the two regional models also showed results comparable to each other, although they are based on structurally different models. The two analysed reanalysis products resemble the results for the global simulations.
However, one striking result was the strong difference between global and regional simulations. The regional models do not seem to inherit the dynamical properties of their driving global models, but simulating a different connection between large-scale parameters and the wind speed distribution.
The different results regarding global and regional data sets demonstrated that the influence of the spatial resolution and the different boundary layer parametrisation can be a

critical factor for the simulation of near-surface wind speeds under climate change.
Moreover, land-use changes could be identified as a modulator of near-surface wind speeds at longer, centennial, time scales. Two global simulations, including land-use change as forcing, exhibited a steadily increasing standard deviation of wind speed during industrialisation over regions with high deforestation rates.

The question as to what large-scale parameters drive changes in the wind speed distribution over Northern Europe could not be answered easily. Although all data sets seemed to be in itself consistent, it was difficult to derive general conclusions on the effect of potential large-scale drivers on the distribution of daily wind. The simulated impact of climate change on wind speed distributions seem to depend strongly on model details such as physical parametrisation and forcings.

These discrepancies and difficulties show the importance for proxy data to verify simulations and extent knowledge about time periods prior observations. This thesis also includes the statistical analysis of a wind proxy based on migrating dunes. This proxy was originally measured and interpreted in cooperation with geologists (Ludwig et al., 2015). Here, a detailed statistical analysis of the link between this proxy and annual and seasonal wind conditions over the past decades was carried out which is required for a quantitative calibration of this proxy to eventually reconstruct past wind conditions in this region.
The analysed dunes at the polish Baltic Sea coast are characterised by alternating white and black layers representing light quartz grains and heavy minerals. The study investigated the relation between the layer thicknesses (migration velocity) and the atmospheric parameters precipitation, temperature and wind. Although it was shown that precipitation and temperature have an influence on the sand transport, this influence strongly depends on wind conditions. Hence, the focus of this analysis lied on the link between wind conditions and dune migration.
The analysed dunes have a west-east orientation, and thus are most prone to westerly (W, SW) and easterly (E, NE) winds. The results showed that the dune migration is most sensitive to autumn and spring wind conditions.
These investigations identified a linear relationship between the dune layer thickness and the frequencies of south-west and west winds exceeding a specific wind speed threshold. The applied linear model regarding this relationship was validated with the leave-one-out-method, which allowed for the conclusion that alternating dune structures can be used as wind proxies also on annual time scales.
Although, the analysed dune system covers only a period of 26 years, the analysis is of relevance for paleoclimate studies because it can be applied to other dune systems covering longer time periods.

The question for a wind proxy in the linear relation between wind and sand dune movement as presented in cooperation with geologists (Ludwig et al., 2015) could be

answered by a statistical validation, which proved this record to be a valid wind proxy.

The presented study allows for numerous possible follow-up analysis. For example, results from Chapter 3 regarding westerly extreme winds and the connection to circulation weather types can be conducted with the model simulations used in Chapter 4. This would extent the presented results in three ways. First, the presented results would cover more than only a few decades. Second, the used HiResAFF data set only allowed for the analysis of the Baltic Sea circulation types, but circulation types over the North-Atlantic-European region would be of interest for the scientific community as well. Third, such an analysis would broaden the knowledge about the pressure influence on wind extremes beyond the North Atlantic Oscillation.
Changes in the wind climate might have a strong influence on sandy coastline processes. The application of the findings of this thesis to available information about changes in the evolution of specific coastlines over several decades can help to verify the main atmospheric drivers of these coastline changes, which might be of great interest in regard to possible climate change induced sea level changes. A first application could be on sandy coastlines of the southern Baltic Sea. A found statistical relation between coastline changes and atmospheric drivers in the observational period might enable us to apply this relation to future climate scenarios.
Furthermore the presented analysis regarding dune proxies could be applied to other proxies, for example lake sediments. The different sediment layers, developing during varying climate parameters, allow for conclusions on past climate conditions. Changing wind speeds can have an effect on the lake mixing ratio, and hence on the sediment deposition. Such proxies might largely extend the time period available from observations or dune proxies and allow for information on data sparse regions.

Abbreviations

AM	Analog Method
CLISCODE	Climate Signals in Coastal Deposits
CRU	Climate Research Unit
diffM	difference between 95^{th} percentile and 50^{th} percentile of wind speed
diffE	difference between 99^{th} percentile and 95^{th} percentile of wind speed
DJF	December-January-February
E	East
ECHAM	General circulation model family from the Max-Planck Institute, Hamburg
EOF	Empirical Orthogonal Function
GCM	Global Circulation Model
HGF	Helmholtz-Gemeinschaft Deutscher Forschungszentren (Hemholtz Research Centres)
HiResAFF	High Resolution Atmospheric Forcing Fields
IPCC	Intergovernmental Panel on Climate Change
JJA	June-July-August
LMM	Late Maunder Minimum
MAM	March-April-May
mTemp	Mean near-surface air Temperature
NAO	North Atlantic Oscillation
NCAR	National Centre for Atmospheric Research
NCEP	National Centres for Environmental Prediction
N	North
NE	North-East
NER	North-East Region
NNE	North-North-East
NNW	North-North-West
NW	North-West
NWR	North-West Region
P50	50^{th} percentile
P95	95^{th} percentile
P99	99^{th} percentile
PC	Principle Component
PCA	Principle Component Analysis
RCAO	Rossby Centre Atmosphere Ocean model
RCM	Regional Circulation Model
REKLIM	Regionale Klimaänderung (Regional Climate Change)
REMO	Regional Climate Model

RMSE	Root Mean Square Error
S	South
SE	South-East
SER	South-East Region
SLP	mean Sea Level Pressure
SMHI	Swedish Meteorological and Hydrological Institute
STD	Standard Deviation
SW	South-West
SWR	South-West Region
tGrad	mean meridional Temperature Gradient
T2M	2-Meter Temperature
WASA	Waves and Storms in the North Atlantic
W	West
WS	Wind Speed
20CR	20^{th} Century Reanalysis

List of Publications

This thesis is related to the following manuscripts:

- Bierstedt, S.E., Hünicke, B. and Zorita, E. (2015): Variability of wind direction statistics of mean and extreme winds over the Baltic Sea region. Tellus A 67, 29073

- Bierstedt, S.E., Hünicke, B., Zorita, E., Wagner, S. and Gómez-Navarro, J.J. (2015): Variability of daily winter wind speed distribution over Northern Europe during the past millennium in regional and global climate simulations. Clim. Past Discuss. 11, 1479-1518.

- Ludwig, J., Lindhorst. S., Bierstedt, S., Betzler C., Borówka, R. (2015): Coastal dunes as archive of annual wind intensity (Łeba, Poland), under revision.

Bibliography

Alexandersson, H., Tuomenvirta, H., Schmith, T., and Iden, K. Trends of storms in NW Europe derived from an updated pressure data set. *Climate Research*, 14:71 – 73, 2000.

Bard, E., Raisbeck, G., Yiou, F., and Jouzel, J. Solar irradiance during the last 1200 years based on cosmogenic nuclides. *Tellus*, 52B:985–992, 2000.

Birks, H. J. B. Quantitative palaeoenvironmental reconstructions. *Maddy, D. and Brew, J. S., editors; Statistical modeling of Quaternary Science Data, Technical Guide, Quaternary Research Association, Cambridge*, 5:161–254, 1995.

Borówka, M. and Rotnicki, K. Balance of the aeolian sand transport on the beach and the problem of sand nourishment of the active dune field on the Łeba Barrier. *J. Coastal Res.*, 22:257–265, 1995.

Borówka, R. K. Present Day Dune Processes and Dune Morphology on the Łeba Barrier, Polish Coast of the Baltic. *Geografiska Annaler. Series A, Physical Geography*, 62(1/2): 75–82, 1980.

Borówka, R. Accumulation and redeposition of eolian sands on the lee slope of dunes and their influence on formation of sedimentary structures. *Quaest. Geogr.*, 5:5–22, 1979.

Borówka, R. Dunes on the Łeba Barrier - their history and dynamics of present-day aeolian processes. *J. Coastal Res.*, 22:247–251, 1995.

Bretagnon, P. and Francou, G. Planetary theories in rectangular and spherical variables – VSOP87 solutions. *Astron. Astrophys.*, 202:309–315, 1988.

Bräuning, A. and Mantwill, B. Summer temperature and summer monsoon history on the Tibetan plateau during the last 400 years recorded by tree rings. *Geophys. Res. Lett.*, 31:L24205, 2004. doi: 10.1029/2004GL020793.

Brönnimann, S., Martius, O., von Waldow, H., Welker, C., Luterbacher, J., Compo, G., Sardeshmukh, P., and Usbeck, T. Extreme winds at northern mid-latitudes since 1871. *Meteor. Z.*, 21(1):013–027, 2012.

Buynevich, I., Bitinas, A., and Pupienis, D. Lithological anomalies in a relict coastal dune: Geophysical and paleoenvironmental markers. *Geophys. Res. Lett.*, 34:1–5, 2007.

Bárdossy, A. and Caspary, H. J. Detection of climate change in europe by analyzing european atmospheric circulation patterns from 1881 to 1989. *Theoretical and Applied Climatology*, 42:155–167, 1990.

Bärring, L. and Fortuniak, K. Multi-indices analysis of southern Scandinavian storminess 1780–2005 and links to interdecadal variations in the NW Europe–North Sea region. *Int. J. Climatol.*, 29:373 – 384, 2009. doi: 10.1002/joc.1842.

Bärring, L. and von Storch, H. Scandinavian storminess since about 1800. *Geophys. Res. Lett.*, 31:L2020, 2004. doi: 10.1029/2004GL020441.

Carretero, J. C., Gomez, M., Lozano, I., de Elvira, A. R., Serrano, O., and Iden, K. Changing waves and storms in the northeast Atlantic? *Bull. Amer. Meteor. Soc.*, 79: 741–760., 1998.

Cattiaux, J. and Cassou, C. Opposite CMIP3/CMIP5 trends in the wintertime Northern Annular Mode explained by combined local sea ice and remote tropical influences. *Geophys. Res. Lett.*, 40:3682–3687, 2013. doi: 10.1002/grl.50643.

Chaverot, S., Hequette, A., and Cohen, O. Changes in storminess and shoreline evolution along the northern coast of France during the second half of the 20(th) century. *Zeitschrift Fur Geomorphologie*, 52:1–20, 2008.

Christensen, O., Kjellström, E., and Zorita, E. *Second Assessment of Climate Change for the Baltic Sea Basin*, chapter Projected Change—Atmosphere, pages 217–233. Springer International Publishing, 2015.

Clemmensen, L. B., Hansen, K. W. T., and Kroon, A. Storminess variation at Skagen, northern Denmark since AD 1860: Relations to climate change and implications for coastal dunes. *Aeolian Research*, 15:101–112, 2014. doi: 10.1016/j.aeolia.2014.09.001.

Compo, G. P., Whitaker, J. S., Sardeshmukh, P. D., Matsui, N., Allan, R. J., Yin, X., Gleason, B. E., Vose, R. S., Rutledge, G., Bessemoulin, P., Brönnimann, S., Brunet, M., Crouthamel, R. I., Grant, A. N., Groisman, P. Y., Jones, P. D., Kruk, M. C., Kruger, A. C., Marshall, G. J., Maugeri, M., Mok, H. Y., Nordli, O., Ross, T. F., Trigo, R. M., Wang, X. L., Woodruff, S. D., and Worley, S. J. The Twentieth Century Reanalysis Project. *Quarterly Journal of the Royal Meteorological Society*, 137(654):1–28, 2011. ISSN 1477-870X. doi: 10.1002/qj.776.

Costas, I. *Climate Archive Dune*. PhD thesis, Hamburg University, 2013.

Costas, I., Reimann, T., Tsukamoto, S., Ludwig, J., Lindhorst, S., Frechen, M., Hass, H., and Betzler, C. Comparison of OSL ages from young dune sediments with a high-resolution independent age model, Quaternary Geochronology. *Quaternary Geochronology*, 10:16–23, 2012a.

Costas, S., Jerez, S., Trigo, R., Goble, R., and Rebêlo, L. Sand invasion along the Portuguese coast forced by westerly shifts during cold climate events. *Quat. Sci. Rev.*, 42: 15–28, 2012b.

Crowley, T. J., Zielinski, G., Vinther, B., Udisti, R., Kreutz, K., Cole-Dai, J., and Castellano, J. Volcanism and the Little Ice Age. *PAGES Newsletter*, 16:22–23, 2008.

Crueger, T., Stevens, B., and Brokopf, R. The Madden–Julian Oscillation in ECHAM6 and the Introduction of an Objective MJO Metric. *J. Climate*, 26:3241–3257, 2013. doi: 10.1175/JCLI-D-12-00413.1.

Dahm, T., Kruger, F., Essen, H. H., and Hensch, M. Historic microseismic data and their relation to the wave-climate in the North Atlantic. *Meteor. Z.*, 14:771–779, 2005.

De Kraker, A. M. J. A method to assess the impact of high tides, storms and storm surges as vital elements in climatic history. The case of stormy weather and dikes in the northern part of Flanders, 1488 to 1609. *Climatic Change*, 43:287–302, 1999.

Dee, D., Fasullo, J., Shea, D., Walsh, J., and the National Center for Atmospheric Research Staff (Eds). The Climate Data Guide: Atmospheric Reanalysis: Overview & Comparison Tables. Retrieved from https://climatedataguide.ucar.edu/climate-data/atmospheric-reanalysis-overview-comparison-tables.

Della-Marta, P. M., Mathis, H., Frei, C., Liniger, M. A., Kleinn, J., and Appenzeller, C. The return period of wind storms over Europe. *Int. J. Climatol.*, 29:437–459., 2009.

Doescher, R., Willen, U., Jones, C., Rutgersson, A., Meier, H. E. M., Hansson, U., and Graham, L. P. The development of the regional coupled ocean-atmosphere model RCAO. *Boreal Environ. Res.*, 7:183–192, 2002.

Doms, J. F., G., Heise, E., Herzog, H.-J., Mrionow, D., Raschendorfer, M., Reinhart, T., Ritter, B., Schrodin, R., Schulz, J.-P., and Vogel, G. A Description of the Nonhydrostatic Regional COSMO Model. Part II: Physical Parameterization. Technical report, Deutscher Wetterdienst, 2011.

Donat, M. G., Renggli, D., Wild, S., Alexander, L. V., Leckebusch, G. C., and Ulbrich, U. Reanalysis suggests long-term upward trends in European storminess since 1871. *Geophys. Res. Lett.*, 38:L14703–L14703, 2011. doi: 10.1029/2011GL047995.

Donnelly, J. P. and Woodruff, J. D. Intense hurricane activity over the past 5,000 years controlled by El Niño and the West African monsoon. *Nature*, 447:465–468, 2007. doi: 10.1038/nature05834.

Ebisuzaki, W. A Method to Estimate the Statistical Significance of a Correlation When the Data Are Serially Correlated. *J. Clim.*, 10:2147–2153, 1997. doi: 10.1175/1520-0442(1997)010⟨2147:AMTETS⟩2.0.CO;2.

Ekman, M. A Secular Change in Storm Activity over the Baltic Sea Detected through Analysis of Sea Level Data. *Small Publications in Historical Geosciences*, 16:1 – 13, 2007.

Esper, J., Düthorn, E., Krusic, P., Timonen, M., and Büntgen, U. Northern European summer temperature variations over the Common Era from integrated tree-ring density records. *J. Quaternary Sci.*, 29:487–494, 2014.

Etheridge, D., Steele, L., Langenfelds, R., Francey, R., Barnola, J., and Morgan, V. Natural and anthropogenic changes in atmospheric CO2 over the last 1000 years from air in Antarctic ice and firn. *J. Geophys. Res.*, 101:4115–4128, 1996.

Fernandez-Donado, L., Gonzalez-Rouco, J. F., Raible, C. C., Ammann, C. M., Barriopedro, D., Garcia-Bustamante, E., Jungclaus, J. H., Lorenz, S. J., Luterbacher, J., Phipps, S. J., Servonnat, J., Swingedouw, D., Tett, S. F. B., Wagner, S., Yiou, P., and Zorita, E. Large-scale temperature response to external forcing in simulations and reconstructions of the last millennium. *Clim. Past*, 9:393–421, 2013. doi: 10.5194/cp-9-393-2013.

Feser, F., Rockel, B., von Storch, H., Winterfeldt, J., and Zahn, M. Regional Climate Models add Value to Global Model Data: A Review and selected Examples. *Bull. Amer. Meteor. Soc.*, 92(9):1181–1192, 2011. doi: 10.1175/2011BAMS3061.1.

Feser, F., Barcikowska, M., Krueger, O., Schenk, F., Weisse, R., and Xia, L. Storminess over the North Atlantic and northwestern Europe—A review. *Q.J.R. Meteorol. Soc.*, 141:350–382, 2015. doi: 10.1002/qj.2364.

Fischer-Bruns, I., von Storch, H., Gonzalez-Rouco, J. F., and Zorita, E. Modelling the variability of midlatitude storm activity on decadal to century time scales. *Clim. Dyn.*, 25:461–476, 2005. doi: 10.1007/s00382-005-0036-1.

Franzén, L. G. The changing frequency of gales on the swedish west coast and its possible relation to the increased damage to coniferous forests of Southern Sweden. *Int. J. Climatol.*, 11:769–793, 1991. doi: 10.1002/joc.3370110705.

Geyer, B. High resolution atmospheric reconstruction for Europe 1948–2012: coastDat2. *Earth Syst. Sci. Data.*, 6:147–164, 2014. doi: 10.5194/essd-6-147-2014.

Gillett, N. P. and Fyfe, J. C. Annular mode changes in the CMIP5 simulations. *Geophys. Res. Lett.*, 40:1189–1193, 2013. doi: 10.1002/grl.50249.

Giorgetta, M. A., Jungclaus, J., Reick, C. H., Legutke, S., Bader, J., Böttinger, M., Brovkin, V., Crueger, T., Esch, M., Fieg, K., Glushak, K., Gayler, V., Haak, H., Hollweg, H.-D., Ilyina, T., Kinne, S., Kornblueh, L., Matei, D., Mauritsen, T., Mikolajewicz, U., Mueller, W., Notz, D., Pithan, F., Raddatz, T., Rast, S., Redler, R., Roeckner, E., Schmidt, H., Schnur, R., Segschneider, J., Six, K. D., Stockhause, M., Timmreck, C., Wegner, J., Widmann, H., Wieners, K.-H., Claussen, M., Marotzke, J., and Stevens, B. Climate and carbon cycle changes from 1850 to 2100 in MPI-ESM simulations for the coupled model intercomparison project phase 5. *J. Adv. Model. Earth Syst.*, 5:572–597, 2013.

Giorgi, F. and Gutowski Jr., W. Regional Dynamical Downscaling and the CORDEX Initiative. *Annual Review of Environment and Resources*, 40:null, 2015. doi: 10.1146/annurev-environ-102014-021217.

Girardi, J. A GPR and mapping study of the evolution of an active parabolic dune system. Master's thesis, Napeague New York. Stony Brook University, Dept. of Geosciences., 2005.

Gulev, S. K. and Hasse, L. Changes of wind waves in the North Atlantic over the last 30 years. *Int. J. Climatol.*, 19:1091 – 1117, 1999.

Gulev, S. K., Zolina, O., and Grigoriev, S. Extratropical cyclone variability in the Northern Hemisphere winter from the NCEP/NCAR reanalysis data. *Climate Dyn.*, 17:795 – 809, 2001.

Gulev, S., Jung, T., and E., R. Climatology and interannual variability in the intensity of synoptic scale processes in the North Atlantic from the NCEP-NCAR reanalysis data. *J. Clim.*, 15:809 – 828, 2002.

Gómez-Navarro, J. J. and Zorita, E. Atmospheric annular modes in simulation over the past millennium: No long-term response to external forcing. *Geophys. Res. Lett.*, 40: 3232–3236, 2013. doi: 10.1002/grl.50628.

Gómez-Navarro, J. J., Montávez, J. P., Jiménez-Guerrero, P., Jerez, S., Lorente-Plazas, R., González-Rouco, J. F., and Zorita, E. Internal and external variability in regional simulations of the Iberian Peninsula climate over the last millennium. *Clim. Past*, 8: 25–36, 2012. doi: 10.5194/cp-8-25-2012.

Gómez-Navarro, J. J., Montávez, J. P., Wagner, S., and Zorita, E. A regional climate palaeosimulation for Europe in the period 1500–1990 – Part 1: Model validation. *Clim. Past*, 9:1667–1682, 2013. doi: 10.5194/cp-9-1667-2013.

Gómez-Navarro, J. J., Bothe, O., Wagner, S., Zorita, E., Werner, J. P., Luterbacher, J., Raible, C. C., and Montávez, J. P. A regional climate palaeosimulation for Europe in the period 1501–1990 – Part II: Comparison with gridded reconstructions. *Clim. Past Discuss.*, 11:307–343, 2015a. doi: 10.5194/cpd-11-307-2015. URL `www.clim-past-discuss.net/11/307/2015/`.

Gómez-Navarro, J. J., Raible, C. C., and Dierer, S. Sensitivity of the WRF model to PBL parametrizations and nesting techniques: evaluation of surface wind over complex terrain. *Geosci. Model Dev. Discuss*, 8:5437–5479, 2015b. doi: 10.5194/gmdd-8-5437-2015.

Hall, A. Projecting regional change. *Science*, 346:1461, 2014. doi: 10.1126/science.aaa0629.

Hall, A. and Qu, X. Using the current seasonal cycle to constrain snow albedo feedback in future climate change. *Geophys. Res. Lett.*, 33:L03502, 2006. doi: 10.1029/2005GL025127.

Hanna, E., Cappelen, J., Allan, R., Jónsson, T., Le Blancq, F., Lillington, T., and Hickey, K. New Insights into North European and North Atlantic Surface Pressure Variability, Storminess, and Related Climatic Change since 1830. *J. Clim.*, 21:6739–6766, 2008.

Hartigan, J. and Wong, M. Algorithm AS 136: A K-means clustering algorithm. *Appl. Stat.*, 28:100–108, 1979.

Hess, P. and Brezowsky, H. Katalog der Großwetterlagen Europas. Technical report, Deutscher Wetterdienst (DWD), 1969.

Hong, S.-Y. and Pan, H.-L. Nonlocal boundary layer vertical diffusion in a medium-range forecast model. *Mon. Wea. Rev.*, 124:2322–2339, 1996.

Hunt, B. The Medieval Warm Period, the Little Ice Age and simulated climatic variability. *Clim. Dyn.*, 27(7-8):677–694, 2006. ISSN 0930-7575. doi: 10.1007/s00382-006-0153-5.

Hurrell, J. W. and van Loon, H. Decadal variations in climate associated with the North Atlantic oscillation. *Climatic Change*, 36:301 – 326, 1997.

Hurrell, J. Decadal trends in the North Atlantic Oscillation – regional temperatures and precipitation. *Science*, 269:676–679, 1995.

Hurrell, J., Y. Kushnir, Y., Ottersen, G., and Visbeck, M. An overview of the North Atlantic Oscillation. The North Atlantic Oscillation: Climatic Significance and Environmental Impact. *Geophys. Monogr.*, 134:1–36, 2003.

Hünicke, B. *Atmospheric forcing of decadal Baltic Sea level variability in the last 200 years: A statistical analysis.* PhD thesis, Department for Geoscience of the University of Hamburg, 2008.

Hünicke, B., Zorita, E., and Haeseler, S. Holocene climate simulations for the Baltic Sea Region -application for sea level and verification of proxy data. *Berichte der RGK*, 92: 211–249, 2011.

Hünicke, B., Zorita, E., Soomere, T., Madsen, K., Johansson, M., and Suursaar, Ü. *Second Assessment of Climate Change for the Baltic Sea Basin*, chapter Recent Change—Sea Level and Wind Waves, pages 155–185. Springer International Publishing, 2015. doi: 10.1007/978-3-319-16006-1_9.

IPCC. Summary for Policymakers. In: Climate Change 2013: The Physical Science Basis. Contribution of Working Group I to the Fifth Assessment Report of the Intergovernmental Panel on Climate Change [Stocker, T.F., D. Qin, G.-K. Plattner, M. Tignor, S.K. Allen, J. Boschung, A. Nauels, Y. Xia, V. Bex and P.M. Midgley (eds.)]. Technical report, Cambridge University Press, Cambridge, United Kingdom and New York, NY, USA., 2013.

Jaagus, J. Long-term changes in frequencies of wind directions on the western coast of Estonia. *Publications of the Institute of Ecology, Tallinn University,*, 11:11 – 24, 2009. [in Estonian, with English summary].

Jaagus, J. and Kull, A. Changes in surface wind directions in Estonia during 1966 - 2008 and their relationships with large-scale atmospheric circulation. *Estonian Journal of Earth Sciences*, 60:220 – 231, 2011. doi: 10.3176/earth.2011.4.03.

Jacob, D. and Podzun, R. Sensitivity studies with the regional climate model REMO. *Meteorology and Atmospheric Physics*, 63:119–129, 1997.

Jungclaus, J. H., Lorenz, S. J., Timmreck, C., Reick, C. H., Brovkin, V., Six, K., Segschneider, J., Giorgetta, M. A., Crowley, T. J., Pongratz, J., Krivova, N. A., Vieira, L. E., Solanki, S. K., Klocke, D., Botzet, M., Esch, M., Gayler, V., Haak, H., Raddatz, T. J., Roeckner, E., Schnur, R., Widmann, H., Claussen, M., Stevens, B., and Marotzke, J. Climate and carbon-cycle variability over the last millennium. *Clim. Past*, 6:723–737, 2010. doi: 10.5194/cp-6-723-2010.

Kalnay, E., Kanamitsu, M., Kistler, R., Collins, W., Deaven, D., Gandin, L., Iredell, M., Saha, S., White, G., Woollen, J., Zhu, Y., Leetmaa, A., Reynolds, R., Chelliah, M., Ebisuzaki, W., Higgins, W., Janowiak, J., Mo, K., Ropelewski, C., Wang, J., Jenne, R., and Joseph, D. The NCEP/NCAR 40-year reanalysis project. *Bull Am Meteorol Soc*, 77:437–471, 1996.

Keevallik, S. Wind speed and velocity at three Estonian coastal stations 1969–1992. *Estonian Journal of Engineering*, 14:209 – 219, 2008. doi: 10.3176/eng.2008.3.02.

Keevallik, S. Shifts in meteorological regime of the late winter and early spring in Estonia during recent decades. *Theor. Appl. Climatol.*, 105:209–215, 2011.

Keevallik, S. and Rajasalub, R. Winds on the 500 hPa isobaric level over Estonia (1953–1998). *Physics and Chemistry of the Earth, Part B: Hydrology, Oceans and Atmosphere*, 26:425–429, 2001.

Kent, E. C., Fangohr, S., and Berry, D. I. A comparative assessment of monthly mean wind speed products over the global ocean. *Int. J. Climatol.*, 33:2520–2541, 2013. doi: 10.1002/joc.3606.

Kistler, R., Kalnay, E., Collins, W., Saha, S., White, G., Woolen, J., Chelliah, M., Ebiszusaki, W., Kanamitsu, M., Kousky, V., van den Dool, H., Jenne, R., , and Fiorino, M. The NCEP/NCAR 50-Year Reanalysis: Monthly Means CD–ROM and Documentation. *Bull. Am. Meteorol. Soc.*, 82:247–267, 2001.

Knippertz, P., Ulbrich, U., and Speth, P. Changing cyclones and surface wind speeds over the North Atlantic and Europe in a transient GHG experiment. *Clim. Res.*, 15:109–122, 2000.

Krivova, N. and Solanki, S. Models of solar irradiance variations: Current status. *Journal of Astrophysics and Astronomy*, 29(1-2):151–158, 2008. ISSN 0250-6335. doi: 10.1007/s12036-008-0018-x.

Krueger, O. The Informational Value of Pressure-Based Proxies for Past Storm Activity. Technical report, HZG Report, 2014.

Krueger, O. and von Storch, H. Evaluation of an Air Pressure–Based Proxy for Storm Activity. *J. Clim.*, 24:2612–2619, 2011. doi: 10.1175/2011JCLI3913.1.

Krueger, O., Schenk, F., Feser, F., and Weisse, R. Inconsistencies between Long-Term Trends in Storminess Derived from the 20CR Reanalysis and Observations. *J. Clim.*, 26:868–874, 2013. doi: 10.1175/JCLI-D-12-00309.1.

Kruizinga, S. and Murphy, A. H. Use of an analogue procedure to formulate objective probabilistic temperature forecasts in the Netherlands, . *Mon. Weather Rev*, 111:2244–2254, 1983. doi: 10.1175/1520-0493(1983)111⟨2244:UOAAPT⟩2.0.CO;2,.

Kull, A. Relationship between inter-annual variation of wind direction and wind speed. *Publicationes Instituti Geographici Universitatis Tartuensis*, 97:62 – 70, 2005.

Kundu, P. K. Ekman Veering Observed near the Ocean Bottom. *J. Phys. Oceanogr.*, 6: 238 – 242, 1975.

Kysely, J. and Huth, R. Changes in atmospheric circulation over europe detected by objective and subjective methods. *Theor. Appl. Climatol.*, 85:19–36, 2006. doi: 10.1007/s00704-005-0164-x.

Kyselý, J. Influence of the persistence of circulation patterns on warm and cold temperature anomalies in europe: Analysis over the 20th century. *Global and Planetary Change*, 62:147–163, 2008.

Lancaster, N. Controls on aeolian activity: some new perspectives from the Kelso Dunes, Mojave Desert, California. *Journal of Arid Environments*, 27:113–125, 1994.

Lancaster, N., Nickling, W., and Neumann, C. Particle size and sorting characteristics of sand in transport on the stoss slope of a small reversing dune. *Geomorphology*, 43: 233–424, 2002.

Legutke, S. and Voss, R. The Hamburg Atmosphere –Ocean Coupled Circulation Model ECHO-G. Technical Report 18, DKRZ, Hamburg, 1999.

Lehmann, A., Getzlaff, K., and Harla, J. Detailed assessment of climate variability of the Baltic Sea area for the period 1958-2009. *Clim. Res.*, 46:185 – 196, 2011.

Leppäranta, M. and Myrberg, K. *Physical Oceanography of the Baltic Sea.* Praxis Publishing Ltd, 2009.

Li, M. and Woollings, T. Extratropical cyclones in a warmer, moister climate: A recent Atlantic analogue. *Geophys. Res. Lett.*, 41(23):8594–8601, 2014.

Lorenz, E. N. Atmospheric predictability as revealed by naturally occurring analogs,. *J. Atmos. Sci.*, 26:639–646, 1969. doi: 10.1175/1520-0469(1969)26⟨636:APARBN⟩2.0.CO;2,.

Ludwig, J., Lindhorst, S., Betzler, C., Bierstedt, S., and Borówka, R. Coastal dunes as archive of annual wind intensity (Łeba, Poland). Aeolian Research (2015) submitted.

Luterbacher, J., Xoplaki, E., Dietrich, D., Rickli, R., Jacobeit, J., Beck, C., Gyalistras, D., Schmutz, C., and Wanner, H. Reconstruction of sea level pressure fields over the Eastern North Atlantic and Europe back to 1500. *Clim. Dyn.*, 18(7):545–561, 2002. ISSN 0930-7575. doi: 10.1007/s00382-001-0196-6.

Luterbacher, J., Dietrich, D., Xoplaki, E., Grosjean, M., and Wanner, H. European seasonal and annual temperature variability, trends, and extremes since 1500. *Science*, 303:1499–1503, 2004.

Marland, G., Boden, T., and Andres, R. Global, Regional, and National Emissions, Trends: a compendium of data on global change. Technical report, Carbon Dioxide Information Center, Oak Ridge National Laboratory, US Department of Energy, Oak Ridge, TN, 2003.

Marsland, S. J., Haak, H., Jungclaus, J. H., Latif, M., and Roeske, F. The Max Planck Institute global ocean/sea ice model with orthogonal curvilinear coordinates. *Ocean Modell*, 5:91–127, 2003.

Matulla, C., Schöner, W., Alexandersson, H., von Storch, H., and Wang, X. L. European storminess: late nineteenth century to present. *Clim. Dyn.*, 31:125–130, 2007. doi: 10.1007/s00382-007-0333-y.

Matulla, C., Hofstätter, I., M .and Auer, Böhm, R., Maugeri, H., M .and von Storch, and Krueger, O. Storminess in Northern Italy and the Adriatic Sea reaching back to 1760. *Physics and Chemistry of the Earth, Parts A/B/C*, 40-41:80–85, 2011.

McCabe, G., Clark, M., and Serreze, M. Trends in Northern Hemisphere Surface Cyclone Frequency and Intensity. *J. Clim.*, 14:2763 – 2768, 2001.

McVicar, T., Roderick, M., Donohuea, R., Lia, L., Van Nielc, T., Thomas, A., Grieser, J., Jhajharia, D., Himri, Y., Mahowald, N., Mescherskaya, A., Kruger, A., Rehman, S., and Dinpashoh, Y. Global review and synthesis of trends in observed terrestrial near-surface wind speeds: Implications for evaporation. *J. Hydrol.*, 416-417:182–205, 2012. doi: 10.1016/j.jhydrol.2011.10.024.

Michaelsen, J. Cross-validation in statistical climate forecast models. *J. Clim. Appl. Met.*, 26:1589–1600, 1987.

Mitchell, T. D. and Jones, P. D. An improved method of constructing a database of monthly climate observations and associated high-resolution grids. *Int. J. Climatol.*, 25: 693–712, 2005. doi: 10.1002/joc.1181.

Nilsson, C. *Windstorms in Sweden - Variations and Impacts.* PhD thesis, Lund University, 2008.

Nilsson, C., Stjernquist, I., Bärring, L., Schlyter, P., Jänsson, A., and H., S. Recorded storm damage in Swedish forests 1901-2000. *Forest Ecol. Manag.*, 199:165 – 173, 2004. doi: 10.1016/j.foreco.2004.07.031.

Nolan, P., Lynch, P., McGrath, R., Semmler, T., and Wang, S. Simulating climate change and its effects on the wind energy resource of Ireland. doi: 10.1002/we.489. *Wind Energ.*, 15:593–608, 2012. doi: 10.1002/we.489.

Paciorek, C., Risbey, J., Ventura, V., and Rosen, R. Multiple Indices of Northern Hemisphere Cyclone Activity, Winters 1949–99. 1590. *J. Clim.*, 15:1573 – 1590, 2002.

PAGES 2k Consortium Continental-scale temperature variability during the past two millennia. *Nature Geoscience*, 6:339–346, 2013. doi: 10.1038/ngeo1797.

Pessacg, N. L. and Solman, S. Effects of land-use changes on climate in southern South America. *Clim. Res.*, 55(1):33–51, 2013. doi: 10.3354/cr01119.

Pithan, F. and Mauritsen, T. Arctic amplification dominated by temperature feedbacks in contemporary climate models. *Nature Geosci*, 7:181–184, 2014. doi: 10.1038/ngeo2071.

Pongratz, J., Reick, C., Raddatz, T., and Claussen, M. A reconstruction of global agricultural areas and land cover for the last millennium. *Global Biogeochem. Cycles,*, 22: GB3018, 2008. doi: 10.1029/2007GB003153.

Raible, C., Yoshimori, M., Stocker, T. F., and Casty, C. Extreme midlatitude cyclonesand their implications for precipitation and wind speed extremes in simulations of the Maunder Minimum versus present day conditions. 8. *Clim. Dyn.*, 28:409–423., 2007.

Reckermann, M., Langner, J., Omstedt, A., von Storch, H., Keevallik, S., Schneider, B., and Arheimer, H. E. M. H. B., B. Meier. BALTEX—an interdisciplinary research network for the Baltic Sea region Focus on Environmental, Socio-Economic and Climatic Changes in Northern Eurasia and Their Feedbacks to the Global Earth System. *Environ. Res. Lett.*, 6:045205, 2011. doi: 10.1088/1748-9326/6/4/045205.

Reimann, T., Tsukamoto, S., Harff, J., Osadczuk, K., and Frechen, M. Reconstruction of Holocene coastal foredune progradation using luminescence dating - An example from the Swina barrier (southern Baltic Sea, NW Poland). *Geomorphology*, 132:1–16, 2011.

Rockel, B. W. and Hense, A. The regional climate model COSMO-CLM (CCLM). *Meteorol. Z.*, 12:347–348, 2008.

Roeckner, E., Arpe, K., Bengtsson, L., Christoph, M., Claussen, M., Dümenil, L., Esch, M., Giorgetta, M., Schlese, U., and Schulzweida, U. The atmospheric general circulation model ECHAM4: model description and simulation of present-day climate. Technical Report 218, MPI-M, Hamburg, 1996.

Roeckner, E., Bäuml, G., Bonaventura, L., Brokopf, R., Esch, M., Giorgetta, M., Hagemann, S., Kirchner, I., Kornblueh, L. ., Manzini, E., Rhodin, A., Schlese, U., Schulzweida, U., and Tompkins, A. The atmospheric general circulation model ECHAM5. Part I: Model description. Technical Report 349, Max Planck Institute for Meteorology, Hamburg, 2003.

Rogers, J. C. Patterns of Low-Frequency Monthly Sea Level Pressure Variability (1899–1986) and Associated Wave Cyclone Frequencies. *J. Clim.*, 3:1364–1379, 1990. doi: 10.1175/1520-0442(1990)003⟨1364:POLFMS⟩2.0.CO;2.

Rutgersson, A., Jaagus, J., Schenk, F., and Stendel, M. Observed changes and variability of atmospheric parameters in the Baltic Sea region during the last 200 years. *Clim. Res.*, 61:177 – 190, 2014.

Rutgersson, A., Jaagus, J., Schenk, F., Stendel, M., Bärring, L., Briede, A., Claremar, B., Hanssen-Bauer, I., Holopainen, J., Moberg, A., Nordli, O., Rimkus, E., and Wibig, J. *Second Assessment of Climate Change for the Baltic Sea Basin*, chapter Recent Change—Atmosphere, pages 69–97. Springer International Publishing, 2015. doi: 10.1007/978-3-319-16006-1_4.

Scaife, A., Ineson, S., Knight, J., Gray, L., Kodera, K., and Smith, D. A mechanism for lagged North Atlantic climate response to solar variability. *Geophys. Res. Lett.*, 40: 434–439, 2013. doi: 10.1002/grl.50099.

Schenk, F. and Zorita, E. Reconstruction of high resolution atmospheric fields for Northern Europe using analog-upscaling. *Clim. Past*, 8:1 – 23, 2012. doi: 10.5194/cp-8-1-2012.

Schimanke, S., Meier, H. E. M., Kjellström, E., Strandberg, G., and Hordoir, R. The climate in the Baltic Sea region during the last millennium simulated with a regional climate model. *Clim. Past*, 8:1419–1433, 2012. doi: 10.5194/cp-8-1419-2012.

Schmidt, G., Jungclaus, C., J.H. andAmmann, Bard, E., Braconnot, P., Crowley, T., Delaygue, G., Joos, F., Krivova, N., Muscheler, R., Otto-Bliesner, B., Pongratz, J., Shindell, D., Solanki, S., Steinhilber, F., and Vieira, L. Climate forcing reconstructions for use in PMIP simulations of the last millennium (v1.0). *Geosci. Model Dev.*, 4:33–45, 2011. doi: 10.5194/gmd-4-33-2011.

Schreiber, T. and Schmitz, A. Improved surrogate data for nonlinearity tests. *Phys. Rev. Lett.*, 77:635, 1996.

Seneviratne, S., Nicholls, N., Easterling, D., Goodess, C., Kanae, S., Kossin, J., Luo, Y., Marengo, J., McInnes, K., Rahimi, M., Reichstein, M., Sorteberg, A., Vera, C., and Zhang, X. Changes in climate extremes and their impacts on the natural physical environment. In: Managing the Risks of Extreme Events and Disasters to Advance Climate Change Adaptation [Field, C.B., V. Barros, T.F. Stocker, D. Qin, D.J. Dokken, K.L. Ebi, M.D. Mastrandrea, K.J. Mach, G.-K. Plattner, S.K. Allen, M. Tignor, and P.M. Midgley (eds.)]. A Special Report of Working Groups I and II of the Intergovernmental Panel on Climate Change (IPCC). Technical report, Cambridge University Press, Cambridge, UK, and New York, NY, USA, 2012.

Serreze, M. C., Walsh, J. E., Chapin, F. S., Osterkamp, T., Dyurgerov, M., Romanovsky, V., Oechel, W. C., Morison, J., Zhang, T., and Barry, R. G. Observational Evidence of Recent Change in the Northern High-Latitude Environment. *Climatic Change*, 46: 159–207, 2000. URL `10.1023/A:1005504031923`.

Siegismund, F. and Schrum, C. Decadal changes in the wind forcing over the North Sea. *Clim. Res.*, 18:39–45, 2001.

Stevens, B., Giorgetta, M., Esch, M., Mauritsen, T., Crueger, T., Rast, S., M., S., Schmidt, H., Bader, J., Block, K., Brokopf, R., Fast, I., Kinne, S., Kornblueh, L., Lohmann, U., Pincus, R., Reichler, T., and Roeckner, E. Atmospheric component of the MPI-M Earth System Model: ECHAM6. *J. Adv. Model. Earth Syst*, 5:146–172, 2013. doi: 10.1002/jame.20015.

Taylor, K. E., Stouffer, R. J., and Meehl, G. A. An Overview of CMIP5 and the Experiment Design. *Bull. Amer. Meteor. Soc.*, 93:485–498, 2012.

Trenberth, K., Jones, P., Ambenje, P., Bojariu, R., Easterling, D., Klein Tank, A., Parker, D., Rahimzadeh, F., Renwick, J., and Rusticucci, M. Climate Change 2007: The Physical Science Basis. Technical report, Contribution of Working Group I to the Fourth Assessment Report of the Intergovernmental Panel on Climate Change (Cambridge University Press, Cambridge, UK and New York, NY, USA, 2007), Chap. Observations: Surface and Atmospheric Climate Change, 2007.

van den Dool, H. Searching for analogs, how long must we wait? *Tellus A*, 46A:314–324, 1994. doi: 10.1034/j.1600-0870.1994.t012-00006.x.

von Storch, H. and Zwiers, F. W. *Statistical Analysis in Climate Research.* Cambridge University Press, 1999.

von Storch, H., Langenberg, H., and Feser, F. A spectral nudging technique for dynamical downscaling purposes. *Mon. Weather Rev.*, 128:3664 – 3673, 2000.

von Storch, H., Zorita, E., Jones, J., Dimitriev, Y., González-Rouco, F., and Tett, S. Reconstructing past climate from noisy data. *Science*, 306:679–682, 2004.

von Storch, H., Omstedt, A., Pawlak, J., and Reckermann, M. *Second Assessment of Climate Change for the Baltic Sea Basin*, chapter Introduction and Summary, pages 1–22. Springer International Publishing, 2015. doi: 10.1007/978-3-319-16006-1_1.

Wang, X. L., Feng, Y., Compo, G. P., Zwiers, F. W., Allan, R. J., Swail, V. R., and Sardeshmukh, R. D. Is the storminess in the Twentieth Century Reanalysis really inconsistent with observations? A reply to the comment by Krueger et al. (2013b). *Clim. Dyn.*, 42:1113–1125, 2013. doi: 10.1007/s00382-013-1828-3.

Wang, X., Swail, V., and Zwiers, F. Climatology and Changes of Extratropical Cyclone Activity: Comparison of ERA-40 with NCEP–NCAR Reanalysis for 1958–2001. *J. Clim.*, 19:3145 – 3166, 2006.

Wang, X., Wan, H., Zwiers, F., Swail, V., Compo, G., Allan, R., Vose, R., Jourdain, S., and X., Y. Trends and low-frequency variability of storminess over western Europe, 1878-2007. *Clim. Dyn.*, 37:2355–2371, 2011. doi: 10.1007/s00382-011-1107-0.

WASA. Changing waves and storms in the northeast Atlantic. *Bull. Am. Meteorol. Soc.*, 79:741 – 760, 1998.

Weidemann, H. *Klimatologie der Ostseewasserstände: Eine Rekonstruktion von 1948 bis 2011.* PhD thesis, University of Hamburg, 2014.

Weisse, R. and von Storch, H. *Marine Climate and Climate Change. Storms, Wind Waves and Storm Surges.* Springer Praxis, 2009. URL `http://www.springer.com/earth+sciences+and+geography/book/978-3-540-25316-7`.

Weisse, R., von Storch, H., and Feser, F. Northeast Atlantic and North Sea Storminess as Simulated by a Regional Climate Model during 1958–2001 and Comparison with Observations. *J. Clim.*, 18:465–479, 2005. doi: 10.1175/JCLI-3281.1.

Weisse, R., von Storch, H., Callies, U., Chrastansky, A., Feser, F., Grabemann, I., Guenther, H., Pluess, A., Stoye, T., Tellkamp, J., Winterfeldt, J., and Woth, K. Regional Meteorological-Marine Reanalyses and Climate Change Projections: Results for Northern Europe and potentials for coastal and offshore applications. *Bull. Am. Meteorol. Soc.*, 90:849–860, 2009. doi: 10.1175/2008BAMS2713.1.

Weisse, R., Gaslikova, L., Geyer, B., Groll, N., and Meyer, E. coastDat – Model Data for Science and Industry. *Die Küste*, 81:5–18, 2014.

Weisse, R., Bisling, P., Gaslikova, L., Geyer, B., Groll, N., Hortamani, M., Matthias, V., Maneke, M., Meinke, I., Meyer, F., E.M.I. Schwichtenberg, Stempinski, F., Wiese, F., and Wöckner-Kluwe, K. Climate services for marine applications in Europe. *Earth Perspectives*, 2:3:1–14, 2015. doi: 10.1186/s40322-015-0029-0.

Wolff, J., Maier-Reimer, E., and Legutke, S. The Hamburg Primitive Equation Model HOPE. Technical Report 8, Germany Climate Computer Center (DKRZ), Hamburg, 1997.

Yao, Z., Wang, T., Han, Z., Zhang, W., and Zhao, A. Migration of sand dunes on the northern Alxa Plateau, Inner Mongolia, China. *J. Arid Environ.*, 70:80–93, 2007.

Yin, J. H. A consistent poleward shift of the storm tracks in simulations of 21st century climate. *Geophys. Res. Lett.*, 32(18):L18701, 2005.

Zanchettin, D., Timmreck, C., Graf, H.-F., Rubino, A., Lorenz, S., Lohmann, K., Krüger, K., and Jungclaus, J. Bi-decadal variability excited in the coupled ocean–atmosphere system by strong tropical volcanic eruptions. *Clim. Dyn.*, 39(1-2):419–444, 2012. doi: 10.1007/s00382-011-1167-1.

Zorita, E. *A Basic Introduction to Climate Modeling and Its Uncertainties*, chapter Climate Impacts on the Baltic Sea: From Science to Policy, pages 105–127. Springer-Verlag Berlin Heidelberg, 2012. doi: 10.1007/978-3-642-25728-5.

Zorita, E., von Storch, H., Gonzalez-Rouco, J. F., Cubasch, U., Luterbacher, J., Legutke, S., Fischer-Bruns, I., and Schlese, U. Climate evolution in the last five centuries simulated by an atmosphere-ocean model: global temperatures, the North Atlantic Oscillation and the Late Maunder Minimum. *Meteorol. Z*, 13:271–289, 2004. doi: 10.1127/0941-2948/2004/0013-0271.

List of Figures

List of Tables

Acknowledgements

First of all, I would like to thank my adviser Birgit Hünicke for her guidance, for her support and for always having her door open for discussions. Also a special thanks to Eduardo Zorita for advising me, for sharing his tremendous knowledge, and for his patience in answering my questions, whenever I needed help. There will never be enough chocolate to pay the both of you off!

A special thanks also to Hans von Storch for supervising this thesis, his constructive comments, and for his encouragement.

I would like to thank Christian Betzler for being the chair of my Advisory Panel and his guidance throughout.

I would also like to thank Frauke Feser for inviting me into the coordination group regarding all storm themes, also 'thank you' to all members of this group.

Thank you to all, former and current, members of the 'System Analysis and Modelling' Division for the great working environment and helpful discussions. Especially, I would like to thank Juliane Ludwig, Sebastian Wagner, Juan José Gómez-Navarro and Dennis Bray for reading and improving large parts of this thesis.

This work was supported through the REKLIM-Initiative, a joint research project of the Helmholtz Association of German research centres (HGF). Additionally, I would like to acknowledge CliSAP for the membership in the School of Integrated Climate System Science (SICSS).

Special thanks goes to my office mate Nele for the perfect mix of working atmosphere and chats of all sorts.

I would also like to thank Saskia and Thomas for proofreading, their encouraging words, support, and motivation.

Most of all, I have to thank my parents for their love and support throughout my life. Thank you both for giving me strength to reach for the stars and chase my dreams.

Eidesstattliche Versicherung

Hiermit erkläre ich an Eides Statt, dass ich die vorliegende Arbeit selbstständig und ohne fremde Hilfe angefertigt, keine anderen als die angegebenen Quellen und Hilfsmittel benutzt und die den benutzten Quellen wörtlich oder inhaltlich entnommenen Stellen als solche kenntlich gemacht habe. Diese Arbeit hat in gleicher oder ähnlicher Form noch keiner Prüfungsbehörde vorgelegen.

Unterschrift: _____

Datum: _____